

The Pennsylvania State University  
The Graduate School  
Department of Electrical Engineering

RESOURCE ALLOCATION TECHNIQUES  
FOR IMPROVED PERFORMANCE OF MULTIUSER SYSTEMS

A Thesis in  
Electrical Engineering  
by  
Changyoon Oh

© 2005 Changyoon Oh

Submitted in Partial Fulfillment  
of the Requirements  
for the Degree of

Doctor of Philosophy

August 2005

The thesis of Changyoon Oh has been reviewed and approved\* by the following:

Aylin Yener

Assistant professor of Electrical Engineering

Thesis Adviser

Chair of Committee

John F. Doherty

Associate professor of Electrical Engineering

John J. Metzner

Professor of Electrical Engineering

Thomas F. La Porta

Professor of Computer Science and Engineering

W. Kenneth Jenkins

Professor of Electrical Engineering

Head of Electrical Engineering

\*Signatures are on file in the Graduate School.

## Abstract

The increasing demand for wireless services necessitates efficient sharing of radio resources. The premise of this thesis is that the performance of multiuser wireless systems can be significantly improved by efficient resource allocation.

This thesis investigates scheduling and power allocation problems for several types of wireless communication systems each employing CDMA as the multiple access mechanism. Scheduling refers to the process of selecting the subset of users to transmit using the available resources. The resources considered are sectorized antennas, orthogonal codes, and time slots. This thesis investigates three distinct scheduling paradigms. The first one is appropriate for real-time CDMA services with constant QoS requirement, whereas the last two are appropriate for delay tolerant CDMA services.

This thesis first considers spatial scheduling and power allocation for a CDMA system employing directional antennas. Spatial scheduling, in this context, refers to scheduling users to sectors served by the directional antennas. The joint optimization problem of cell sectorization, transmit power control, and receiver filter design is studied for both uplink and downlink. Specifically, we determine the optimum sector beam width, such that the total transmit power is minimized, while each user satisfies the minimum signal to interference ratio (SIR) at receivers capable of employing linear multiuser detection. Near optimum solutions with reduced complexity are also sought.

This thesis next investigates the multiuser scheduling and power allocation problem for interference limited multiuser systems. Scheduling, in this context, refers to

scheduling a subset of users to allocate the downlink bandwidth so as to maximize the throughput. The aim is to characterize the optimum base station transmission strategy and to find the corresponding power allocation. We model the interference level by the aid of the orthogonality factor, and find the optimum policy for a range of the orthogonality factor values.

Lastly, this thesis considers the temporal scheduling and power allocation problem for delay constrained CDMA services, i.e., scheduling users to time slots. The motivation is to design an energy-efficient transmission strategy, while each user satisfies a short term throughput fairness requirement. We provide the optimum scheduling policy which minimizes the total transmit power.

## Table of Contents

List of Tables . . . . .	ix
List of Figures . . . . .	xi
Acknowledgments . . . . .	xvi
Chapter 1. Introduction . . . . .	1
1.1 Spatial Scheduling and Power Allocation . . . . .	2
1.2 Multiuser Scheduling and Power Allocation . . . . .	4
1.3 Temporal Scheduling and Power Allocation . . . . .	7
1.4 Thesis Road Map . . . . .	9
Chapter 2. Adaptive CDMA Cell Sectorization with Linear Multiuser Detection	13
2.1 Introduction . . . . .	13
2.2 Model . . . . .	15
2.3 Transmit Power Optimization . . . . .	16
2.3.1 Problem Statement . . . . .	16
2.3.2 Large System with Random Sequences . . . . .	19
2.3.3 Finite Size System with shifted versions of m-sequence . . . . .	21
2.3.4 Graph Theoretic Formulation of the Problem . . . . .	22
2.4 Numerical Results . . . . .	24
2.5 Conclusion . . . . .	24

Chapter 3. Power Controlled CDMA Cell Sectorization with Multiuser Detection:	
A Comprehensive Analysis of Uplink and Downlink . . . . .	31
3.1 Introduction . . . . .	31
3.2 Antenna Pattern and System Model . . . . .	34
3.2.1 Antenna Pattern-I . . . . .	34
3.2.2 Antenna Pattern-II . . . . .	36
3.2.3 System Model . . . . .	37
3.3 Problem Formulation . . . . .	40
3.4 Uplink and Downlink Sectorization . . . . .	43
3.5 Optimum Sectorization . . . . .	46
3.6 Near-Optimum Sectorization . . . . .	51
3.6.1 Ignoring ISecI . . . . .	51
3.6.2 Variations on equal loading . . . . .	51
3.7 Numerical Results . . . . .	53
3.7.1 Perfect Channel Estimation . . . . .	53
3.7.2 Channel Estimation Error . . . . .	55
3.8 Conclusion . . . . .	57
3.9 Appendix-I . . . . .	58
3.10 Appendix-II: Adaptive Cell Sectorization: Joint Transmit and Receiver filter Design . . . . .	60
Chapter 4. Downlink Throughput Maximization for Interference Limited Multiuser Systems: TDMA versus CDMA . . . . .	82

4.1	Introduction . . . . .	82
4.2	System Model and Problem Formulation . . . . .	85
4.3	Optimum Transmit Strategy and Power Allocation . . . . .	88
4.3.1	User Centric Approach . . . . .	88
4.3.2	System-Wide Approach . . . . .	92
4.3.3	Algorithms for Transmit Strategy and Power Allocation . . . . .	96
4.4	Downlink Transmission policies with individual power constraints . . . . .	98
4.4.1	Observations on the Constrained Problem . . . . .	99
4.4.2	Utility Maximization with Individual Constraints . . . . .	101
4.4.3	Algorithms with Individual Power Constraints . . . . .	103
4.5	Numerical Results . . . . .	106
4.6	Conclusion . . . . .	108
Chapter 5. Energy Efficient Rate Scheduling for Interference Limited CDMA Sys-		
	tems: Short Term Throughput Fairness . . . . .	119
5.1	Introduction . . . . .	119
5.2	System Model and Problem Formulation . . . . .	121
5.2.1	System Model . . . . .	121
5.2.2	Problem Formulation . . . . .	122
5.3	Optimum Scheduling . . . . .	124
5.4	Numerical Results . . . . .	128
5.5	Conclusion . . . . .	130
Chapter 6. Conclusion and Future Work . . . . .		
		136

	viii
6.1 Thesis Summary . . . . .	136
6.2 Future Work . . . . .	138
6.3 Publications . . . . .	139
References . . . . .	140



## List of Tables

2.1	Optimum total transmit powers [WATTS] of a large system with random signature sequences for three linear detectors. . . . .	26
2.2	Optimum total transmit powers [WATTS] of a finite size system with m-sequences for three linear detectors. . . . .	26
3.1	Results for the system in Figure 3.5. Total transmit power is in WATTS	64
3.2	Results for the system in Figure 3.6 . . . . .	64
3.3	Results for the system in Figure 3.7 . . . . .	65
3.4	Results for the system in Figure 3.8 . . . . .	65
3.5	Results for the system in Figure 3.9 . . . . .	66
3.6	Results for the system in Figure 3.10 . . . . .	66
3.7	Uplink of a CDMA system with uniform user distribution. Antenna pattern-II . . . . .	67
3.8	Uplink of a CDMA system with nonuniform user distribution. Antenna pattern-II . . . . .	67
3.9	Downlink of a CDMA system with uniform user distribution. Antenna pattern-II . . . . .	68
3.10	Downlink of a CDMA system with nonuniform user distribution. Antenna pattern-II . . . . .	68
3.11	Total Transmit Power (TP) for uniform terminal distribution, $\gamma^* = 5$ . . . . .	69
3.12	Total Transmit Power (TP) for nonuniform terminal distribution, $\gamma^* = 5$ . . . . .	69

3.13 Robustness of optimum sectorization against Gaussian estimation error	70
3.14 Results of method with joint transmit and receiver filter optimization (TR) and method with receiver filter optimization only (RO) for uniform (UNI) and nonuniform (NONUNI) user distributions. K=30. Total transmit power is in WATTS . . . . .	70
3.15 Results of method with joint transmit and receiver filter optimization (TR) and method with receiver filter optimization only (RO) for uniform (UNI) and nonuniform (NONUNI) user distributions. K=50. Total transmit power is in WATTS . . . . .	71

## List of Figures

1.1	An example where the system is infeasible by conventional sectorization: Users in the heavily congested sector (sector 1) can not achieve their QoS requirements. . . . .	10
1.2	The same system as Figure 1.1 where now the system is feasible by adaptive sectorization. . . . .	10
1.3	An example where the relation between utility and power is linear. $\text{gain1} >$ $\text{gain2} > \text{gain3} > \text{gain4}$ . . . . .	11
1.4	Utility functions for different orthogonality factor values. . . . .	11
1.5	System model of scheduling the virtual users in time slots . . . . .	12
2.1	Sector boundaries in a cell for a large system with random signature sequences with Matched Filter (MF), Decorrelator (DD) and MMSE de- tector (MMSE) where the number of users, $K=60$ , number of sectors, $N=6$ , processing gain, $G=64$ , target SIR, $\gamma^*=5$ and noise power, $\sigma^2=$ $10^{-13}$ . Distribution of terminals is uniform. . . . .	27
2.2	Sector boundaries in a cell for a large system with random signature sequences with Matched Filter (MF), Decorrelator (DD) and MMSE de- tector (MMSE) where the number of users, $K=60$ , number of sectors, $N=6$ , processing gain, $G=64$ , target SIR, $\gamma^*=5$ and noise power, $\sigma^2=$ $10^{-13}$ . Distribution of terminals is nonuniform. . . . .	28

2.3	Sector boundaries in a cell for finite size system with m-sequences with Matched Filter (MF), Decorrelator (DD) and MMSE detector (MMSE) where the number of users, $K=36$ , number of sectors, $N=6$ , processing gain, $G=7$ , target SIR, $\gamma^*=5$ and noise power, $\sigma^2=10^{-13}$ . Distribution of terminals is uniform. . . . .	29
2.4	Sector boundaries in a cell for finite size system with m-sequences with Matched Filter (MF), Decorrelator (DD) and MMSE detector (MMSE) where the number of users, $K=36$ , number of sectors, $N=6$ , processing gain, $G=7$ , target SIR, $\gamma^*=5$ and noise power, $\sigma^2=10^{-13}$ . Distribution of terminals is nonuniform. . . . .	30
3.1	(a) Uplink/Downlink Antenna Pattern Model-I (b) Intersector Interference Model . . . . .	35
3.2	Uplink/Downlink Antenna Pattern Model-II . . . . .	36
3.3	(a) User locations in a cell (b) Ring network constructed from the user locations. Node $N_i$ in the ring corresponds to user $U_i$ . . . . .	39
3.4	The network constructed for $K=5$ users, and $M=3$ sectors. . . . .	47
3.5	Comparison of optimum sectorization with random signature for uplink and downlink; uniform terminal distribution . . . . .	72
3.6	Comparison of optimum sectorization with random signature for uplink and downlink; nonuniform terminal distribution. . . . .	73

3.7	Sector boundaries for the uplink of a CDMA system with uniform user distribution. Number of users, $K=25$ , Processing gain, $N=16$ , Number of sectors, $M=6$ , noise power, $\sigma^2 = 10^{-13}$ . . . . .	74
3.8	Sector boundaries for the uplink of a CDMA system with nonuniform user distribution. Number of users, $K=25$ , Processing gain, $N=16$ , Number of sectors, $M=6$ , noise power, $\sigma^2 = 10^{-13}$ . . . . .	75
3.9	Sector boundaries for the downlink of a CDMA system with uniform user distribution. Number of users, $K=25$ , Processing gain, $N=16$ , Number of sectors, $M=6$ , noise power, $\sigma^2 = 10^{-13}$ . . . . .	76
3.10	Sector boundaries for the downlink of a CDMA system with nonuniform user distribution. Number of users, $K=25$ , Processing gain, $N=16$ , Number of sectors, $M=6$ , noise power, $\sigma^2 = 10^{-13}$ . . . . .	77
3.11	Uplink Probability ( $SIR > \gamma^*$ ) vs. TSIR for Gaussian channel estimation error $\sigma_h^2 = 0.001, 0.01, 0.05, 0.1, 0.15$ , $\gamma^* = 5$ . . . . .	78
3.12	Downlink Probability ( $SIR > \gamma^*$ ) vs. TSIR for Gaussian channel estimation error $\sigma_h^2 = 0.001, 0.01, 0.05, 0.1, 0.15$ , $\gamma^* = 5$ . . . . .	79
3.13	Uplink individual user's SIR convergence for Gaussian channel estimation error. $\sigma_h^2 = 0.001$ , $\bar{\gamma} = 5.4$ . . . . .	80
3.14	Uplink individual user's SIR convergence for Gaussian channel estimation error. $\sigma_h^2 = 0.01$ , $\bar{\gamma} = 5.8$ . . . . .	81
4.1	Downlink system model. . . . .	110

4.2	Utility versus transmit power. $gain_1 > gain_2 > gain_3 > gain_4$ . An example where individual utility functions for all users are concave. . . .	111
4.3	Utility versus transmit power. $gain_1 > gain_2 > gain_3 > gain_4$ . An example where individual utility functions for some users are not concave.	112
4.4	Percentage of channel realizations in which the TDMA mode is optimum.	113
4.5	System Utility versus number of users in the system. . . . .	114
4.6	System Utility versus number of users in the system. . . . .	115
4.7	CDMA-mode gain over TDMA-mode for different $\alpha$ values. . . . .	116
4.8	System utilities with no power constraint (NPC), minimum power constraint (PCMIN), maximum power constraint (PCMAX) and maximum and minimum power constraints (PC). $k = 2.4$ ( $\Gamma = 0.15$ , $N = 16$ ), $\alpha = 0.1$ .	117
4.9	Discrete system utilities with no power constraint (NPC), minimum power constraint (PCMIN), maximum power constraint (PCMAX) and maximum and minimum power constraints (PC). $k = 2.4$ ( $\Gamma = 0.15$ , $N = 16$ ), $\alpha = 0.1$ . . . . .	118
5.1	A string constructed based on optimum virtual users scheduling ordering	130
5.2	Network constructed by 3-partitioning the string having 5 nodes ( $\cdots$ : Infeasible edge, $-$ : Feasible edge). . . . .	131
5.3	Power Consumption of Optimum Scheduling (OS) and TDMA-type (TD) $K = 5$ , $n = 5$ . . . . .	132
5.4	Transmission rate allocation in time slots. $g_1 > g_2 > g_3 > g_4 > g_5$ . . . .	133
5.5	Transmission rate allocation in time slots. $g_1 > g_2 > g_3 > g_4 > g_5$ . . . .	134

5.6 Power Consumption of Optimum Scheduling (OS) and Equal Loading	
(EL), $K = 20$ , $n = 10$ . . . . .	135

## Acknowledgments

I am most grateful and indebted to my thesis advisor, Dr. Aylin Yener, for the large doses of guidance, patience, and encouragement she has shown me during my Ph.D. program at Penn State. I also thank my thesis committee members, Dr. John J. Metzner, Dr. Thomas La Porta, and Dr. John Doherty for their insightful commentary on my work. I would like to thank my parents for their continued love and support through my entire life. Finally, I would like to thank my wife, Junghye for her love, belief and understanding.



## Chapter 1

### Introduction

Future wireless systems are expected to provide high capacity flexible services. Code division multiple access (CDMA) shows promise in meeting the demand for future wireless services [1]. Third generation wireless systems, W-CDMA and cdma2000, are both CDMA based standards. In CDMA systems, users share the same time and frequency resources. Each user modulates its symbols with a unique signature sequence, identifying its transmission. Although signatures may be designed to be orthogonal to each other, in practice, due to the asynchronous transmissions and multipath, the orthogonality between codes is destroyed. As a result, each user's transmission creates interference for other users. This interference limits the performance of CDMA systems. To improve the capacity of CDMA systems, efficient resource allocation techniques are necessary.

In this thesis, we investigate resource allocation techniques for a variety of CDMA systems. Specifically, we consider the **scheduling** and **power allocation** problems by utilizing different degrees of freedom, such as sectorized antennas, orthogonal codes, and time slots. We aim to maximize the performance metric that translates to improved system capacity, given quality of service requirements, such as signal to interference ratio (SIR) corresponding to a bit error rate (BER), and maximum delay tolerance.

Scheduling refers to choosing the users to be served. Optimum power allocation is found for the transmissions of the scheduled users.

This thesis investigates three distinct scheduling and power allocation problems, namely, *spatial scheduling* and power allocation, *multiuser scheduling* and power allocation, and *temporal scheduling* and power allocation. The first one is appropriate for real-time CDMA services with constant QoS requirement, and the last two are appropriate for delay tolerant CDMA services.

## 1.1 Spatial Scheduling and Power Allocation

We first present jointly optimum spatial scheduling, power allocation, and linear multiuser detection for real time CDMA services as an effective interference management tool to improve user capacity.

Interference management techniques, such as power control, multiuser detection, beamforming, and cell sectorization have been addressed extensively up to date. Power control has been extensively studied for the past decade, especially for CDMA systems. For voice services, the main purpose of power control is to provide an adequate level of quality of service without causing unnecessary interference to other users [17, 64, 65, 37, 3, 67, 68, 22]. Multiuser detection is the process of demodulating the signals of the users in the time domain to suppress the interference [60]. Beamforming and cell sectorization strive to better receive the desired signal in the spatial domain [32].

While earlier work on the interference management techniques proposed each aforementioned method as an alternative to another, more recent research efforts recognized the capacity improvement by employing these techniques jointly. To that end,

jointly optimum transmit power control and multiuser detection, or beamforming, jointly optimum transmit power control, multiuser detection, and beamforming, and jointly optimum power control and cell sectorization have been considered in references [57, 46, 51, 66].

In chapter 2, to further improve the capacity of CDMA system, we investigate *cell sectorization, transmit power control, and multiuser detection* jointly. A perfect antenna pattern, i.e., no intersector interference, is assumed in chapter 2. Reference [51] reports that substantial capacity improvement by employing adaptive cell sectorization, can be achieved as compared to conventional cell sectorization, i.e., equal angular beamwidth sectorization, and shows that the best cell sectorization arrangement is achieved by solving a shortest path problem when perfect antennas are assumed. When the users' location distribution is uniform, the conventional cell sectorization performs adequately. However, as the users' distribution becomes non-uniform, one or more sectors may be heavily congested. Hence, each user requires more transmit power to compensate for the interference. In this case, by sectorizing the cell adaptive to the users' distribution, system capacity can be increased. Figures 1.1, 1.2 illustrate examples of adaptive cell sectorization.

We jointly optimize the cell sectorization pattern, transmit power levels, and linear receiver filters. The resulting optimization problem may have high complexity for arbitrary signature sequences. We first list the cases under which the optimum solution is guaranteed to have a relatively low complexity. These cases include large systems employing random signatures and finite size systems employing m-sequences or equal square crosscorrelation sequences. For these cases, we observe that the optimum

sectorization problem with linear multiuser detectors has the same complexity as the same problem with matched filters. By intelligently scheduling the users in the pool of spatially orthogonal channels provided by perfect directional antennas, the system wide performance metric, i.e., the total transmit power, is minimized, while each user satisfies the minimum required SIR.

In practice, it is not possible to expect the directional antennas to completely filter out all transmission and reception outside its main beam-width. This fact leads to intersector interference and alters the optimum sectorization arrangement found in chapter 2. In chapter 3, we investigate more realistic antenna patterns. To efficiently manage the interference, we incorporate linear multiuser detection at the base station (for uplink) or at the mobile (for downlink) and formulate the joint optimization problem of the power control, multiuser detection and cell sectorization for uplink and downlink. The existence of the intersector interference may result in a significant increase in the computational complexity requirement. We propose low complexity sectorization algorithms that perform near optimum. We provide a comprehensive analysis of practical scenarios, and answer the question of how to adjust the sector boundaries to optimize the user capacity in conjunction with optimum transmit power and receiver filter design.

## 1.2 Multiuser Scheduling and Power Allocation

Current and future wireless services are a lot more data centric than the previous generation, and often require higher data rate for downlink communications [24, 5, 7]. Data services typically require higher reliability, but are delay tolerant. For delay tolerant data services, conventional power control is not efficient in that, the transmit power would

be wasted to compensate for the constant interference. By exploiting the nature of delay tolerance, power control for data services has been investigated in [50, 16, 49, 63, 26].

In chapter 4, we investigate the multiuser scheduling and power allocation problem for the downlink of delay tolerant CDMA systems by taking the channels of the users into account. Specifically, the problem is to characterize the optimum base station transmission strategy (TDMA or CDMA) and to find the corresponding power allocation for a range of the values of the orthogonality factor. We aim to maximize the system utility, i.e., the sum of the individual utility values. The individual utility we consider is the transmission rate.

Previous research efforts have been focused on the issue of the multiple access schemes, *one-user* transmission or *more than one-user* transmissions for throughput maximization for non-real time services [6, 27, 2, 8]. In references [41, 56], aggregate throughput maximization is investigated for uplink CDMA systems. Reference [6] considers the downlink throughput maximization and shows the optimality of one-user transmission. To overcome the possible unfairness that may result from one-user transmission, reference [27] imposes a minimum service rate constraint and shows the greedy optimality, i.e., allocation of maximum available resource to the users in the order of decreasing channel gains.

When the relation between the transmission rate and power is *linear*, such as schemes with variable processing gain or multicode, the optimality of greedy policy where users with better channels are allocated the power resources, is well described in references [6, 27]. Figure 1.3 illustrates an example of the linear relation between utility and power. The slope between utility and power represents the utility increase per

power, which is a constant for each user. In this case, allocation of power to the user with higher channel gain produces higher system utility. However, when the relation between the transmission rate and power is *logarithmic*, such as a scheme with adaptive modulation, optimality of the greedy policy is no longer guaranteed. Reference [2] considers such a case with an assumption of orthogonal transmissions. The resulting optimization problem for throughput maximization, which assumes orthogonality between the transmissions is preserved, is a convex program. For the CDMA downlink, typically orthogonal codes are used, however, due to the multipath fading, assuming complete orthogonality between transmissions may not be realistic [36]. The *orthogonality factor* designates the level of multipath fading and represents the degree of interference in practical scenarios. In reference [8], multiuser scheduling gain over CDMA, i.e., gain by transmissions of a fraction of users over transmissions of all users in the system, is investigated for a given orthogonality factor. Optimum scheduling and power allocation is not considered in [8].

In chapter 4, we attempt to find the optimum multiuser scheduling strategy and power allocation. We observe that the relation between the rate and power is a function of the orthogonality factor. Depending on the orthogonality factor and users' channel conditions, the optimum number of users to be scheduled may be different. In chapter 4, we define the utility of user  $i$  as:

$$U_i(p_i) = \log\left(1 + k \frac{p_i}{\alpha(P_T - p_i) + \frac{I}{g_i}}\right) \quad (1.1)$$

where  $p_i$ ,  $g_i$  denote the transmit power, channel gain of user  $i$ , respectively.  $k$ ,  $I$  denote the product of modulation index and processing gain, the sum of the thermal noise and the intercell interference, respectively.  $P_T$  denotes the base station maximum power. Figure 1.4 shows the utilities with the transmit power for different orthogonality factor values. When the level of interference is low, simultaneous transmissions by sharing the power  $P_T$  can produce significantly higher system utility than one-user transmission. As the orthogonality factor increases, the utility value for any fixed power level ( $1 < p_i < P_T$ ) decreases due to the increase of interference which more than one-user transmissions create. When the level of interference is high, simultaneous transmissions do not produce higher system utility than one-user transmission. In this case, transmitting a user with best channel gain with maximum power  $P_T$  is the optimum policy.

In each time slot, a subset of users are scheduled to transmit such that the system utility is maximized. For the scheduled users, optimum power values are allocated. For maximum system utility, in general a fraction of the users are scheduled. The resulting optimization problem is non-convex. Fortunately, valuable properties regarding the optimum policy can be observed, and as a result of our observations, we propose an *exact* and a *near-exact* algorithm to determine whether and when TDMA is the optimum strategy. In the later stages of chapter 4, maximum and minimum power constraints are imposed for practical issue and fairness.

### 1.3 Temporal Scheduling and Power Allocation

The service classes in multimedia services are often differentiated by their delay constraints. Limited battery life of mobile terminals prompts careful consideration of

power allocation and delay for multimedia wireless systems [12, 43, 18]. The main idea is to utilize the convex relationship between power and delay: by increasing the transmission time, the transmit power required decreases, while the delay increases. In reference [12], power-delay tradeoff is considered for a single user system. Reference [43] considers efficient transmission scheduling by varying the packet transmission time. In reference [18], power minimization problem is considered with a deadline constraint for a single user system.

In contrast, wireless resources are shared by simultaneous users in CDMA systems. Reference [10] investigates power efficient power and rate allocation for delay tolerant CDMA services with minimum service rate. By greedy packing the transmit power in the order of decreasing channel gain, total transmit power is minimized for achieving any instantaneous total throughput. In greedy packing, a user with higher channel gain always has a higher instantaneous throughput. Thus, the unfairness due to different channel gains among users can not be resolved. To avoid this possible throughput unfairness, short term average throughput requirement, rather than a minimum throughput requirement, is appropriate. This motivates our investigation of a power efficient schedule with a short term average throughput requirement.

In chapter 5, we consider the temporal scheduling and power allocation for delay constrained CDMA systems. Specifically, the aim is to determine the power efficient scheduling policy, while each user maintains the short term average throughput. We consider a multirate CDMA system with the aid of multicodes. In each time slot, multicodes become virtual users, and each virtual user interferes with each others. The problem is to schedule these virtual users such that the transmit power of all users is minimized.



Figure 1.5 shows the system model of scheduling these virtual users in time slots. At the outset, this problem is similar to bin packing problem which is NP-complete [19]. However, by observing the specific structure of the problem, we determine that it can be transformed into a graph partitioning problem which can be solved by a shortest path algorithm in polynomial time. We provide the optimum scheduling policy and compare the performance of the optimum scheduling with that of TDMA-type scheduling.

## 1.4 Thesis Road Map

In this thesis, three distinct scheduling and power allocation problems are studied. Chapter 2 and 3 describe the adaptive CDMA cell sectorization with linear multiuser detection. Chapter 2 considers uplink and a perfect antenna pattern, i.e., no intersector interference, is assumed. Chapter 3 relaxes the assumption of the perfect antenna model, and solves the joint optimization problem of cell sectorization, transmit power control, and receiver filter design. Chapter 3 considers both uplink and downlink. Chapter 4 deals with the throughput maximization problem for delay constrained time slotted CDMA systems. Chapter 5 investigates the power efficiency temporal scheduling with short term average throughput for CDMA uplink. Chapter 6 presents the conclusions of this thesis along with future work.

Each chapter provides a detailed introduction and a detailed relevant literature review. Following the introduction in each chapter, we present the corresponding system model in an effort to have the chapters self contained.

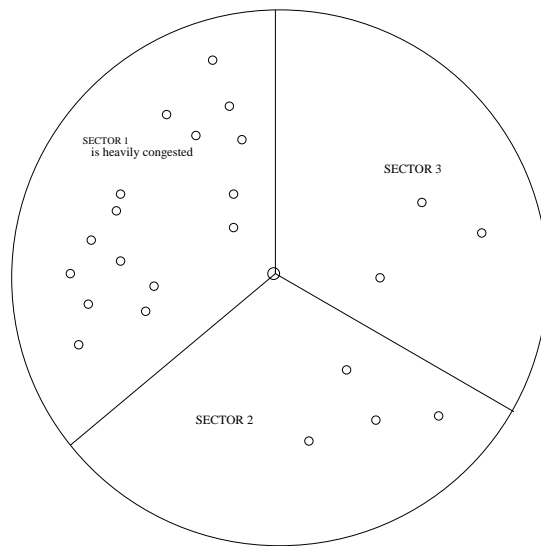


Fig. 1.1. An example where the system is infeasible by conventional sectorization: Users in the heavily congested sector (sector 1) can not achieve their QoS requirements.

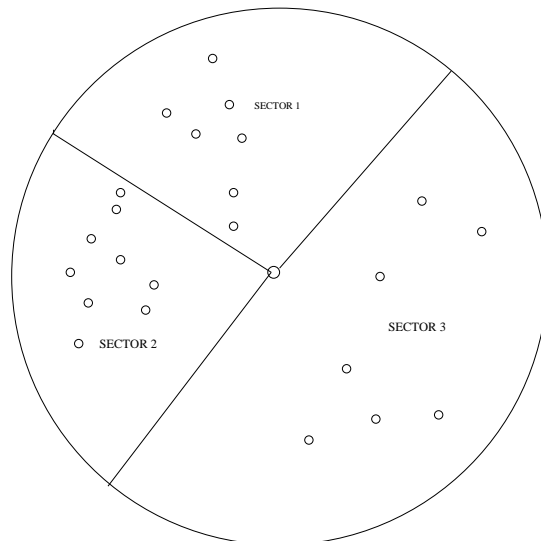


Fig. 1.2. The same system as Figure 1.1 where now the system is feasible by adaptive sectorization.

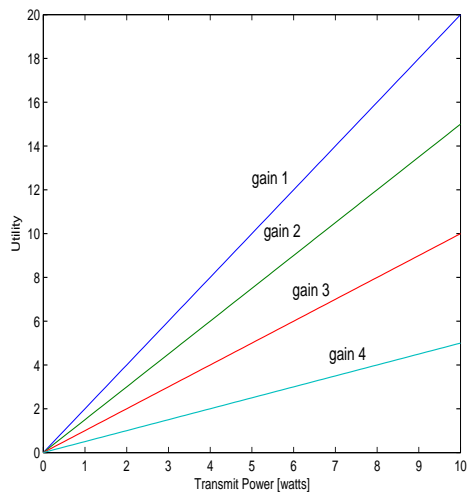


Fig. 1.3. An example where the relation between utility and power is linear.  $\text{gain1} > \text{gain2} > \text{gain3} > \text{gain4}$ .

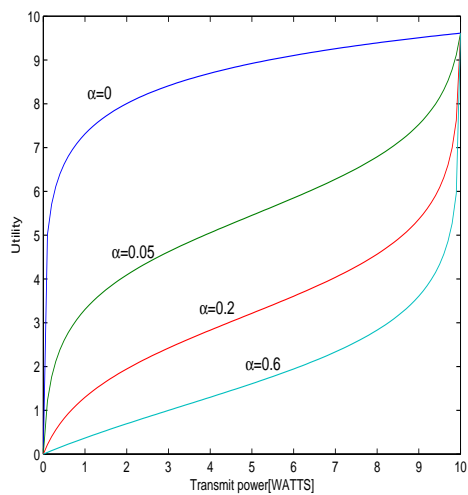


Fig. 1.4. Utility functions for different orthogonality factor values.

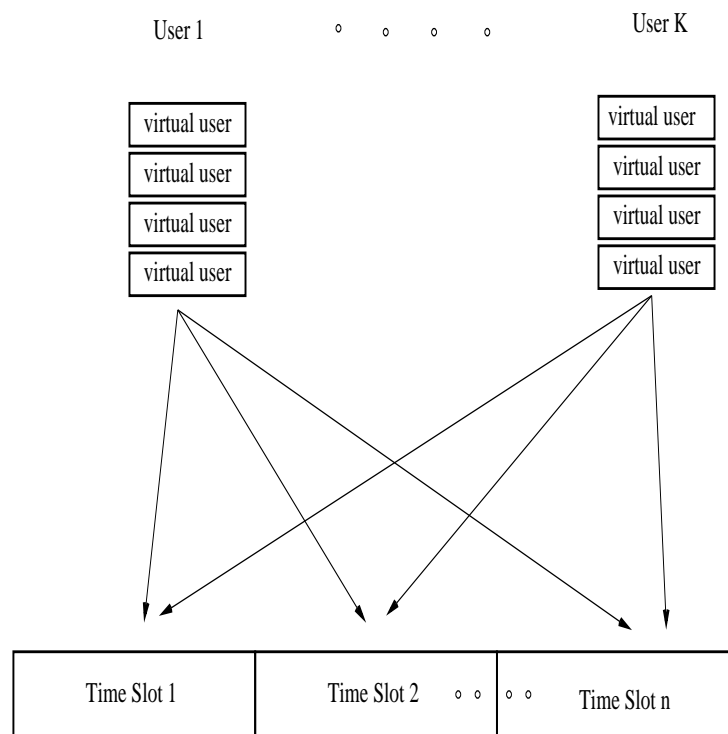


Fig. 1.5. System model of scheduling the virtual users in time slots

## Chapter 2

# Adaptive CDMA Cell Sectorization with Linear Multiuser Detection

### 2.1 Introduction

The demand for high capacity flexible wireless services is ever growing. CDMA shows promise in meeting this demand [1]. It is well known that CDMA systems are interference limited, so interference management techniques are necessary to improve the capacity of CDMA systems. Many techniques that control or suppress interference in CDMA systems such as transmit power control, multiuser detection and cell sectorization have been proposed to date [51, 66, 57, 60, 64]. In this work, we investigate adaptive cell sectorization with multiuser detection. Specifically, given the number of sectors and terminal locations, the problem we investigate is to appropriately sectorize the cell, such that the total transmit power is minimized, while each user has acceptable quality of service, under the assumption that the base station employs linear multiuser detection.

Conventional cell sectorization, where the cell is sectorized to equal angular regions, may not perform well especially in systems where the user distribution is nonuniform. Adaptive cell sectorization, where the cell is sectorized in response to the user distribution, is a promising method to improve the capacity in CDMA systems [51]. Previous work showed that, if the aim is to minimize the total received power of all

users, the best sectorization arrangement is to assign equal number of users to each sector, whereas the solution for the minimum total transmit power sectorization is achieved by solving a shortest path problem [51]. Reference [51] reported substantial power savings as compared to conventional cell sectorization. We note that sectorization related previous work is based on the assumption that the receiver structure is the conventional matched filter (MF), see [51] and references therein.

Multiuser detection is the process of demodulating the signals of the users in a multiple access environment. It was shown in [60] that the optimum multiuser detector has computational complexity which increases exponentially with the number of users. This result prompted the development of several suboptimum detectors. Two key linear multiuser detectors are the decorrelating detector (DD) and the Minimum Mean Square Error (MMSE) detector. The decorrelating detector chooses the linear filter to completely eliminate the multiple access interference (MAI); the MMSE detector chooses the filter to minimize the mean squared error, or equivalently maximize the signal to interference ratio (SIR) [60].

In this work, we consider adaptive cell sectorization when the receiver is equipped with linear multiuser detector (MUD) for all users. The premise of this work is that further capacity improvement is possible with adaptive cell sectorization when matched filters are replaced by linear multiuser detectors. Thus, we address the problem of finding the best sectorization arrangement with minimum transmit power and linear receiver filters. The resulting joint optimization problem has high complexity for arbitrary signature sequences, so we concentrate on the tractable case where the square of the

crosscorrelation values between the users' signatures are equal. Two such cases are considered. First, we consider a large system employing random signatures as is considered in [55]. We formulate the sectorization problem for different linear multiuser detectors for the large system. Second, for finite size deterministic systems, we consider m-sequences, which have equal crosscorrelations. In both cases, the optimum sectorization problem with linear MUD has the same complexity as the same problem with MF.

We provide performance comparisons between different linear detectors in uniform distribution and nonuniform distribution environment. We observe that the incorporation of a better receiver structure, such as the MMSE detector, or the decorrelating detector, provides significant power savings, and user capacity can be improved by employing linear multiuser receivers in conjunction with adaptive sectorization.

## 2.2 Model

A single cell DS-CDMA system with processing gain  $G$  and  $K$  users is considered. The user locations in the cell are assumed to be known. This is a reasonable assumption in very slow mobility environment. For example, in a Wireless Local Loop (WLL), this information is readily available through the addresses of the subscribers. We assume the cell is to be sectorized into  $N$  sectors and there is no intersector interference. All users within the same sector interfere with each other and each user has a pre-assigned signature sequence.

Conventional cell sectorization, or equal angular width cell sectorization may not perform well especially in systems where the user distribution is nonuniform. Adaptive cell sectorization, where the cell is sectorized in response to the user distribution, is

a promising method to improve the capacity of CDMA systems. Our purpose is to investigate the best sectorization arrangement such that the total transmit power is minimized, while each user has acceptable quality of service, under the assumption that the base station employs linear multiuser detection. The quality of service is represented by signal to interference ratio (SIR). A user has an acceptable quality of service if its SIR is greater than a target SIR,  $\gamma^*$ .

## 2.3 Transmit Power Optimization

### 2.3.1 Problem Statement

For the synchronous system, using chip matched filtering and sampling the signal at the chip rate, the received signal vector at the front end of the receiver filter at the base station is given by

$$\mathbf{r} = \sum_{j=1}^K \sqrt{p_j} \sqrt{h_j} b_j \mathbf{s}_j + \mathbf{n} \quad (2.1)$$

where  $p_j$ ,  $h_j$ ,  $b_j$  and  $\mathbf{s}_j$  denote the transmit power, the uplink gain, the information bit and the signature sequence of the  $j$ th user,  $\mathbf{n}$  denotes a Gaussian random vector with  $E[\mathbf{n}\mathbf{n}^\top] = \sigma^2 \mathbf{I}$ . SIR for user  $j$  at the receiver filter output can be expressed as

$$\text{SIR}_j = \frac{(\mathbf{c}_j^\top \mathbf{s}_j)^2 p_j h_j}{\sum_{l \neq j} (\mathbf{c}_j^\top \mathbf{s}_l)^2 p_l h_l + \sigma^2 (\mathbf{c}_j^\top \mathbf{c}_j)} \quad (2.2)$$

where  $\mathbf{c}_j$  denotes the receiver filter for user  $j$ . Equivalently, we may use bank of matched filters each of which is matched to the signature waveform of a user. In one symbol



interval this yields

$$\mathbf{y} = \mathbf{S}^\top \mathbf{r} = \mathbf{R}\mathbf{A}\mathbf{b} + \sigma\mathbf{n} \quad (2.3)$$

where  $\mathbf{R}$  denotes the normalized crosscorrelation matrix of users with  $\mathbf{R}_{k,l} = \rho_{k,l} = \langle \mathbf{s}_k, \mathbf{s}_l \rangle$ ,  $\mathbf{S} = [\mathbf{s}_1, \dots, \mathbf{s}_K]$ ,  $\mathbf{A} = \text{diag}(\sqrt{p_1 h_1}, \dots, \sqrt{p_K h_K})$ ,  $\mathbf{b}$  is K-vector whose  $j$ th component is  $b_j$ , and  $\langle, \rangle$  denotes inner product.

The decision for user  $j$  will be made as

$$\hat{b}_k = \text{sgn}((\mathbf{L}\mathbf{y})_k)$$

with

$$\mathbf{L} = \mathbf{I} \quad \text{for matched filter}$$

$$\mathbf{L} = \mathbf{R}^{-1} \quad \text{for decorrelator}$$

$$\mathbf{L} = (\mathbf{R} + \sigma^2 \mathbf{A}^{-2})^{-1} \quad \text{for MMSE detector}$$

where  $\mathbf{I}$  is identity matrix. SIR for user  $j$  at the output of a linear MUD  $\mathbf{L}$  can be expressed as

$$\text{SIR}_j = \frac{(\mathbf{L}_{jj} + \sum_{k \neq j} \rho_{kj} \mathbf{L}_{jk})^2 p_j h_j}{\sum_{l \neq j} (\mathbf{L}_{jl} + \sum_{t \neq l} \rho_{tl} \mathbf{L}_{jt})^2 p_l h_l + \sigma^2 (\mathbf{LRL})_{jj}}. \quad (2.4)$$

The sectorization problem we consider can be formulated as the transmit power optimization problem.

$$\min_{\theta, \mathbf{P}} \sum_{i=1}^N \sum_{j \in g_i(\theta)} p_j \quad (2.5)$$

$$\begin{aligned}
s.t. \quad \gamma_j &= \frac{(\mathbf{c}_j^\top \mathbf{s}_j)^2 p_j h_j}{\sum_{l \neq j, l \in g_i(\theta)} (\mathbf{c}_j^\top \mathbf{s}_l)^2 p_l h_l + \sigma^2 (\mathbf{c}_j^\top \mathbf{c}_j)} \geq \gamma^* \\
i &= 1, \dots, N \quad \mathbf{p} \geq \mathbf{0} \quad \mathbf{1}^T \theta = 2\pi
\end{aligned}$$

where  $\gamma_j$  is the SIR of the  $j$ th user,  $g_i(\theta)$  is the set of users that reside in the area spanned by sector  $i$ ,  $\theta$  is the  $N$ -tuple vector that denotes the sector angles,  $\mathbf{0}$  and  $\mathbf{1}$  denote the all zero and all one vectors, respectively.

In (2.5), the minimum transmit power is achieved when the SIR constraints are satisfied with equality [64]. In general, the above optimization problem in (2.5) has high complexity for arbitrary signature sequences. However, when all the users have equal squared crosscorrelation, transmit power optimization can be formulated as a graph partitioning problem, and can be solved by a shortest path algorithm, see [51] and references therein. In this particular case, minimum power is achieved by assigning equal received powers to all users belonging to the same sector. Under this assumption, (2.5) is simplified as

$$\min_{\theta, \mathbf{p}} \sum_{i=1}^N q_i^* \sum_{j \in g_i(\theta)} \frac{1}{h_j} \tag{2.6}$$

where  $q_i^*$  is equal received power for sector  $i$ . This optimization problem can be solved by shortest path algorithm with computational complexity  $O(K^3 N)$  as we will see shortly.

In this work, we consider two cases where the optimum received power in each sector turns out to be identical for all users in that sector. First, we consider a large system employing random signature sequences as is considered in [55]. Second, for finite

sized deterministic systems, we consider the shifted versions of m-sequence, which have equal crosscorrelation.

### 2.3.2 Large System with Random Sequences

Reference [55] shows that if the signature sequences are random, as  $N \rightarrow \infty$ , and the ratio  $\alpha = \frac{K}{N}$  is fixed, the empirical distribution of users' powers converges to a fixed distribution  $F(P)$ , and  $\beta_1^N$  will converge in probability to a deterministic value  $\beta_1^*$  which is the unique solution to the equation

$$\beta_1^* = \frac{P_1}{\sigma^2 + \alpha \int I(P, P_1, \beta_1^*) dF(P)} \quad (2.7)$$

$$I(P, P_1, \beta_1^*) = \frac{PP_1}{P_1 + P\beta_1^*} \quad \text{for MMSE receiver}$$

$$I(P, P_1, \beta_1^*) = P \quad \text{for Matched Filter}$$

$$\beta_1^* = \frac{P_1(1 - \alpha)}{\sigma^2}; \quad \alpha < 1 \quad \text{for Decorrelator} \quad (2.8)$$

where  $P_1$  and  $\beta_1^N$  are the received power and SIR of user 1, respectively.  $\beta_1$  is deterministic in a large system and approximately satisfies

$$\beta_{1,MMSE} \simeq \frac{P_1}{\sigma^2 + \frac{1}{N} \sum_{i=2}^K \frac{P_i P_1}{P_1 + P_i \beta_1^*}} \quad (2.9)$$

$$\beta_{1,MF} \simeq \frac{P_1}{\sigma^2 + \frac{1}{N} \sum_{i=2}^K P_i} \quad (2.10)$$

$$\beta_{1,Decorrelator} \simeq \frac{P_1(1 - \alpha)}{\sigma^2} \quad \alpha < 1. \quad (2.11)$$

Also it is shown that minimum power solution is achieved by assigning the same received power  $P(\beta^*)$  to all users for a given SIR  $\beta^*$ . In this case, the minimum received powers for the three receivers are

$$P_{MF}(\beta^*) = \frac{\beta^* \sigma^2}{1 - \alpha \beta^*} \quad \alpha < \frac{1}{\beta^*} \quad (2.12)$$

$$P_{MMSE}(\beta^*) = \frac{\beta^* \sigma^2}{1 - \alpha \frac{1 + \beta^*}{\beta^*}} \quad \alpha < \frac{1 + \beta^*}{\beta^*} \quad (2.13)$$

$$P_{DD}(\beta^*) = \frac{\beta^* \sigma^2}{1 - \alpha} \quad \alpha < 1. \quad (2.14)$$

Under the large system assumption<sup>1</sup>, the cost function of our transmit power optimization problem (2.6) for three linear receivers can be expressed as

$$\min_{\theta, \mathbf{P}} \sum_{i=1}^N P_{MF,i}(\beta^*) \sum_{j \in g_i(\theta)} \frac{1}{h_j} \quad (2.15)$$

$$\min_{\theta, \mathbf{P}} \sum_{i=1}^N P_{DD,i}(\beta^*) \sum_{j \in g_i(\theta)} \frac{1}{h_j} \quad (2.16)$$

$$\min_{\theta, \mathbf{P}} \sum_{i=1}^N P_{MMSE,i}(\beta^*) \sum_{j \in g_i(\theta)} \frac{1}{h_j} \quad (2.17)$$

where  $P_{MF,i}(\beta^*)$ ,  $P_{DD,i}(\beta^*)$  and  $P_{MMSE,i}(\beta^*)$  are minimum received powers for the sector  $i$ .

---

<sup>1</sup>In reference [55], it is shown that the random SIR in finite sized system is close to the deterministic SIR in large system.

### 2.3.3 Finite Size System with shifted versions of m-sequence

We now consider the shifted versions of m-sequence with processing gain  $G$ , which satisfy the equal crosscorrelation between users,  $\rho = -\frac{1}{G}$ <sup>2</sup>. In this case, the SIR for user  $j$  in a sector  $i$  at the output of linear MUD  $\mathbf{L}$  can be expressed as

$$\text{SIR}_j = \frac{(\mathbf{L}_{jj} + \rho \sum_{k \neq j} \mathbf{L}_{jk})^2 p_j h_j}{\sum_{l \neq j} (\mathbf{L}_{jl} + \rho \sum_{t \neq l} \mathbf{L}_{jt})^2 p_l h_l + \sigma^2 (\mathbf{LRL})_{jj}} \quad (2.18)$$

The transmit power optimization problem (2.5) is

$$\min_{\theta, \mathbf{p}} \sum_{i=1}^N \sum_{j \in g_i(\theta)} p_j \quad (2.19)$$

$$s.t. \gamma_j = \frac{(\mathbf{L}_{jj} + \rho \sum_{k \neq j} \mathbf{L}_{jk})^2 p_j h_j}{\sum_{l \neq j} (\mathbf{L}_{jl} + \rho \sum_{t \neq l} \mathbf{L}_{jt})^2 p_l h_l + \sigma^2 (\mathbf{LRL})_{jj}} \geq \gamma^*$$

$$l, k \in g_i(\theta) \quad i = 1, \dots, N \quad \mathbf{p} \geq \mathbf{0} \quad \mathbf{1}^T \theta = 2\pi.$$

Minimum power is achieved when all users within the sector have the same received power. In this case, (3.21) is given by

$$\min_{\theta, \mathbf{p}} \sum_{i=1}^N q_i^* \sum_{j \in g_i(\theta)}^{K_i} \frac{1}{h_j}. \quad (2.20)$$

---

<sup>2</sup>m-sequence with length  $G = 2^m - 1$  bits is generated by an  $m$ -stage shift register with linear feedback. Generated m-sequence has  $2^{m-1} - 1$  1's and  $2^{m-1} - 1$  -1's. One property of m-sequence is that shifted versions of m-sequence have equal crosscorrelation with  $-\frac{1}{G}$  [35].

For Matched Filter and Decorrelator,  $q_i^*$ , the received power for the users in sector  $i$ , is given by

$$q_i^* = \frac{\gamma^* \sigma^2}{1 - \gamma^* \frac{(K_i - 1)}{\rho^2}}, \quad q_i \geq 0 \quad (2.21)$$

$$q_i^* = \gamma^* \sigma^2 R_{11}^{-1}, \quad \rho > \frac{-1}{K_i - 1} \quad (2.22)$$

where  $K_i$  denotes the number of users in sector  $i$ . For MMSE receiver,  $q_i^*$  satisfies the following three equations.

$$q_i^* = \frac{(\mathbf{L}_{jj} + \rho \sum_{k \neq j, k \in g_i(\theta)} \mathbf{L}_{1k})^2 p_j h_j}{\sum_{l \neq j, l \in g_i(\theta)} (\mathbf{L}_{1l} + \rho \sum_{t \neq l, t \in g_i(\theta)} \mathbf{L}_{1t})^2 p_l h_l + \sigma^2 (\mathbf{LRL})_{jj}} \quad (2.23)$$

$$L_{jj} = [1 + \frac{\sigma^2}{q_i^*} + (K_i - 1)\rho]^{-1} [1 + \frac{\rho(K_i - 1)}{1 - \rho + \frac{\sigma^2}{q_i^*}}] \quad (2.24)$$

$$L_{jk} = [1 + \frac{\sigma^2}{q_i^*} + (K_i - 1)\rho]^{-1} [\frac{-\rho}{1 - \rho + \frac{\sigma^2}{q_i^*}}]. \quad (2.25)$$

### 2.3.4 Graph Theoretic Formulation of the Problem

Transmit power optimization problem (TP) does not have a closed form solution. However, when the minimum received powers in a sector are equal, through an appropriate transformation, TP can be formulated as a graph partitioning problem which is guaranteed to find the optimal solution in polynomial time. First, the angular and radial coordinate is assigned to each terminal in a cell. The angular position is the angular

distance of the terminal to a reference terminal. The radial position is the distance of the terminal to the base station. Each terminal in a cell is represented by a vertex along the ring. The position of vertex is determined by the angular position of the terminal regardless of its radial position. This constitutes the elements of an undirected connected graph with vertex set  $V$  and edge set  $E$ ,  $G = (V, E)$ . The vertex set and the edge set are  $V = \{v_1, \dots, v_K\}$  and  $E = \{(v_i, v_{i+1}) | i = 1, \dots, K - 1\} \cup \{(v_K, v_1)\}$ , respectively. Vertex  $i$  has weight  $w_i = \frac{1}{h_i}$ , where  $h_i$  is the uplink gain of the  $i$ th terminal. Sectorization problem for minimum transmit power is to find optimum connected partition on this ring. The set of terminals are partitioned into disjoint subsets  $\{V_1, \dots, V_N\}$  along the ring. Subset  $i$  has weight  $q_i^* \sum_{j \in g_i(\theta)} \frac{1}{h_i}$  and the cost of all subsets is  $\sum_{i=1}^N q_i^* \sum_{j \in g_i(\theta)} \frac{1}{h_i}$ . The graph partitioning problem is to find a feasible partition such that some given cost is minimized.

$$\arg \min_{\{V_1, \dots, V_N\}} \sum_{i=1}^N q_i^* \sum_{j \in g_i(\theta)} \frac{1}{h_i}. \quad (2.26)$$

TP in (2.6) is a graph partitioning problem. Graph theoretic formulation returns the optimal sectors in terms of a list of terminals that belong to each sector. In the previous subsection we already formulated the TP, which is suitable to be transformed into the problem of graph partitioning. When the cost function is separable as is in (2.26), the problem of graph partitioning a string can be reduced to a shortest path problem with computational complexity  $O(K^2N)$  [51]. The cost function in (2.26) is separable, but the corresponding graph is a ring instead of string. When disconnected at some arbitrary edge, the ring is easily transformed into a string. A shortest path algorithm can be applied to the resulting network constructed out of the string. By repeating the same

procedure for each  $K$  edge in  $E$ , graph partitioning problem for the ring can be solved by a shortest path algorithm with complexity  $O(K^3N)$ .

## 2.4 Numerical Results

We provide sectorization results by three linear detectors for transmit power optimization. Figure 2.1 and 2.2 show sector boundaries for a large system with random signature sequences in uniform and nonuniform user distribution, respectively. In addition to the benefit from exploiting other users' power and crosscorrelation, linear multiuser detectors have more flexible choice for selecting sector boundaries than MF, which has a strict constraint for maximum number of users supportable. This leads to significant power saving of linear multiuser detectors over the MF. Table 2.1 shows the optimum transmit power of the large system with random signature sequences. The MMSE detector has 65%, 43% power savings over MF in the case of uniform and nonuniform distribution, respectively. Figure 2.3 and 2.4 show sector boundaries for a finite size system with m-sequences in uniform and nonuniform user distribution, respectively. M-sequence has low squared crosscorrelation, which is beneficial to MF. Table 2.2 shows the optimum transmit power of a finite size system with m-sequences. The MMSE detector has 40%, 20% power savings over MF in case of uniform and nonuniform distribution, respectively.

## 2.5 Conclusion

In this chapter, we studied the joint transmit power optimization and adaptive cell sectorization under the assumption that the base station employs linear multiuser



detectors. In general, this joint optimization problem has high complexity, so tractable cases where the squares of crosscorrelation between users are equal were investigated. First, a large system with random signature sequences was considered. In the second case, we considered the finite size system with m-sequences. We note that besides these two cases, any sequence set with a crosscorrelation matrix where non-diagonal entries are  $\pm\rho$  fits in the same framework.

We provided numerical results for uniform and nonuniform distribution cases. In both cases, the MMSE detector has significant power saving over the MF, while the optimum sectorization problem with linear multiuser detection has the same complexity as the same problem with MF. We conclude that the incorporation of a better receiver structure, such as the MMSE detector, or the decorrelator, provides significant power savings, and user capacity can be improved by employing linear multiuser receivers in conjunction with adaptive sectorization.

Table 2.1. Optimum total transmit powers [WATTS] of a large system with random signature sequences for three linear detectors.

User-distribution	Uniform	Nonuniform
MF	11.46	17.02
DD	4.04	9.70
MMSE	3.92	9.62

Table 2.2. Optimum total transmit powers [WATTS] of a finite size system with m-sequences for three linear detectors.

User-distribution	Uniform	Nonuniform
MF	3.20	6.03
DD	2.18	5.06
MMSE	1.89	4.80

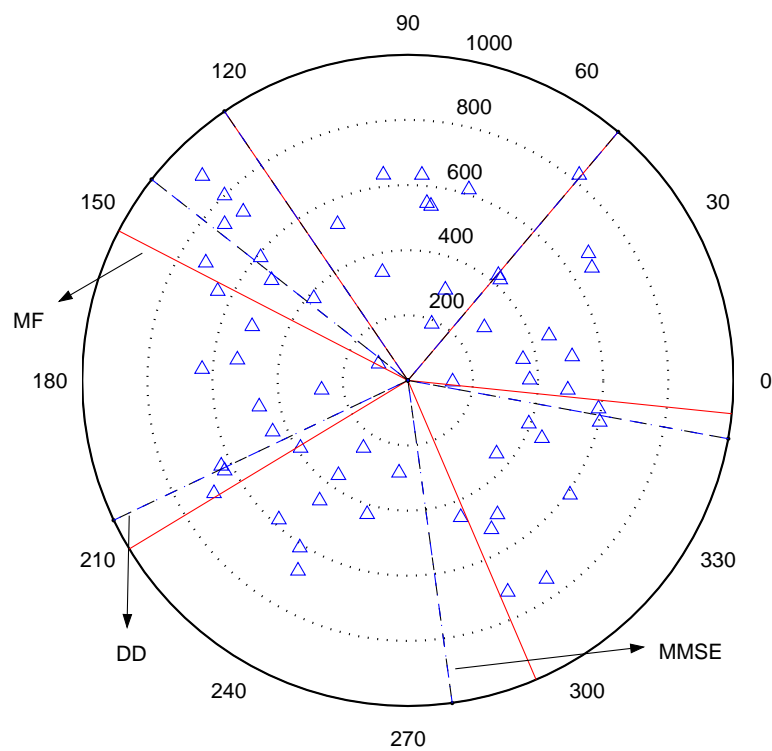


Fig. 2.1. Sector boundaries in a cell for a large system with random signature sequences with Matched Filter (MF), Decorrelator (DD) and MMSE detector (MMSE) where the number of users,  $K=60$ , number of sectors,  $N=6$ , processing gain,  $G=64$ , target SIR,  $\gamma^*=5$  and noise power,  $\sigma^2=10^{-13}$ . Distribution of terminals is uniform.

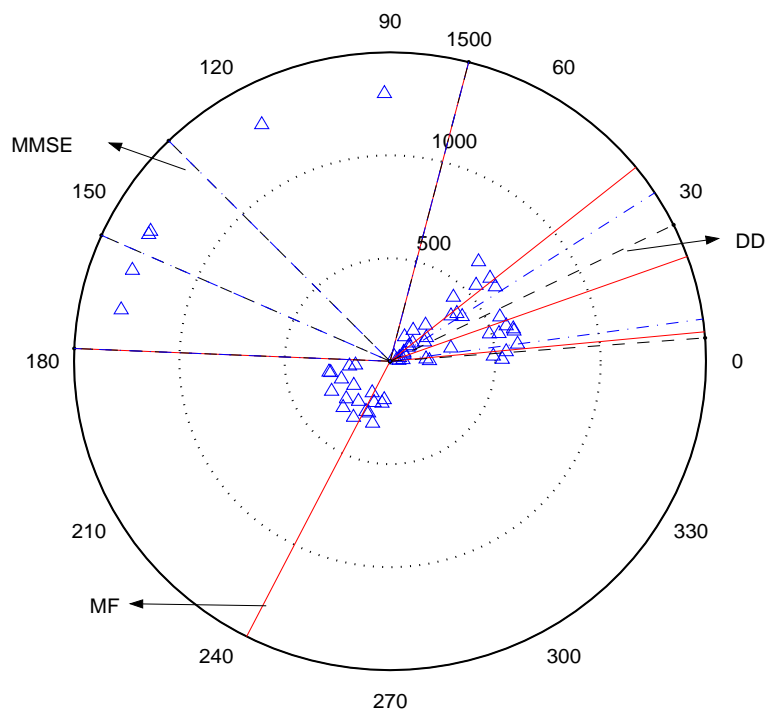


Fig. 2.2. Sector boundaries in a cell for a large system with random signature sequences with Matched Filter (MF), Decorrelator (DD) and MMSE detector (MMSE) where the number of users,  $K=60$ , number of sectors,  $N=6$ , processing gain,  $G=64$ , target SIR,  $\gamma^*=5$  and noise power,  $\sigma^2=10^{-13}$ . Distribution of terminals is nonuniform.

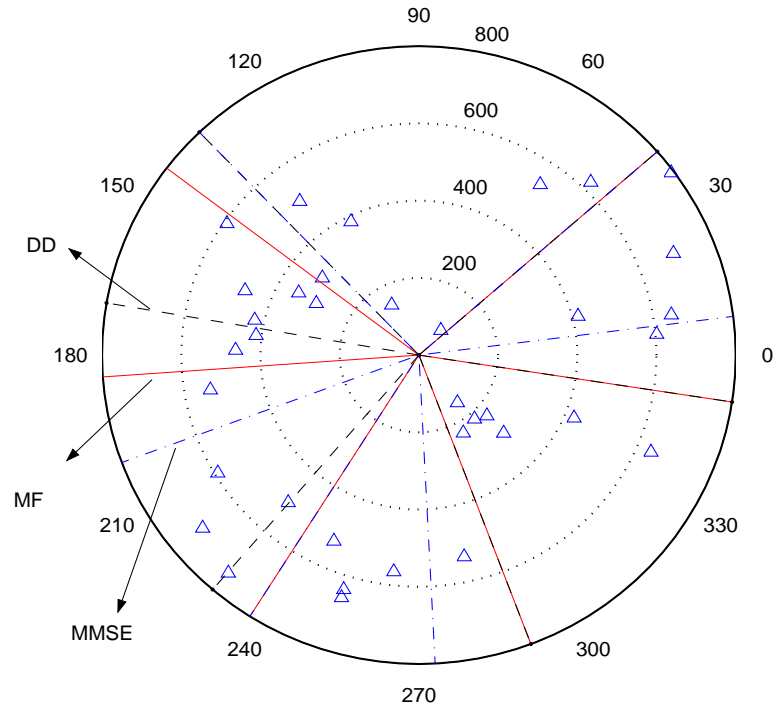


Fig. 2.3. Sector boundaries in a cell for finite size system with m-sequences with Matched Filter (MF), Decorrelator (DD) and MMSE detector (MMSE) where the number of users,  $K=36$ , number of sectors,  $N=6$ , processing gain,  $G=7$ , target SIR,  $\gamma^*=5$  and noise power,  $\sigma^2=10^{-13}$ . Distribution of terminals is uniform.

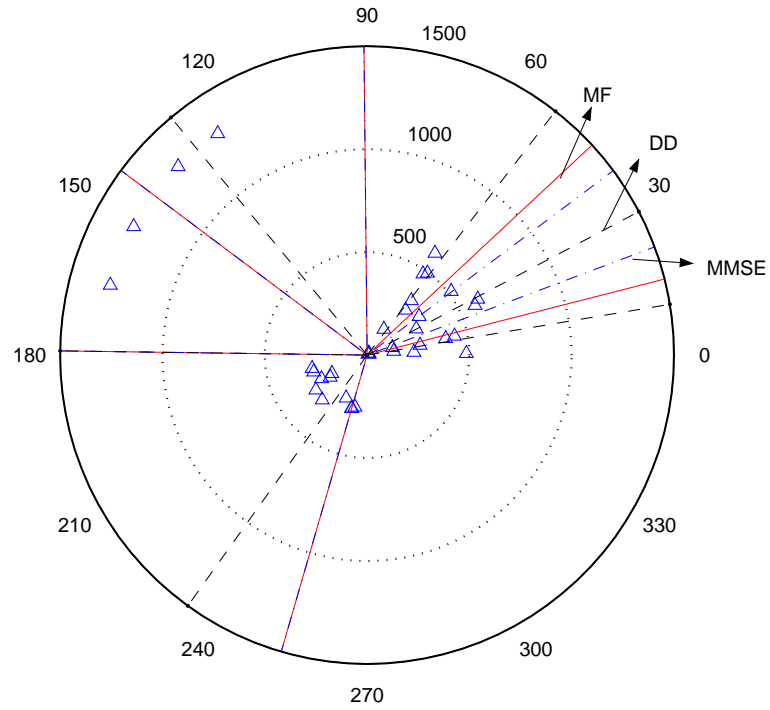


Fig. 2.4. Sector boundaries in a cell for finite size system with m-sequences with Matched Filter (MF), Decorrelator (DD) and MMSE detector (MMSE) where the number of users,  $K=36$ , number of sectors,  $N=6$ , processing gain,  $G=7$ , target SIR,  $\gamma^*=5$  and noise power,  $\sigma^2=10^{-13}$ . Distribution of terminals is nonuniform.

## Chapter 3

# Power Controlled CDMA Cell Sectorization with Multiuser Detection: A Comprehensive Analysis of Uplink and Downlink

### 3.1 Introduction

Future wireless systems are expected to provide high capacity flexible services. Code Division Multiple Access (CDMA) shows promise in meeting the demand for future wireless services [1]. It is well known that CDMA systems are interference limited and the capacity of CDMA systems can be improved by various interference management techniques. These techniques include transmit power control where transmit power levels are adjusted to control interference, multiuser detection where receiver filters are designed to separate interfering signals, and beamforming and cell sectorization where arrays and directional antennas are utilized to suppress interference [51, 66, 67, 33, 34, 57, 17, 64, 60]. While earlier work on interference management techniques proposed each aforementioned method as an alternative to another, more recent research efforts recognize the capacity improvement by employing these techniques jointly. To that end, jointly optimum transmit power control and receiver design, and jointly optimum transmit power control and cell sectorization have been considered in [51, 57].

In this chapter, we consider a CDMA system where the base station is equipped with directional antennas with variable beam width [32], and investigate the joint optimization problem of cell sectorization, power control and multiuser detection. Given the

number of sectors and terminal locations, and the fact that the base station (for uplink), and the terminals (for downlink) employ linear multiuser detection, the problem we consider is to appropriately sectorize the cell, i.e., to determine the main beam width of the directional antennas to be used at the base station, such that the total transmit power is minimized, while each terminal has an acceptable quality of service. The quality of service (QoS) measure we adopt is the signal to interference ratio (SIR). In the sequel, we use the terms terminal and user interchangeably.

Conventional cell sectorization, where the cell is sectorized to equal angular regions, may not perform sufficiently well especially in systems where user distribution is nonuniform [51]. Previous work has shown that *adaptive cell sectorization*, where sector boundaries are adjusted in response to terminal locations, greatly improves the uplink user capacity [51]. Preliminary results also indicate that uplink capacity can be further improved when adaptive cell sectorization is employed in conjunction with linear multiuser detection [40]. Adaptive cell sectorization, [51, 40, 20, 69, 48], can be interpreted as dynamically grouping users in the pool of spatial orthogonal channels provided by perfect directional antennas. In the special case, when the system employs random signatures or a deterministic equicorrelated signature set, the minimum received power in each sector is achieved when all users' received powers are equal, and there exists a closed form solution for the optimum received power in each sector. In this case, the transmit power optimization problem can be transformed into a graph partitioning problem whose solution complexity is polynomial in the number of users and sectors. References [51] and [40] considered such special cases, when matched filters and linear multiuser



detectors are employed at the base station. Both references also assumed perfect directional antenna response, i.e., complete orthogonality between sectors. We also note that, for improvement of the downlink user capacity, heuristic methods to adjust sector boundaries have been reported previously, e.g., [20].

In general, it is more reasonable to assume that users (for uplink) and the base station (for downlink) experience a frequency selective channel in which case it becomes difficult to justify the equi-correlated signature assumption in [51]. In addition, it is not possible to expect the directional antenna to completely filter out all transmission/reception outside its main beam width. This fact leads to inter-sector interference (ISecI) and, as we observe in the sequel, alters the optimum sectorization arrangement found in [51].

The preceding discussion suggests that, while previous work [51, 40, 20, 69, 48] has paved the way in demonstrating the benefits of adapting the size of each sector to improve user capacity, a comprehensive mathematical analysis of more practical scenarios, where the limiting system model assumptions are relaxed, is needed to demonstrate the real value of adaptive cell sectorization both for the uplink and the downlink. This chapter aims to provide that analysis, and answer the question of how to adjust the sector boundaries to optimize the user capacity in conjunction with optimum transmit power and receiver filter design. We consider both the uplink and the downlink problems, and observe that the two problems in general do not lead to identical sectorization arrangements. We examine the optimum solution in each case and propose near-optimum methods with reduced complexity. Our numerical results suggest that the uplink/downlink user capacity in realistic scenarios significantly benefits from intelligently combining cell

sectorization, power control and receiver filtering. Lastly, our numerical results also consider the effect of channel estimation errors on adaptive sectorization. We observe that adaptive sectorization is robust against users' channel estimation errors, i.e., slightly increased user transmit power can compensate for user's channel estimation errors, while optimum sectorization arrangement remains the same.

## 3.2 Antenna Pattern and System Model

### 3.2.1 Antenna Pattern-I

Following references [54, 32], we use the antenna pattern shown in Figure 3.1 for transmission and reception at the base station. Due to the existence of side lobes in the antenna pattern, interference (ISecI) results from adjacent sectors. Main lobe between  $\theta_1$  and  $-\theta_1$  (within the sector) has a constant antenna gain, and the side lobes between  $\theta_1$  and  $\theta_2$ ,  $-\theta_2$  and  $-\theta_1$  (out of sector) have linear attenuated antenna gain in dB. The larger  $\delta = \theta_2 - \theta_1$  is, the larger the area spanned by the sector antenna, which causes increased ISecI. Typically,  $\delta$  is small compared to the size of the main lobe, but non-negligible. Note that, if the directional antenna were perfect, i.e., there were no side lobes ( $\delta = 0^\circ$ ), there would be no ISecI [51]. Uplink and downlink ISecI patterns are in general quite different as explained in the following.

**Uplink ISecI Pattern:** All users within a sector between  $\theta_1$  and  $-\theta_1$  experience interference from the same set of out-of-sector users. Thus, the amount of ISecI at the *front end* of the receiver filters, for all users in the sector is the same. The base station receives all in-sector users' signals (users whose angular locations lie between  $\theta_1$  and

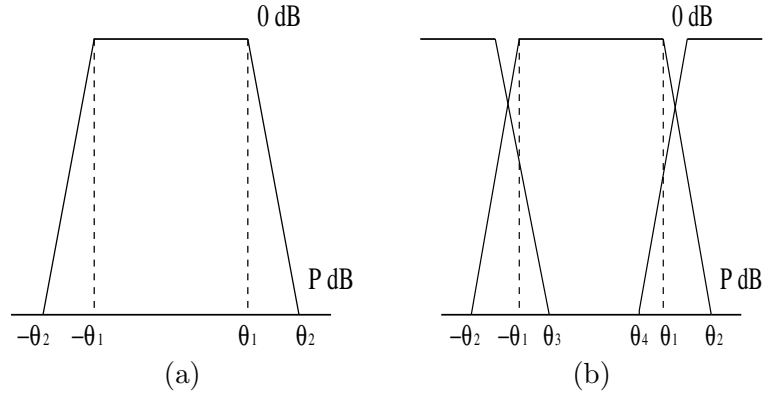


Fig. 3.1. (a) Uplink/Downlink Antenna Pattern Model-I (b) Intersector Interference Model

$-\theta_1$ ) with unity antenna gain and, all out-of-sector users' signals (users whose angular locations lie between  $-\theta_2$  and  $-\theta_1$  and  $\theta_1$  and  $\theta_2$ ) with attenuated antenna gain following the pattern in Figure 3.1. Increased number of out of sector users in between  $\theta_1$  and  $\theta_2$ ,  $-\theta_1$  and  $-\theta_2$  increase ISecI.

**Downlink ISecI Pattern:** The base station transmits users' signal through their assigned sector antennas as in Figure 3.1.b. When we look at a given sector area, we see that, each user experiences a different level of ISecI depending on the user's angular location. Users between  $\theta_3$  and  $\theta_4$  experience no ISecI, because adjacent sector antennas do not reach that region between  $\theta_3$  and  $\theta_4$ . On the other hand, users between  $-\theta_1$  and  $\theta_3$ ,  $\theta_4$  and  $\theta_1$  do experience ISecI. The level of ISecI these users experience depends on the side lobe antenna gain of the adjacent sectors. Clearly, users closer to the boundaries,  $-\theta_1$  or  $\theta_1$ , will experience more ISecI. Users whose angular locations lie in all neighbor sectors, i.e., sectors whose antenna reaches that region between  $-\theta_1$  and

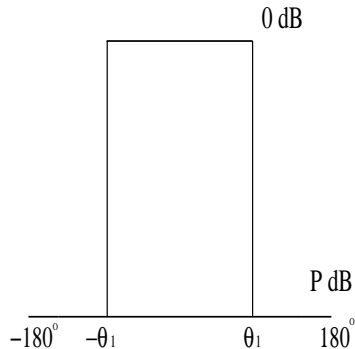


Fig. 3.2. Uplink/Downlink Antenna Pattern Model-II

$\theta_3$ , and,  $\theta_4$  and  $\theta_1$ , contribute to the ISeCI. Note that the uplink side lobe antenna gain for user  $i$  from out of sector interferer  $l$ ,  $v_{li}^{up}$  is a function of the angular location of out of sector interferer  $l$ . On the other hand, the downlink side lobe antenna gain for user  $i$  from out of sector interferer  $l$ ,  $v_{li}^{down}$  is a function of the angular location of user  $i$ . Consequently,  $v_{li}^{up}$  is different from  $v_{li}^{down}$  in general.

### 3.2.2 Antenna Pattern-II

We use antenna pattern shown in Figure 3.2 for transmission and reception at the base station. With this model, for both uplink and downlink, users within a sector between  $-\theta_1$  and  $\theta_1$  receive interference from all out-of-sector users with constant antenna gain  $P \text{ dB}$ . Thus,  $v_{li} = v_{il} = \text{Constant}$ .

### 3.2.3 System Model

A DS-CDMA cell with processing gain  $N$ , and  $K$  users is considered. The locations and the channels of the users in the cell are assumed to be known at the base station and will not change in the duration of interest. This is a reasonable assumption in a slow mobility environment or in fixed wireless systems. Our formulation will assume perfect channel knowledge. In the numerical results, we show the robustness of cell sectorization in the presence of channel estimation errors. We assume the cell is to be sectorized to  $M$  sectors.

**Uplink:** Given that the channels are perfectly acquired at the base station, without loss of generality, we assume single path synchronous channel for each user with non-orthogonal signatures. Asynchronous and multipath channel models can be easily accommodated in the appropriate discrete time model [60].

After chip matched filtering and sampling, the received signal vector for user  $i$  at the base station is

$$\mathbf{r}_i = \sqrt{p_i h_i} b_i \mathbf{s}_i + \sum_{j \neq i, j \in g_k(\underline{\theta})} \sqrt{p_j h_j} b_j \mathbf{s}_j + \sum_{l \notin g_k(\underline{\theta})} \sqrt{p_l h_l v_{li}} b_l \mathbf{s}_l + \mathbf{n} \quad (3.1)$$

where  $p_i$ ,  $h_i$ ,  $b_i$  are the transmit power, the channel gain, and the information bit for user  $i$ .  $\mathbf{s}_i$  is the signature sequence of length  $N$  for user  $i$ .  $\mathbf{n}$  denotes the zero-mean Gaussian noise vector with  $E(\mathbf{n}\mathbf{n}^\top) = \sigma^2 \mathbf{I}_N$ .  $\underline{\theta}$  is the  $N$ -tuple vector whose  $j$ th component denotes the main beam width for sector  $j$  in radians.  $g_k(\underline{\theta})$  is the set of users that reside in the area spanned by sector  $k$ . The second term in (3.1) represents the intra-sector interference, while the third term represents the ISecI.  $v_{li}$  is antenna gain between interferer  $l$  and

user  $i$ . If user  $i$  experiences no ISecI,  $v_{li} = 0$ . It is important to note that  $v_{li} \neq v_{il}$  for antenna model-I, that is the interference that two mutually out of sector terminals cause for each other may be different, depending on the antenna pattern and the users' locations. In particular, user  $l$  may lie within the receive range of the antenna serving the sector where user  $i$  resides, hence contribute to the ISecI for user  $i$ , while user  $i$  may reside outside the range of the receive antenna of the sector in which user  $l$  resides, not contributing to the ISecI for user  $l$ .

**Downlink:** In the downlink, we assume that each user has a multipath channel. This is because we would like to consider the general case where each user experiences (intra- and inter-sector) interference even if orthogonal sequences are used within each sector.

Following reference [28], the transmitted signal vector from the sector antenna  $k$  can be expressed as:

$$\mathbf{x} = \sum_{j \in g_k(\theta)} \sqrt{p_j} b_j \mathbf{s}_j \quad k = 1, \dots, K \quad (3.2)$$

where  $p_j$  and  $\mathbf{s}_j$  are the transmit power and the signature sequence the base station uses to transmit  $b_j$  to user  $j$ .

User  $i$  receives  $\mathbf{r}_i$  through the multipath channel  $\mathbf{G}_i$ , which is an  $N \times N$  matrix whose  $(i, j)$ th entry  $G_{ij}$  represents  $j$ th multipath gain for user  $i$ . We define the pathloss based channel gain for user  $i$ ,  $h_i$  as a separate quantity, that is, the overall channel response is a scalar multiple of  $\mathbf{G}_i$ . This model assumes that the multiple paths are chip synchronized, and the  $j$ th path represents the copy that arrives at the receiver with

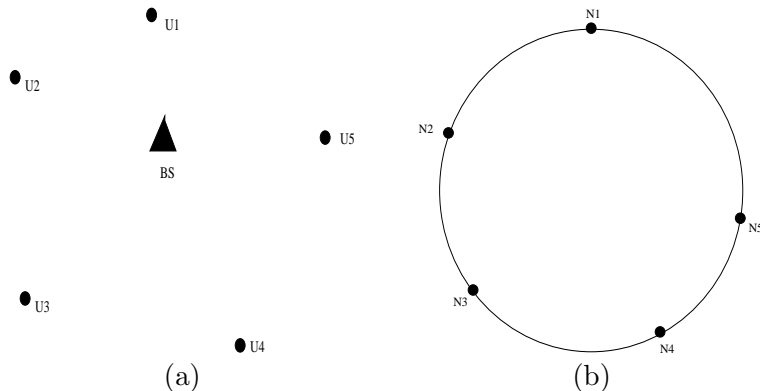


Fig. 3.3. (a) User locations in a cell (b) Ring network constructed from the user locations. Node  $N_i$  in the ring corresponds to user  $U_i$ .

a delay of  $j$  chips. We assume that the number of resolvable paths is less than the processing gain. We consider the bit duration as our observation interval, and ignore intersymbol interference for clarity of exposition. We compensate for this however, by normalizing the multipath gains of each user to unity, i.e.,  $\sum_{l=1}^N G_{il}^2 = 1$  for all  $i = 1, \dots, K$ . Let the signature of user  $j$  after going through the multipath channel of user  $i$  be  $\mathbf{s}_j^i = \mathbf{G}_i \mathbf{s}_j$ . Then, following the description of our model, the received signal for user  $i$  is given by

$$\mathbf{y}_i = \sqrt{p_i h_i} b_i \mathbf{s}_i^i + \sum_{j \neq i, j \in g_k(\varrho)} \sqrt{p_j h_i} b_j \mathbf{s}_j^i + \sum_{l \notin g_k(\varrho)} \sqrt{p_l h_i} v_{li} b_l \mathbf{s}_l^i + \mathbf{n}_i \quad (3.3)$$

where  $\mathbf{n}_i$  is the white Gaussian noise vector. Once again,  $v_{li}$  is antenna gain between interferer  $l$  and user  $i$ , and that  $v_{li} \neq v_{il}$  for antenna model-I, see Figure 3.1.

### 3.3 Problem Formulation

Our aim in this chapter is to improve the user capacity of the CDMA cell, i.e., increase the number of simultaneous users that achieve their quality of service requirements. This will be accomplished by employing jointly optimal power control, and multiuser detection, and designing variable width sectors that lead to the assignment of each user to its corresponding directional antenna. We consider the user capacity enhancement problem for both the uplink and the downlink. In each case, our metric is the transmit power expended in the cell, while guaranteeing each user with its minimum quality of service. A user is said to have an acceptable quality of service if its SIR is greater than or equal to a target SIR,  $\gamma^*$ . In the uplink, the minimum total transmit power minimization problem has the additional advantage of battery conservation for each user. In the downlink, the problem can be interpreted as one that yields strategies that can accommodate more simultaneous users for a given transmit power at the base station. In each case, we need to find non-negative power values and design the sectors such that the entire cell is covered. The corresponding transmit power optimization problem is given by

$$\begin{aligned}
 \min_{\underline{\theta}, \mathbf{p}, \mathbf{c}_i} \quad & \sum_{k=1}^K \sum_{i \in g_k(\underline{\theta})} p_i & (3.4) \\
 \text{s.t.} \quad & \text{SIR}_i = \frac{P_{i,S}}{P_{i,INTRA} + P_{i,INTER} + P_{i,NOISE}} \geq \gamma^* \quad i = 1, \dots, K \\
 & \mathbf{p} \geq \mathbf{0} \quad \mathbf{1}^\top \underline{\theta} = 2\pi
 \end{aligned}$$



where  $P_{i,S}$ ,  $P_{i,INTRA}$ ,  $P_{i,INTER}$  and  $P_{i,NOISE}$  represent the desired signal power, intra-sector interference power, inter-sector interference power, and the noise power, experienced by user  $i$ , respectively. Each of these terms will vary for uplink and downlink leading to the corresponding SIR expressions. In addition, the SIR is a function of the transmit powers and receiver filters that we will optimize over. A moments thought reveals that, the receiver filter of user  $i$  affects the SIR of user  $i$  only, and similar to the single sector joint power control and multiuser detection [57], the filter optimization can be moved to the SIR constraint:

$$\begin{aligned}
& \min_{\underline{\theta}, \mathbf{p}} \quad \sum_{k=1}^K \sum_{i \in g_k(\underline{\theta})} p_i & (3.5) \\
& \text{s.t.} \quad \max_{\mathbf{c}_i} \text{SIR}_i \geq \gamma^* \quad i = 1, \dots, K \\
& \quad \mathbf{p} \geq \mathbf{0} \quad \mathbf{1}^\top \underline{\theta} = 2\pi
\end{aligned}$$

For the uplink, the terms that contribute to the SIR expression for user  $i$  is found by filtering  $\mathbf{r}_i$  in (3.1) by the receiver filter of user  $i$ ,  $\mathbf{c}_i$ , leading to

$$\begin{aligned}
P_{i,S} &= p_i h_i (\mathbf{c}_i^\top \mathbf{s}_i)^2, & P_{i,INTRA} &= \sum_{j \neq i, j \in g_k(\underline{\theta})} p_j h_j (\mathbf{c}_i^\top \mathbf{s}_j)^2 \\
P_{i,INTER} &= \sum_{l \notin g_k(\underline{\theta})} p_l h_l v_{li} (\mathbf{c}_i^\top \mathbf{s}_l)^2, & P_{i,NOISE} &= \sigma^2 (\mathbf{c}_i^\top \mathbf{c}_i). & (3.6)
\end{aligned}$$

The transmit power optimization problem for the uplink (UTP) entails finding radial value of each directional antenna beam-width, the transmit power of each user, and the linear receiver filter for each user at the base station, in a jointly optimum fashion. It is

straightforward to see that, in this case, (3.5) becomes

$$\begin{aligned}
& \min_{\underline{\theta}, \mathbf{p}} \sum_{k=1}^K \sum_{i \in g_k(\underline{\theta})} p_i && \text{(UTP)} && (3.7) \\
& \text{s.t.} && p_i \geq \min_{\mathbf{c}_i} \frac{\gamma^* (\sum_{j \neq i, j \in g_k(\underline{\theta})} p_j h_j(\mathbf{c}_i^\top \mathbf{s}_j)^2 + \sum_{l \notin g_k(\underline{\theta})} p_l h_l v_{li} (\mathbf{c}_i^\top \mathbf{s}_l)^2 + \sigma^2 (\mathbf{c}_i^\top \mathbf{c}_i))}{h_i(\mathbf{c}_i^\top \mathbf{s}_i)^2} \\
& && \mathbf{p} \geq \mathbf{0} \quad \mathbf{1}^\top \underline{\theta} = 2\pi
\end{aligned}$$

For the downlink, the SIR for user  $i$  residing in sector  $k$  is found by filtering  $\mathbf{y}_i$  in (3.3), with user  $i$ 's receiver filter,  $\mathbf{c}_i$ , and includes contributions from intra- and inter-sector interference that arises from the base station's transmission to other users going through the multipath channel of user  $i$  as described in Section 3.2.3. This leads to

$$\begin{aligned}
P_{i,S} &= p_i h_i(\mathbf{c}_i^\top \mathbf{s}_i)^2, & P_{i,INTRA} &= \sum_{j \neq i, j \in g_k(\underline{\theta})} p_j h_i(\mathbf{c}_i^\top \mathbf{s}_j^i)^2 \\
P_{i,INTER} &= \sum_{l \notin g_k(\underline{\theta})} p_l h_i v_{li} (\mathbf{c}_i^\top \mathbf{s}_l^i)^2, & P_{i,NOISE} &= \sigma^2 (\mathbf{c}_i^\top \mathbf{c}_i). && (3.8)
\end{aligned}$$

The downlink transmit power optimization problem (DTP) becomes

$$\begin{aligned}
& \min_{\underline{\theta}, \mathbf{p}} \sum_{k=1}^K \sum_{i \in g_k(\underline{\theta})} p_i && \text{(DTP)} && (3.9) \\
& \text{s.t.} && p_i \geq \min_{\mathbf{c}_i} \frac{\gamma^* (\sum_{j \neq i, j \in g_k(\underline{\theta})} p_j h_i(\mathbf{c}_i^\top \mathbf{s}_j^i)^2 + \sum_{l \notin g_k(\underline{\theta})} p_l h_i v_{li} (\mathbf{c}_i^\top \mathbf{s}_l^i)^2 + \sigma^2 (\mathbf{c}_i^\top \mathbf{c}_i))}{h_i(\mathbf{c}_i^\top \mathbf{s}_i^i)^2} \\
& && \mathbf{p} \geq \mathbf{0} \quad \mathbf{1}^\top \underline{\theta} = 2\pi
\end{aligned}$$

where  $p_i$  represents the power transmitted by the base station to communicate to user  $i$ , and the cost function in (3.9) is the total power transmitted by the base station.

### 3.4 Uplink and Downlink Sectorization

Given the problem formulations in the previous section, a valid question to ask is whether the optimum sectorization arrangement would be identical both from the uplink and downlink perspective.

At the outset, by comparing UTP and DTP, one might believe that the optimum solutions should be identical. However, a closer look reveals that such a statement can be made only under a specific set of conditions. In particular, for a cellular system with no sectorization, it is well known that, if the base station for each user to maintain an acceptable level of SIR is fixed and given, under the assumption of identical channel gains for uplink and downlink between each user and base station, the condition for feasibility of the uplink and the downlink power control problems is the same [37, 46]. Further, reference [46] shows that, in this case, the optimum total transmit power of all users (uplink) is identical to the optimum total transmit power of all base stations (downlink).

Let us consider a similar scenario for the system model we have at hand. Consider the case, where there is no ISecI, i.e., each sector is perfectly isolated. Assume that matched filter receivers are used, i.e., no receiver filter optimization is done. We note that this scenario, in the uplink, is a slightly more general model than that of reference [51], in that we assume arbitrarily correlated sequences as opposed to pseudo-random sequences. Also, assume that the signature sequence for each user is identical to the downlink signature used to transmit to this user from a single path channel. Uplink and

downlink channel gain between a user and the base station, and noise power values at all receivers are also identical. We will call this setting a “symmetric system”. Note that in this case, the UTP and DTP becomes

$$\begin{aligned} \min_{\underline{\theta}, \mathbf{p}} \quad & \sum_{k=1}^K \sum_{i \in g_k(\underline{\theta})} p_i & (3.10) \\ \text{s.t.} \quad & \frac{p_i h_i}{\sum_{j \neq i, j \in g_k(\underline{\theta})} p_j h_j (\mathbf{s}_i^\top \mathbf{s}_j)^2 + \sigma^2} \geq \gamma^*, \quad i = 1, \dots, K \end{aligned}$$

$$\begin{aligned} \min_{\underline{\theta}, \mathbf{p}} \quad & \sum_{k=1}^K \sum_{i \in g_k(\underline{\theta})} q_i & (3.11) \\ \text{s.t.} \quad & \frac{q_i h_i}{\sum_{j \neq i, j \in g_k(\underline{\theta})} q_j h_j (\mathbf{s}_i^\top \mathbf{s}_j)^2 + \sigma^2} \geq \gamma^* \quad i = 1, \dots, K \end{aligned}$$

where we denoted the downlink power used to transmit to user  $i$  as  $q_i$  to distinguish from the uplink power user  $i$  transmits with  $p_i$ . Noting that the minimum transmit power is achieved when the SIR constraints are satisfied with equality [64, 28], we first make the following observation:

**OBSERVATION 3.1.** *For the symmetric system, under a given sectorization arrangement, the minimum total sector transmit powers for uplink/downlink are equal.*

**Proof:** The proof of this observation is straight forward using simple linear algebra and is given in the Appendix.  $\square$

An immediate corollary of the above observation is that the total *cell transmit power* for uplink and downlink are equal for any given sectorization arrangement. We can now make the following observation.

**OBSERVATION 3.2.** *If under a given sectorization arrangement, the minimum total transmit power for uplink and downlink are identical, then the optimum sectorization arrangements in terms of minimum transmit power for uplink and downlink are also identical.*

**Proof:** Assume that the observation is false. Let  $\{g_k(\underline{\theta}_1)\}_{k=1,\dots,M}$  be optimum uplink sectorization arrangement and,  $\{g_k(\underline{\theta}_2)\}_{k=1,\dots,M}$ , where  $\underline{\theta}_2 \neq \underline{\theta}_1$  is the optimum downlink sectorization arrangement. Since the cell total transmit powers for uplink and downlink are identical, we have

$$\sum_{k=1}^M \sum_{i \in g_k(\underline{\theta}_1)} p_i = \sum_{k=1}^M \sum_{i \in g_k(\underline{\theta}_1)} q_i > \sum_{k=1}^M \sum_{i \in g_k(\underline{\theta}_2)} q_i = \sum_{k=1}^M \sum_{i \in g_k(\underline{\theta}_2)} p_i \quad (3.12)$$

which implies  $\{g_k(\underline{\theta}_1)\}_{k=1,\dots,M}$  can not be optimum uplink sectorization arrangement. Therefore, we have shown by contradiction that, the uplink and downlink optimum sectorization arrangement have to be identical.  $\square$

We note that Observation 4.2 is independent of the symmetry assumptions and a general statement. However, for the statement to be true, we need the equivalence of the uplink and downlink total transmit power values. The symmetric system is one for which this is guaranteed, and consequently we can easily claim the converse of Observation 4.2 is also true.

We have seen that, under a set of system assumptions, we can hope to have same optimum sectorization arrangement for the uplink and downlink. Such a scenario would simplify the calculation of the optimum transmit powers for the downlink once the uplink sectorization problem is solved. Unfortunately, once we introduce the receiver filter optimization to the problem, i.e., as in UTP (3.7) and DTP (3.9), we can no longer guarantee the validity of observation 4.1 even under reciprocal channel gains and signature sequences. The reason for this is that the resulting receiver filters are a function of the received power values [57]. In addition, in cases where we must take into account the inter-sector-interference, as explained in Section 3.2.3, the fact that the ISecI one user causes to another user is not reciprocal, i.e.,  $v_{li} \neq v_{il}$ , and the fact that  $v_{li}^{up} \neq v_{li}^{down}$  prevent us from claiming that the sectorization arrangement would be identical in general. Hence, we conclude that in general each direction should be optimized separately, by solving UTP and DTP. In the numerical results section, we will see by an example that, the resulting sectorization arrangements in each direction are different.

### 3.5 Optimum Sectorization

The previous sections have formulated UTP and DTP and argued that in the most general formulation, they each lead to different sectorization arrangements. In this section, we will describe how to obtain the optimum solution.

We first note that, unlike the case where each sector is perfectly isolated, i.e., the no ISecI case, we can not consider each sector independently, and that we need to run “cell-wide” power control.

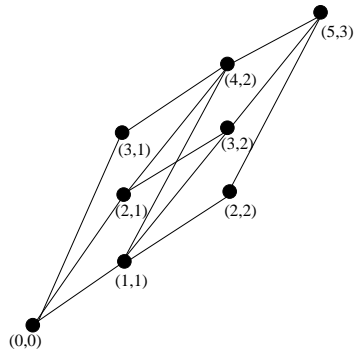


Fig. 3.4. The network constructed for  $K = 5$  users, and  $M = 3$  sectors.

Although for each sectorization pattern, there is an iterative algorithm that is guaranteed to converge to the optimum powers and receiver filters as will be described shortly, there is no simple algorithm to choose the best sectorization arrangement. Hence, to find the jointly optimum sectorization arrangement, receiver filters and transmit powers for all users in the cell, we need to consider all sectorization arrangements for which the corresponding grouping of users yield a feasible power control problem.

We note that, the difference of the sectorization problem, from the channel allocation/scheduling type problems that have exponential complexity in the number of users [19] is the fact that, in the sectorization problem, the number of possible grouping of users is limited due to the physical constraints, that is their angular positions in the cell. Similar to [51], we can represent the system by a graph that is a ring, where each user's angular position in the cell is mapped to the same angular position on the ring (Figure 3.3). It is easy to see that the number of all possible sectorization arrangements is  $\binom{K}{M}$ .

For each feasible sectorization arrangement, an iterative algorithm that finds the minimum power solution along with the best linear filters is easily obtained as outlined below. Consider the minimum total power solution, given a feasible sectorization arrangement. Define the power vector for all users in the cell

$$\mathbf{p} = [p_1, \dots, p_{K_1}, p_1, \dots, p_{K_2}, \dots, p_1, \dots, p_{K_M}]$$

where  $K_i$  is number of user in the sector  $i$ , and

$$I_{ki}(\mathbf{p}, \mathbf{c}_i) = \frac{\gamma^*(P_{i,INTRA} + P_{i,INTER} + P_{i,NOISE})}{h_i(\mathbf{c}_i^\top \mathbf{s}_i)^2} \quad (\mathbf{IF-UTP}) \quad (3.13)$$

for the uplink and

$$I_{ki}(\mathbf{p}, \mathbf{c}_i) = \frac{\gamma^*(P_{i,INTRA} + P_{i,INTER} + P_{i,NOISE})}{h_i(\mathbf{c}_i^\top \mathbf{G}_i \mathbf{s}_i)^2} \quad (\mathbf{IF-DTP}) \quad (3.14)$$

for the downlink. We define the interference function  $I(\mathbf{p})$  as

$$I_{ki}(\mathbf{p}) = \min_{\mathbf{c}_i} I_{ki}(\mathbf{p}, \mathbf{c}_i) \quad (3.15)$$

$$\mathbf{I}(\mathbf{p}) = [I_{11}(\mathbf{p}), \dots, I_{1K_1}(\mathbf{p}), \dots, I_{M1}(\mathbf{p}), \dots, I_{MK_M}(\mathbf{p})]. \quad (3.16)$$

Reference [64] showed that power control algorithms in the form of  $\mathbf{p}(n+1) = \mathbf{I}(\mathbf{p}(n))$  converge to the minimum power solution if  $\mathbf{I}(\mathbf{p})$  is a standard interference function. The proof that (3.16) is a standard interference function follows directly from the proof given in reference [57] for single-sector systems. The resulting power control algorithm first



finds the receiver filter for user  $i$  to be the MMSE filter for fixed power vector:

$$\text{(U-PC)} \quad \mathbf{A}_{ki}(\mathbf{p}(n)) = \sum_{j \neq i, j \in g_k(\varrho)} p_j h_j \mathbf{s}_j \mathbf{s}_j^\top + \sum_{l \notin g_k(\varrho)} p_l h_l v_{li} \mathbf{s}_l \mathbf{s}_l^\top + \sigma^2 \mathbf{I} \quad (3.17)$$

$$\mathbf{c}_i = \frac{\sqrt{p_i(n)}}{1 + p_i(n) \mathbf{s}_i^\top \mathbf{A}_{ki}^{-1}(\mathbf{p}(n)) \mathbf{s}_i} \mathbf{A}_{ki}^{-1}(\mathbf{p}(n)) \mathbf{s}_i. \quad (3.18)$$

for the uplink and

$$\text{(D-PC)} \quad \mathbf{A}_{ki}(\mathbf{p}(n)) = \sum_{j \neq i, j \in g_k(\varrho)} p_j h_i (\mathbf{s}_j^i) (\mathbf{s}_j^i)^\top + \sum_{l \notin g_k(\varrho)} p_l h_i v_{li} (\mathbf{s}_l^i) (\mathbf{s}_l^i)^\top + \sigma^2 \mathbf{I} \quad (3.19)$$

$$\mathbf{c}_i = \frac{\sqrt{p_i(n)}}{1 + p_i(n) (\mathbf{s}_i^i)^\top \mathbf{A}_{ki}^{-1}(\mathbf{p}(n)) (\mathbf{s}_i^i)} \mathbf{A}_{ki}^{-1}(\mathbf{p}(n)) (\mathbf{s}_i^i) \quad (3.20)$$

for the downlink. The power for user  $i$  is then adjusted to meet the SIR constraint:

$$\mathbf{p}(n+1) = \mathbf{I}(\mathbf{p}(n)). \quad (3.21)$$

We should note that due to the presence of ISecI, the iterative power control algorithms that are run in each sector for a given arrangement interact with each other. However, cell-wide convergence is guaranteed no matter which order the sector power updates are executed thanks to the asynchronous convergence theorem in [64]. We also note that the resulting MMSE filters suppresses both the intra-sector interference and the ISecI that each user experiences.

When the number of feasible sectorization arrangements is  $S_f$ , the jointly optimum sectorization arrangement, power control and receiver filters are found by the following algorithm:

1. For  $l = 1, \dots, S_f$ : for sectorization arrangement  $l$ , find the minimum total transmit power,  $TP_l$  using the MMSE power control algorithm described above.
2. Choose the sectorization arrangement that yields  $\min_l TP_l$ , along with the corresponding transmit power values and receiver filters found in step 1.

As explained before, the number of feasible sectorization arrangements,  $S_f \leq \binom{K}{M}$ . Thus, the number of power control algorithms to be run is  $O(MK^M)$ . In practice, however, the number of feasible scenarios can be significantly smaller. We note that cells that are heavily loaded are ones that would significantly benefit from employing several interference management techniques in a jointly optimum fashion. In such cases, it is unlikely that, sectorization arrangements where a small fraction of the sectors serving most of the users would turn out to be infeasible, i.e., not all users can achieve their target SIR. Also, physical constraints of the directional sector antennas typically impose a minimum angular separation constraint between users, and a minimum and a maximum sector angle constraint. Nevertheless, when the number of users/sectors is relatively large, we may opt to look for solutions with reduced complexity that result in near optimum performance. Such algorithms are presented next.

## 3.6 Near-Optimum Sectorization

### 3.6.1 Ignoring ISecI

If the directional antenna patterns have a fast decay for the out of sector range, the amount of ISecI experienced by a user would be small as compared to intra-sector interference. In such cases, sectorizing the cell by ignoring the inter-sector interference is expected to perform close to the optimum.

Ignoring the existence of ISecI leads to perfectly isolated sectors, as considered in [51]. In this case, as reference [51] shows, the sectorization problem can be converted to a shortest path problem on a network that is constructed from the string that is obtained from breaking the ring in Figure 3.1 between any two nodes.  $K$  such shortest path problems should be solved each of which has complexity  $O(MK^2)$ . Reference [40] showed that in the special case where equi-correlated signature sequences are used, a closed form expression for sector received power exists for UTP, and the weight of each edge of the network can be calculated readily. However, for arbitrary signature sequences, as we consider here, the calculation of each weight entails, running the iterative power control algorithm, U-PC or D-PC. Thus, the sectorization complexity is reduced only when  $M > 3$ .

### 3.6.2 Variations on equal loading

An intuitively pleasing and simple solution is to design sectors such that an equal number of users reside in each sector. The intuition behind is to try to equalize the “load” per sector as much as possible. The angular boundaries of sectors are determined

such that, equal number of users reside in each sector with respect to a reference point. Next, the corresponding power transmit power values and receiver filters are found via running the power control algorithm described in Section 3.5. This process has to be repeated  $\lceil \frac{K}{M} \rceil$  times by shifting the reference point with  $0^\circ$  angle to the next user from the previous reference point. The sectorization arrangement with minimum total transmit power is selected as the best “equal number of users per sector solution”.

When the terminal distribution is uniform, equal load per sector solution is expected to work well. However, as the terminal distribution becomes nonuniform, equal load per sector solution needs to be improved to achieve near optimum performance. We have observed that the following algorithm improves the equal load per sector solution and works near-optimum in a range of scenarios. Once the equal load per sector solution that yields the minimum (cell) total power is found, we move the boundaries of the sector with *the minimum total power* to include users from neighboring cells, in an effort to try to shift a user that may cause substantial increase in sector power, to the neighboring sector that has the least power expenditure. Specifically, we try to maximize the minimum  $P_k$ , where  $P_k$  is the sector received power in the uplink case, or the sector transmit power in the downlink case for the  $k$ th sector antenna. Although it is difficult to draw general conclusions for a system with no particular channel or signature set structure, we find that running a couple of the above iterations improved the performance in all our simulation scenarios considerably as compared to equal number of users per sector, and performed near optimum.

## 3.7 Numerical Results

### 3.7.1 Perfect Channel Estimation

We consider a heavily loaded CDMA cell with processing gain  $N = 16$  and number of users  $K = 25$ . We assume a single path for the uplink and three paths for the downlink. In the multipath model, the delay of the first path  $\tau_{i1}$  is set to 0. For all other channel taps, each successive tap is delayed by either 1 or 2 chips, with probability  $\frac{1}{2}$ , i.e., the delay spread is at most 4 chips. The channel tap difference between two successive tap gains is  $|A|$  dB where  $A \sim \mathcal{N}(0, 20)$ . The cell is to be partitioned to  $M = 6$  sectors. In the antenna pattern model-I, we set  $\theta_2 - \theta_1 = 15^\circ$ ,  $P = -10$ dB, and the maximum angle constraint ( $\max(2\theta_1)$ ) =  $120^\circ$ . Similarly, we set  $P = -10$ dB in the antenna pattern model-II. We assume no channel estimation error in this section.

We first consider the case with antenna pattern model-I. The numerical results demonstrate the performance of optimum sectorization (OS), sectorization done ignoring the ISecI as explained in Section 3.6.1 (NOS-1), sectorization done using the algorithm described in Section 3.6.2 (NOS-2). To assess the benefit of adaptive uplink and downlink cell sectorization with multiuser detection (receiver filter optimization), we compared our results with (i) conventional sectorization (equal angular partition) when the base station (for the uplink) or each terminal (for the downlink) employs MMSE multiuser detection (EAP), and (ii) adaptive optimum sectorization when the base station or each terminal uses matched filters (AMF). For clarity of presentation of our results, we number all  $K$  users in the cell, in order of increasing angular distance from a reference line. In the tables we present, “the sector arrangement” identifies the users that belong to each sector.

Sector arrangement  $(K_1 K_2 \cdots K_M)$  corresponds to sector 1:(user  $K_1, \cdots, K_2-1$ ), sector 2:(user  $K_2, \cdots, K_3-1$ ), ..., sector  $M$ : (user  $K_M, \cdots, K, 1, \cdots, K_1-1$ ).

Our first set of numerical results aim to show the difference between the optimum sectorization arrangements for uplink and downlink. Figures 3.5 and 3.6 show the optimum sectorization for uplink and downlink with random signatures and single path, for uniform and nonuniform user distributions over the cell. Tables 3.1 and 3.2 show the corresponding optimum total transmit power values. They also tabulate the resulting transmit powers for uplink when downlink OS arrangement is used, and for downlink when uplink OS arrangement is used. As expected, the optimum arrangements are different.

Figures 3.7, 3.8, 3.9, and 3.10 show uplink and downlink sector boundaries for uniform and nonuniform user distributions, respectively. Tables 3.3, 3.4, 3.5 and 3.6 show the total transmit power and sectorization arrangement of the optimum sectorization (OS), NOS-1 and NOS-2 in uniform and nonuniform distribution, respectively. It is seen that the optimum, as well as near-optimum algorithms we proposed, outperform EAP and AMF; that is, employing all three interference management methods, power control, receiver filter optimization and adaptive sectorization jointly, results in better performance than both employing power control and receiver optimization (EAP), and power control and adaptive sectorization with matched filters (AMF). In fact, AMF [51] returns a feasible solution only for the downlink uniform distribution example. As expected, for uniform user distribution, equal number of users per sector solution works well with the added advantage of MMSE receiver filters to suppress intra- and inter-sector interference. However, for nonuniform user distribution, EAP has poor performance and

requires about 3dB more transmit power than OS for the uplink (Table 3.4). Lastly, we note that, NOS-2, the computationally simplest of the three algorithms we propose, generally performs near optimum and better than NOS-1. NOS-1, which simply ignores the ISecI, also has good performance, at the expense of computational complexity that may not be much lower than that of OS. The degree of suboptimality of NOS-1 is strictly a function of the antenna patterns, i.e., the smaller the out of sector range of the directional antenna (fast decay of side lobes), the closer NOS-1 will perform to OS.

We then consider the case with antenna pattern model-II. Similar to antenna pattern model-I, we compared the performances of OS, NOS-I, NOS-II, EAP, and AMF for uplink and downlink in tables 3.7, 3.8, 3.9, and 3.10. Since all out of sector users cause ISecI, more transmit power is required to compensate for additional ISecI. Hence, total transmit power with antenna pattern-II is higher than that with antenna pattern-I.

### 3.7.2 Channel Estimation Error

The adaptive cell sectorization concept relies on the fact that users' channels/physical locations are known. Hence, it is appropriate to investigate the robustness of the methods against channel estimation errors. In this section, we provide numerical results to show the robustness of optimum sectorization against Gaussian channel estimation errors. Estimated pathloss gain  $\hat{h}$  is modeled as

$$\hat{h} = h + e; \quad \frac{E(\hat{h} - h)^2}{h^2} = \sigma_h^2. \quad (3.22)$$

where  $h$  is the true channel gain and  $E(e) = 0$ . Figures 3.11 show Probability(SIR  $>$   $\gamma^*$ ) vs. target SIR in MMSE power control, for uplink and downlink, respectively. The target SIR in MMSE power control (TSIR) is the actual target SIR value used in the power control algorithms U-PC and D-PC, whereas  $\gamma^*$  is the minimum QoS requirement for reliable communication. In the presence of estimation errors, TSIR should be chosen such that, the original target for reliable communication  $\gamma^*$  should be achieved most of the time. Hence, TSIR should include a margin to compensate for channel estimation errors. We set TSIR to the value that satisfies Probability(SIR  $>$   $\gamma^*$ )=0.9 in Figures 3.11 and term it *effective target SIR*,  $\bar{\gamma}$ . Tables 3.11 and 3.12 show the resulting total transmit power for different  $\sigma_h^2$  values. Figures 3.13, 3.14 show the convergence of the SIR for each user for  $\sigma_h^2 = 0.001$  and  $\sigma_h^2 = 0.01$ , respectively. As expected, increased normalized estimation error variance causes the total minimum transmit power to increase. Table 3.13 shows the robustness of optimum sectorization against Gaussian channel estimation error. The percentages shown represent the percentages of channel estimation error realizations that yield the same optimum adaptive cell sectorization arrangement as the ones that use the perfect channel estimates. For example, at  $\sigma_h^2 = 0.01$  for nonuniform distribution, for 99.9% of the time, the optimum sectorization arrangement does not change. It is observed that the scenario with the uniform distribution of users is more vulnerable to estimation errors as compared to the nonuniform distribution. This may be attributed to the fact that, when the users are uniformly distributed in the cell, the number of feasible sectorization arrangements is a lot higher than the case of nonuniform distribution. However, note that, in general, the cases of nonuniform user distribution,



which appears to be fairly robust to estimation errors, is of interest, since adaptive sectorization is more beneficial in such scenarios.

### 3.8 Conclusion

In this chapter, we considered the joint optimization problem of cell sectorization, transmit power control and linear receiver filters, and provided a comprehensive study for CDMA cells where the base station is equipped with variable beam-width directional antennas, and the base station (for uplink) and the terminals (for downlink) have the ability to perform linear multiuser detection. We formulated the problems for uplink and downlink for arbitrary signature sequences and, observed that, in general, the resulting sectorization arrangements that optimize the uplink user capacity would be different from the downlink. We proposed algorithms that would find the optimum solution, as well as near-optimum solutions with reduced complexity. Numerical results confirm that intelligently combining power control, receiver filter design and cell sectorization lead to improved uplink and downlink user capacity as compared to employing one or a couple of these interference management methods. That is, the cell can serve more simultaneous users with the same resources. We also numerically tested the robustness of cell sectorization arrangements against channel gain estimation errors and found that, for a range of scenarios of interest, the optimum sectorization arrangement stays the same, and we can compensate for channel estimation errors by a slight elevation in the total transmit power.

In conclusion, although exploring the interactions of the three interference management methods considered in this chapter, power control, sectorization, and multiuser

detection, requires more complexity on system design as compared to an unoptimized system, the improvement in user capacity that is achieved may very well justify the additional complexity. This is true especially for slowly changing environments where channel gains and user activity status do not change frequently.

### 3.9 Appendix-I

Uplink transmit power is minimized when the SIR constraint in (3.10) is achieved with equality for all users, that is

$$\begin{bmatrix} (\mathbf{s}_1^\top \mathbf{s}_1)^2 & -\gamma^*(\mathbf{s}_1^\top \mathbf{s}_2)^2 & \cdot & -\gamma^*(\mathbf{s}_1^\top \mathbf{s}_K)^2 \\ -\gamma^*(\mathbf{s}_2^\top \mathbf{s}_1)^2 & (\mathbf{s}_2^\top \mathbf{s}_2)^2 & \cdot & -\gamma^*(\mathbf{s}_2^\top \mathbf{s}_K)^2 \\ \cdot & \cdot & \cdot & \cdot \\ -\gamma^*(\mathbf{s}_K^\top \mathbf{s}_1)^2 & -\gamma^*(\mathbf{s}_K^\top \mathbf{s}_2)^2 & \cdot & (\mathbf{s}_K^\top \mathbf{s}_K)^2 \end{bmatrix} \begin{bmatrix} p_1 h_1 \\ p_2 h_2 \\ \cdot \\ p_K h_K \end{bmatrix} = \begin{bmatrix} \gamma^* \sigma^2 (\mathbf{s}_1^\top \mathbf{s}_1) \\ \gamma^* \sigma^2 (\mathbf{s}_2^\top \mathbf{s}_2) \\ \cdot \\ \gamma^* \sigma^2 (\mathbf{s}_K^\top \mathbf{s}_K) \end{bmatrix}. \quad (3.23)$$

Equation (3.23) has the form:

$$[\mathbf{I} - \gamma^* \mathbf{F}] \mathbf{p}_r = \gamma^* \sigma^2 \mathbf{1} \quad (3.24)$$

where  $\mathbf{p}_r = [p_1 h_1 p_2 h_2 \cdots p_K h_K]^\top$  is the uplink received power vector. Note that  $\mathbf{s}_i^\top \mathbf{s}_i = 1$  due to the assumption of unit energy signatures.  $\mathbf{F}$  is the squared crosscorrelation matrix whose diagonal entries are zeros. A nonnegative solution  $\mathbf{p}_r$  exists if and only if the Perron-Frobenius eigenvalue of  $\mathbf{F}$  is less than  $\frac{1}{\gamma^*}$  [4]. The solution is

$$\mathbf{p}_r = \gamma^* \sigma^2 [\mathbf{I} - \gamma^* \mathbf{F}]^{-1} \mathbf{1} = \gamma^* \sigma^2 \mathbf{A} \mathbf{1} \quad (3.25)$$

Observe that, since  $\mathbf{F}$  is symmetric,  $\mathbf{A}$  is symmetric, i.e.,  $A_{ij} = A_{ji}$ . The optimum transmit power value for user  $i$  is

$$p_i = \frac{\gamma^* \sigma^2}{h_i} \sum_j A_{ij} \quad i = 1, \dots, K \quad (3.26)$$

and the total minimum sector transmit power is

$$\sum_i p_i = \gamma^* \sigma^2 \sum_i \frac{1}{h_i} \sum_j A_{ij} \quad i, j = 1, \dots, K. \quad (3.27)$$

For the downlink, we also have to satisfy all SIR constraints with equality leading to the matrix equation:

$$\begin{bmatrix} (\mathbf{s}_1^\top \mathbf{s}_1)^2 & -\gamma^* (\mathbf{s}_1^\top \mathbf{s}_2)^2 & \cdot & -\gamma^* (\mathbf{s}_1^\top \mathbf{s}_K)^2 \\ -\gamma^* (\mathbf{s}_2^\top \mathbf{s}_1)^2 & (\mathbf{s}_2^\top \mathbf{s}_2)^2 & \cdot & -\gamma^* (\mathbf{s}_2^\top \mathbf{s}_K)^2 \\ \cdot & \cdot & \cdot & \cdot \\ -\gamma^* (\mathbf{s}_K^\top \mathbf{s}_1)^2 & -\gamma^* (\mathbf{s}_K^\top \mathbf{s}_2)^2 & \cdot & (\mathbf{s}_K^\top \mathbf{s}_K)^2 \end{bmatrix} \begin{bmatrix} q_1 \\ q_2 \\ \cdot \\ q_K \end{bmatrix} = \begin{bmatrix} \frac{\gamma^* \sigma^2 (\mathbf{s}_1^\top \mathbf{s}_1)}{h_1} \\ \frac{\gamma^* \sigma^2 (\mathbf{s}_2^\top \mathbf{s}_2)}{h_2} \\ \cdot \\ \frac{\gamma^* \sigma^2 (\mathbf{s}_K^\top \mathbf{s}_K)}{h_K} \end{bmatrix}. \quad (3.28)$$

Defining  $\mathbf{u} = [1/h_1 \ 1/h_2 \ \dots \ 1/h_K]^\top$ , the solution for the optimum downlink powers is

$$\mathbf{q} = \gamma^* \sigma^2 [\mathbf{I} - \gamma^* \mathbf{F}]^{-1} \mathbf{u} = \gamma^* \sigma^2 \mathbf{A} \mathbf{u} \quad (3.29)$$

The downlink transmit power for user  $i$  is

$$q_i = \gamma^* \sigma^2 \sum_j \frac{A_{ij}}{h_j}. \quad (3.30)$$

The total minimum downlink sector power is

$$\sum_i q_i = \gamma^* \sigma^2 \sum_i \sum_j \frac{A_{ij}}{h_j} = \gamma^* \sigma^2 \sum_j \frac{1}{h_j} \sum_i A_{ij}. \quad (3.31)$$

Therefore,

$$\sum_i p_i = \sum_i q_i \quad (3.32)$$

because  $A_{ij} = A_{ji}$ .

### 3.10 Appendix-II: Adaptive Cell Sectorization: Joint Transmit and Receiver filter Design

By knowing that further capacity improvement is possible by jointly optimizing transmit filter, receiver filter, cell sectorization, and transmit power, we formulate the optimization problem. Perfect antenna pattern is assumed for simplicity of analysis.

We find non-negative power values, transmit filters (signature sets), receiver filters, and sectorization arrangement such that the total transmit power is minimized, while all users in a cell satisfy the quality of service which is defined as the target SIR.

The corresponding joint optimization problem is formulated as:

$$\begin{aligned} \min_{\underline{\theta}, \mathbf{p}, \mathbf{c}_i, \mathbf{s}_i} \quad & \sum_{k=1}^M \sum_{i \in g_k(\underline{\theta})} p_i \\ \text{s.t.} \quad & \text{SIR}_i \geq \gamma^* \quad i = 1, \dots, K \\ & \mathbf{p} \geq \mathbf{0} \quad \mathbf{1}^\top \underline{\theta} = 2\pi \end{aligned} \quad (3.33)$$

The  $SIR_i$  is a function of the transmit powers, signature sequence set and receiver filters that we will optimize over.

Under the perfect antenna pattern, for any given sectorization arrangement, power level, signature, and receiver filter of any user in one sector do not affect the performance of users in other sectors. In other words, each sector is independently optimized. Thus we consider any one sector for a given sectorization arrangement.

When the number of users  $K_i$  in  $k$ th sector is less than the processing gain  $N$ , the optimum solution is to assign the orthogonal signature set to users in a sector. Accordingly, the optimum receiver filter is the matched filter. In this case, each user does not create interference to other users in a sector, i.e., single user transmission

When the number of users in a sector is larger than the processing gain, i.e., large system, the number of orthogonal signature set is not enough to support all users in a sector. Recent research efforts [61, 59, 58] have considered the signature set optimization problem. In [61], it is shown that the optimum signature set and receiver filter are WBE sequence set and MMSE filter, when  $K_i > N$ . In [59, 58], the iterative algorithm to find the optimum sequence set has been considered. Each user takes MMSE filter as a signature sequence and as a receiver filter. The results of this iterative algorithm are WBE sequences as an optimum signature set and matched filter as an optimum receiver. We rely on this result to solve our optimization problem over power, signature sets and receiver filters. Starting from random signature set and initial equal power value, the iterative algorithm in reference [59, 58] generates WBE sequences set. With this WBE

signature sets and equal received power  $p$ ,  $SIR$  for user  $i$  is given by [61] :

$$SIR_i = \frac{p}{\frac{K_i - N}{N}p + \sigma^2} \quad (3.34)$$

For a given target SIR  $\gamma^*$ , the equal power is given by [61]

$$p = \frac{\sigma^2}{1 + \frac{1}{\gamma^*} - \frac{K_i}{N}} \quad (3.35)$$

Therefore, the optimization problem above can be transformed as follows:

$$\min_{\underline{\theta}, \mathbf{P},} \quad \sum_{k=1}^M q_k^* \sum_{i \in g_k(\underline{\theta})} \frac{1}{h_i} \quad (3.36)$$

$$q_k^* = \sigma^2 \gamma^* \quad \text{when } |g_k(\underline{\theta})| \leq N \quad (3.37)$$

$$q_k^* = \frac{\sigma^2}{1 + \frac{1}{\gamma^*} - \frac{K_i}{N}} \quad \text{when } |g_k(\underline{\theta})| > N \quad (3.38)$$

When  $K_i > N$ , optimum signature set is WBE sequences and optimum receiver filter is matched filter. When  $|g_k(\underline{\theta})| \leq N$ , optimum signature set is orthogonal signature set and optimum receiver filter is matched filter.

The optimization problem above has the same form as that in chapter 2. The optimum problem above is solved by a shortest path algorithm.

We consider  $M = 3$  sectors, processing gain  $N = 16$ . We consider two cases,  $K = 50$ , i.e., loaded system ( $K > N \times M$ ) and  $K = 30$ , i.e., unloaded system ( $K < N \times M$ ).

We compare the performance of this method with jointly transmit and receiver filter optimization (TR) with that of method with receiver filter optimization only (RO) in tables 3.14, 3.15.

For unloaded case, method with TR has power saving about 70%, 50% for uniform and nonuniform distribution, respectively.

For loaded case, the method with RO is infeasible, while the method with TR can support users larger than processing gain. This shows the benefit of method with TR over method with RO.

Table 3.1. Results for the system in Figure 3.5. Total transmit power is in WATTS

Method	Total Trans. Power	Sector Arrangement
Uplink with uplink OS	1.7872	3 8 10 17 20 23
Uplink with downlink OS	2.2096	1 8 13 18 19 23
Downlink with downlink OS	2.5114	1 8 13 18 19 23
Downlink with uplink OS	2.5823	3 8 10 17 20 23

Table 3.2. Results for the system in Figure 3.6

Method	Total Trans. Power	Sector Arrangement
Uplink with uplink OS	9.1039	3 6 13 15 21 25
Uplink with downlink OS	10.1200	1 5 6 13 15 21
Downlink with downlink OS	10.8223	1 5 6 13 15 21
Downlink with uplink OS	10.8537	3 6 13 15 21 25



Table 3.3. Results for the system in Figure 3.7

Method	Total Trans. Power	Sector Arrangement
OS	1.7812	3 8 10 17 20 23
NOS-1	2.114	3 6 10 15 21 24
NOS-2	1.8622	3 8 10 15 19 23
EAP	2.2532	1 6 8 15 20 23
AMF		Infeasible

Table 3.4. Results for the system in Figure 3.8

Method	Total Trans. Power	Sector Arrangement
OS	9.1039	3 6 13 15 21 25
NOS-1	12.4404	3 8 10 15 19 24
NOS-2	10.5815	2 6 10 13 18 21
EAP	20.6124	1 3 5 7 20 25
AMF		Infeasible

Table 3.5. Results for the system in Figure 3.9

Method	Total Trans. Power	Sector Arrangement
OS	2.5114	1 8 13 18 19 23
NOS-1	2.5457	1 8 12 18 19 24
NOS-2	2.5300	1 8 10 13 18 22
EAP	2.5977	1 6 8 15 20 23
AMF	2.8262	1 6 10 17 19 23

Table 3.6. Results for the system in Figure 3.10

Method	Total Trans. Power	Sector Arrangement
OS	10.8223	1 5 6 13 15 21
NOS-1	11.7079	1 3 8 10 17 20
NOS-2	10.9893	1 5 8 13 17 21
EAP	13.7195	1 3 5 7 20 25
AMF		Infeasible

Table 3.7. Uplink of a CDMA system with uniform user distribution. Antenna pattern-

II

Method	Total Trans. Power	Sector Arrangement
OS	3.1265	3 8 12 19 21 25
NOS-1	3.5650	3 6 10 15 21 24
NOS-2	3.3134	3 8 10 15 19 23
EAP	3.7221	1 6 8 15 20 23
AMF		Infeasible

Table 3.8. Uplink of a CDMA system with nonuniform user distribution. Antenna pattern-II

Method	Total Trans. Power	Sector Arrangement
OS	15.7469	1 3 6 10 16 21
NOS-1	19.7590	3 8 10 15 19 24
NOS-2	18.0995	2 6 10 13 18 21
EAP	29.7357	1 3 5 7 20 25
AMF		Infeasible

Table 3.9. Downlink of a CDMA system with uniform user distribution. Antenna pattern-II

Method	Total Trans. Power	Sector Arrangement
OS	2.7376	1 6 10 16 19 21
NOS-1	3.1381	1 8 12 18 19 24
NOS-2	2.8786	1 8 10 13 18 22
EAP	3.4459	1 6 8 15 20 23
AMF		Infeasible

Table 3.10. Downlink of a CDMA system with nonuniform user distribution. Antenna pattern-II

Method	Total Trans. Power	Sector Arrangement
OS	11.4009	1 5 8 12 17 21
NOS-1	13.9480	1 3 8 10 17 20
NOS-2	11.7370	1 5 8 13 17 21
EAP	16.3909	1 3 5 7 20 25
AMF		Infeasible

Table 3.11. Total Transmit Power (TP) for uniform terminal distribution,  $\gamma^* = 5$ .

	$\sigma_h^2$	0.001	0.01	0.05	0.1	0.15
Uplink	$\bar{\gamma}$	5.4	5.8	6.6	7.2	7.8
	TP	1.9327	2.0965	2.5086	3.0674	4.5773
Downlink	$\bar{\gamma}$	5.2	5.8	6.4	7.0	7.4
	TP	2.6148	2.9510	3.4680	4.2674	5.2034

Table 3.12. Total Transmit Power (TP) for nonuniform terminal distribution,  $\gamma^* = 5$ .

	$\sigma_h^2$	0.001	0.01	0.05	0.1	0.15
Uplink	$\bar{\gamma}$	5.2	5.8	6.6	7.2	8.0
	TP	9.5024	10.7366	13.0274	16.3130	23.4325
Downlink	$\bar{\gamma}$	5.2	5.8	6.4	7.0	7.4
	TP	11.2585	12.6676	14.7034	17.7137	22.1825

Table 3.13. Robustness of optimum sectorization against Gaussian estimation error

		$\sigma_h^2$	0.001	0.01	0.05	0.1	0.15
Uniform	Uplink	Robustness	85%	65 %	54%	49%	46%
	Downlink	Robustness	99.9%	96 %	63%	50%	44%
Nonuniform	Uplink	Robustness	99.9%	99.9 %	94%	87%	82%
	Downlink	Robustness	99.9%	99 %	90%	83%	72%

Table 3.14. Results of method with joint transmit and receiver filter optimization (TR) and method with receiver filter optimization only (RO) for uniform (UNI) and nonuniform (NONUNI) user distributions. K=30. Total transmit power is in WATTS

Method	Total Trans. Power	Sector Arrangement
TR (UNI)	1.5533	3 16 30
RO (UNI)	4.7767	7 16 26
TR (NONUNI)	4.6366	2 11 27
RO (NONUNI)	8.0770	4.7767

Table 3.15. Results of method with joint transmit and receiver filter optimization (TR) and method with receiver filter optimization only (RO) for uniform (UNI) and nonuniform (NONUNI) user distributions.  $K=50$ . Total transmit power is in WATTS

Method	Total Trans. Power	Sector Arrangement
TR (UNI)	4.5564	1 7 34
RO (UNI)	Infeasible	
TR (NONUNI)	7.9109	6 22 38
RO (NONUNI)	Infeasible	

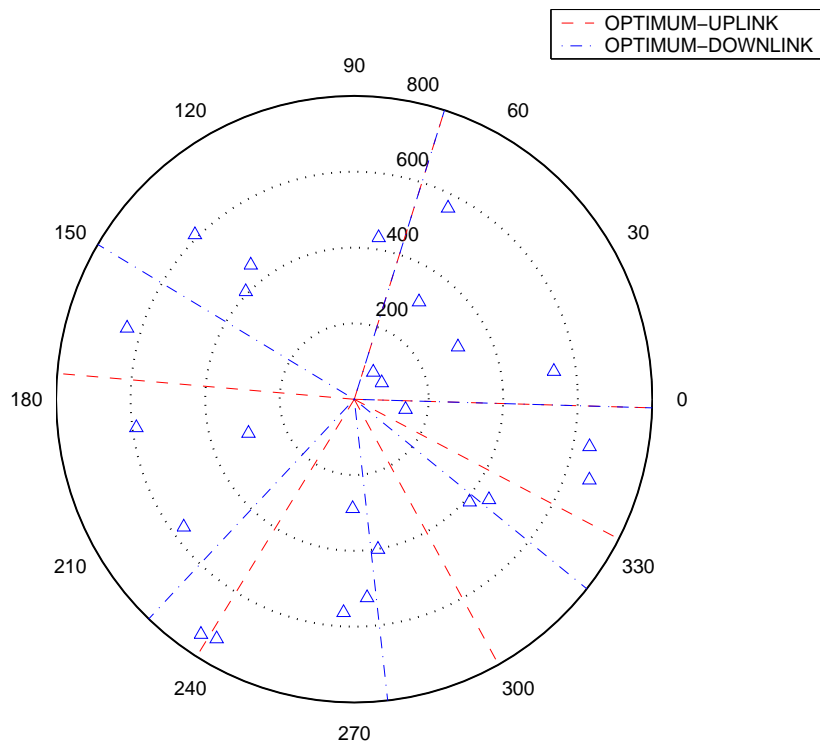


Fig. 3.5. Comparison of optimum sectorization with random signature for uplink and downlink; uniform terminal distribution



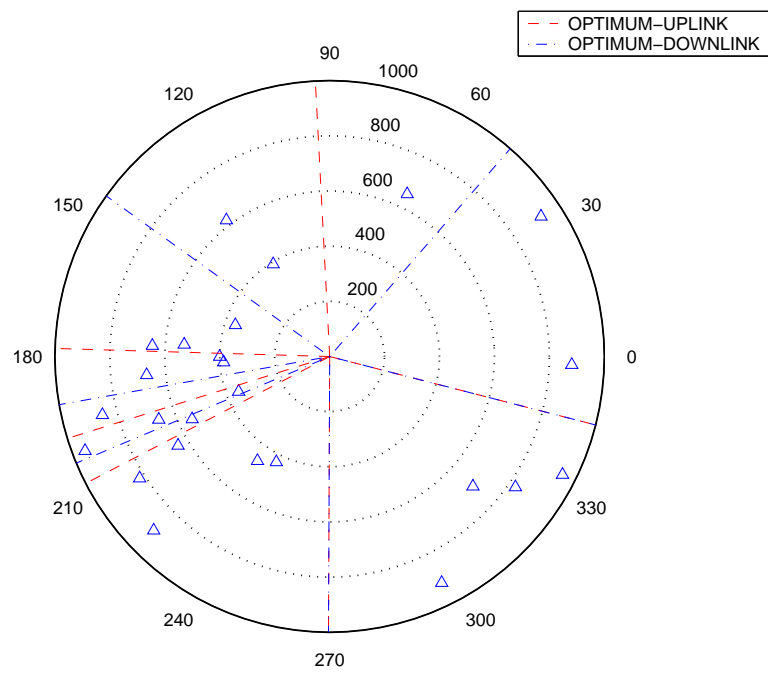


Fig. 3.6. Comparison of optimum sectorization with random signature for uplink and downlink; nonuniform terminal distribution.

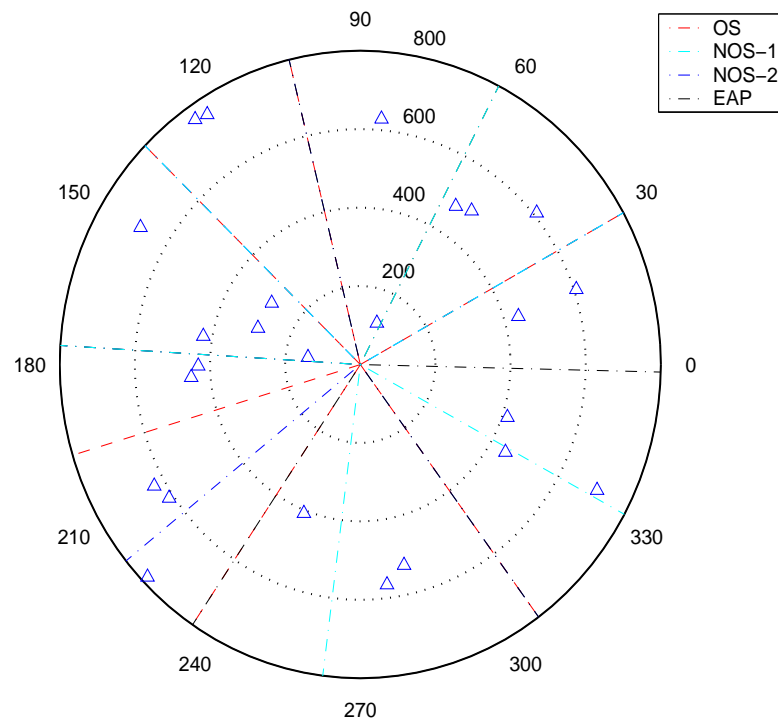


Fig. 3.7. Sector boundaries for the uplink of a CDMA system with uniform user distribution. Number of users,  $K=25$ , Processing gain,  $N=16$ , Number of sectors,  $M=6$ , noise power,  $\sigma^2 = 10^{-13}$ .

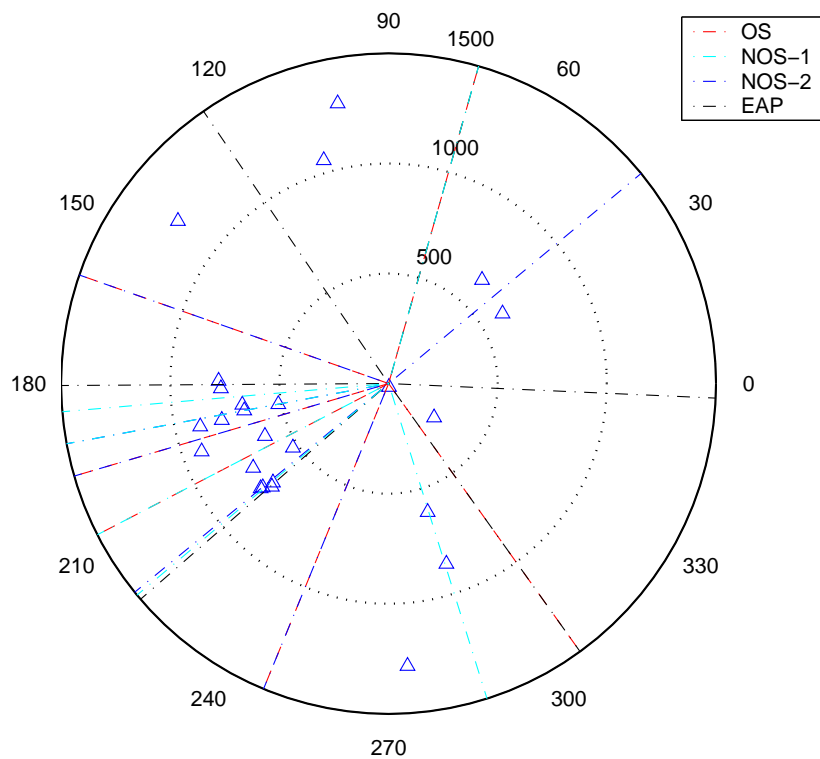


Fig. 3.8. Sector boundaries for the uplink of a CDMA system with nonuniform user distribution. Number of users,  $K=25$ , Processing gain,  $N=16$ , Number of sectors,  $M=6$ , noise power,  $\sigma^2 = 10^{-13}$ .

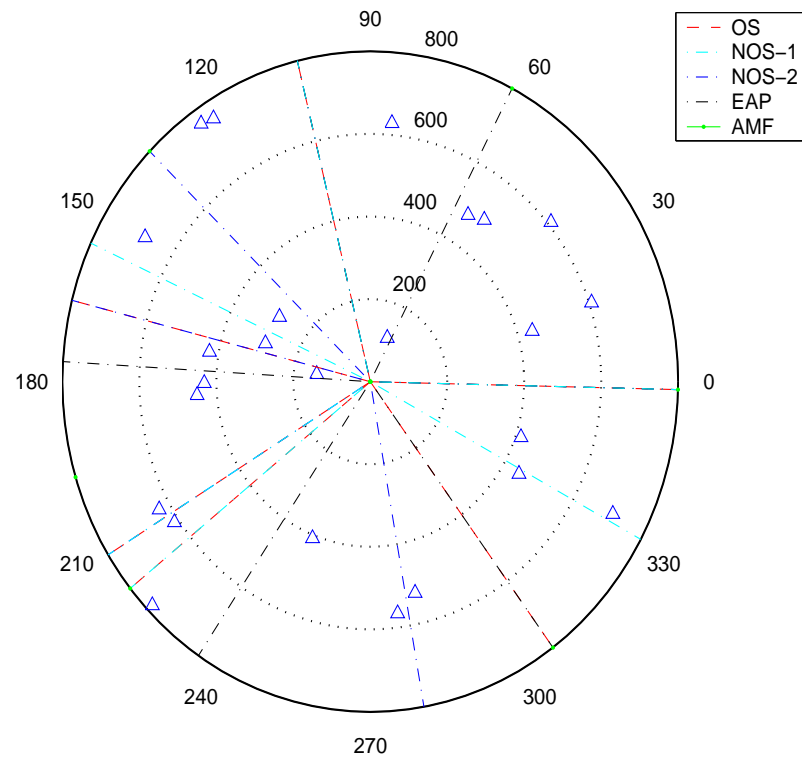


Fig. 3.9. Sector boundaries for the downlink of a CDMA system with uniform user distribution. Number of users,  $K=25$ , Processing gain,  $N=16$ , Number of sectors,  $M=6$ , noise power,  $\sigma^2 = 10^{-13}$ .

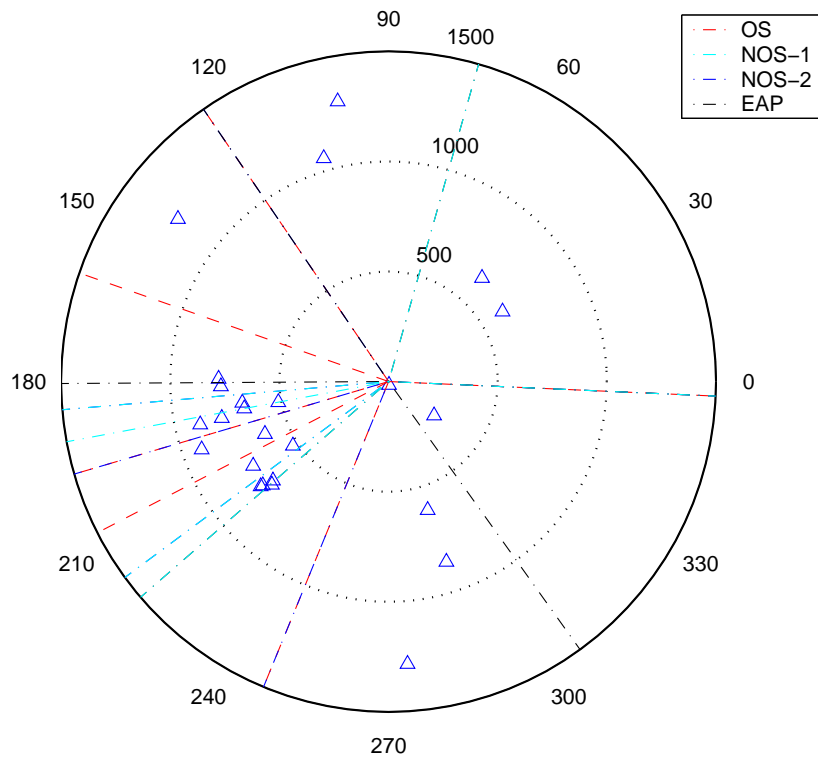


Fig. 3.10. Sector boundaries for the downlink of a CDMA system with nonuniform user distribution. Number of users,  $K=25$ , Processing gain,  $N=16$ , Number of sectors,  $M=6$ , noise power,  $\sigma^2 = 10^{-13}$ .

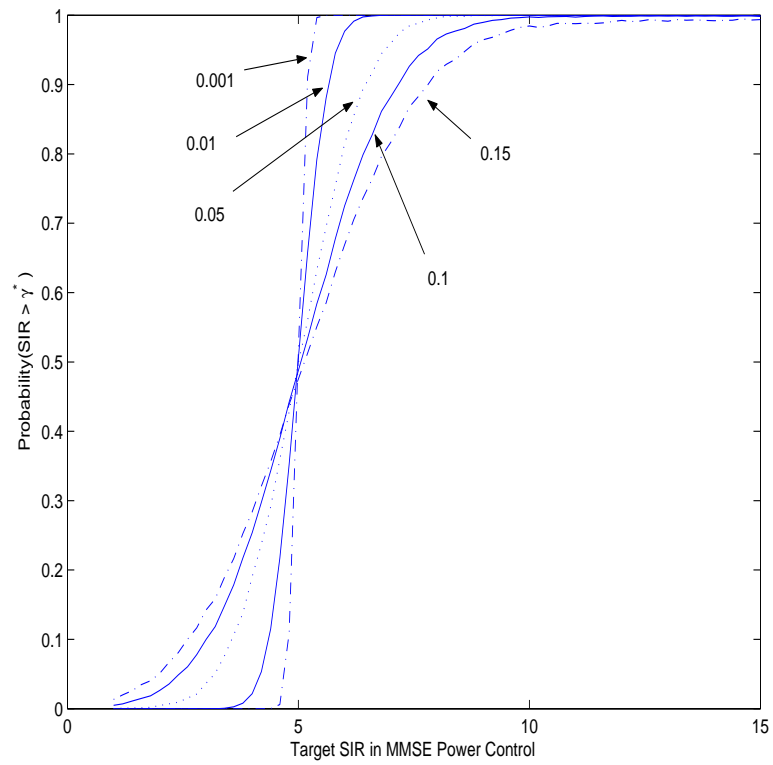


Fig. 3.11. Uplink Probability ( $\text{SIR} > \gamma^*$ ) vs. TSIR for Gaussian channel estimation error  $\sigma_h^2 = 0.001, 0.01, 0.05, 0.1, 0.15$ ,  $\gamma^* = 5$ .

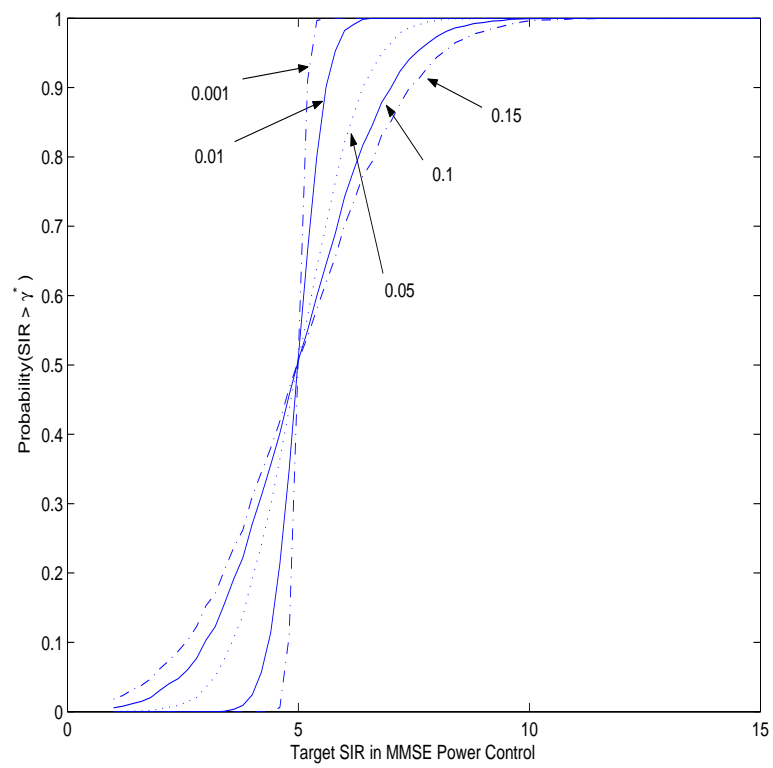


Fig. 3.12. Downlink Probability ( $\text{SIR} > \gamma^*$ ) vs. TSIR for Gaussian channel estimation error  $\sigma_h^2 = 0.001, 0.01, 0.05, 0.1, 0.15$ ,  $\gamma^* = 5$ .

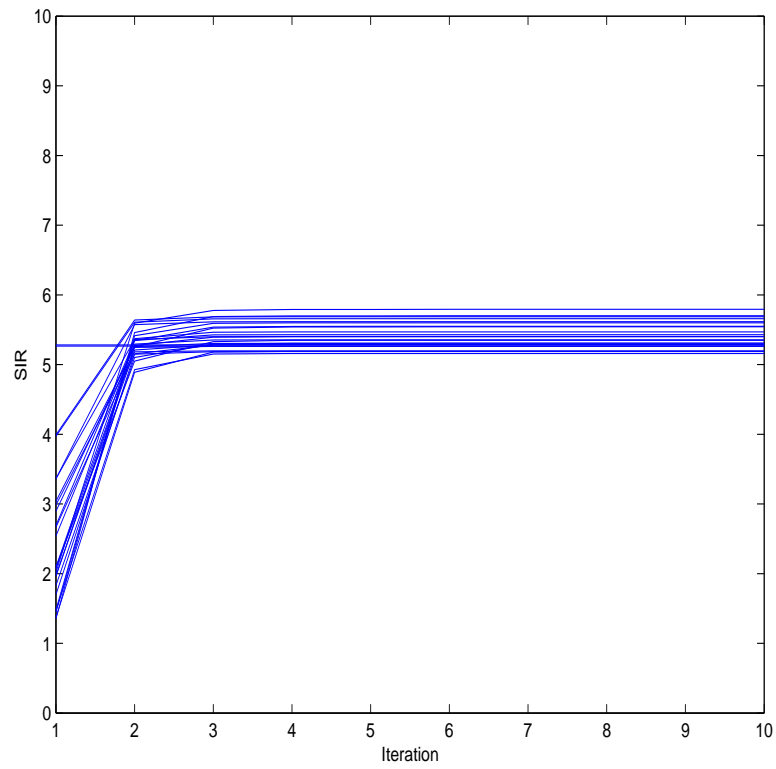


Fig. 3.13. Uplink individual user's SIR convergence for Gaussian channel estimation error.  $\sigma_h^2 = 0.001$ ,  $\bar{\gamma} = 5.4$ .



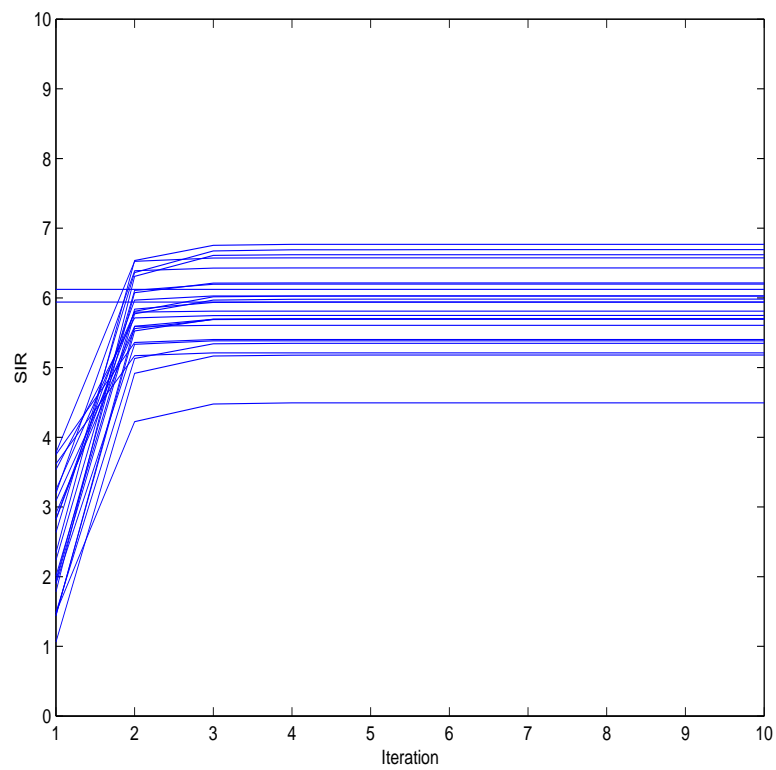


Fig. 3.14. Uplink individual user's SIR convergence for Gaussian channel estimation error.  $\sigma_h^2 = 0.01$ ,  $\bar{\gamma} = 5.8$ .

## Chapter 4

# Downlink Throughput Maximization for Interference Limited Multiuser Systems: TDMA versus CDMA

### 4.1 Introduction

Due to the scarcity of wireless resources, efficient resource management is crucial for high speed wireless communications. Power control is one important resource management technique [3, 67, 64]. For voice CDMA services, the main purpose of power control is to maintain the signal to interference ratio (SIR) to satisfy the minimum quality of service for all voice users constantly. Current and future wireless services are becoming more data centric, and often require higher data rate for downlink communications [24, 5, 7]. Data services typically require higher reliability but are delay tolerant. Conventional power control as described above is not efficient for data services in that, the transmit power would be wasted to compensate for constant interference. Instead, delay tolerance can be exploited by efficiently scheduling users in favorable channel conditions to increase overall system throughput [9].

In this chapter, we consider the scheduling and power allocation problem for the downlink of delay tolerant CDMA systems, by taking the channels of the users into account. For the CDMA downlink, typically, orthogonal codes are used to communicate to each user [24]. However, due to multipath fading, orthogonality between codes is not preserved at the mobile side. In such cases, orthogonality factor is often used to represent

the level of interference from other users [36]. This is precisely the scenario we focus on with the aim to find the optimum transmission policy, i.e., the user(s) the base station will transmit to and the corresponding transmit power levels so as to maximize the total system utility. The total system utility is defined simply as the sum of the individual utilities. The individual utility we consider is the transmission rate to a user, which is an increasing function of the user's transmit power. Utility based power control for data services has previously been considered in [49, 50, 16], for the uplink, where the quality of service (QoS) of each user, e.g. signal to interference ratio (SIR), is defined as the utility. Power allocation problem for CDMA data services is considered in the uplink in [41, 56] and the downlink in [11, 6, 27, 2]. References [41, 56], consider the jointly uplink power control and spreading gain allocation problem for the non-real time users. The jointly power and spreading gain control results in the optimum spreading gain being inversely proportional to the user's SIR, i.e., the optimum rate is proportional to the user's SIR. When no minimum spreading gain constraint exists, users are served in the order of decreasing channel gain [41].

Power allocation problem in the downlink differs from that of the uplink in that a total power constraint is required in downlink, while typically an individual power constraint is imposed in the uplink. In references [6, 11], all available power from the base station is transmitted to one user for the sake of increased throughput, and no compensation for the intracell interference is needed. To overcome the possible unfairness that may result from the one-user-transmission strategy, reference [27] imposes a minimum service rate requirement for each user, and considers the throughput maximization problem for downlink multirate CDMA system where the multirate is achieved

by either multicode or orthogonal variable spreading factor (OVSF). The optimality of greedy power allocation is shown in this scenario [27]. Also provided in [27] are numerical results which demonstrate that the value of the orthogonality factor significantly affects the system performance.

References [6, 11, 27] promote a formulation where the transmission rate and the power have a *linear* relation. In references [2, 8], on the other hand, rate and power have a *logarithmic* relation. Reference [2] considers the optimization of the sum of the individual weighted throughput values in the downlink of a multirate CDMA system with orthogonal codes. It is assumed that the orthogonality is preserved at the receiver side. The resulting problem then becomes a convex program, which for the special case of the equal weight scenario, i.e., throughput maximization, produces one-user-transmission as the optimum policy [2]. Reference [8] investigates the multiuser scheduling gain, i.e., gain by transmissions of a fraction of users over transmissions of all users for a given orthogonality factor, with the assumption of equal power transmission for the scheduled users without the consideration of optimum scheduling and power allocation.

In this chapter, we will adopt a model similar to [2, 8], but consider the downlink of an *interference limited* CDMA system. We determine the optimum number of users to be scheduled and find the corresponding power allocation. The key observation is that the optimum policy is a function of the orthogonality factor. Specifically, given the channel realization of the users and the orthogonality factor, the TDMA-mode, i.e., the base station transmits to one-user, or the CDMA-mode, i.e., the base station transmits to multiple users, can be the optimum strategy. If the CDMA-mode is optimum, that is, if more than one-user should be served by the base station, then the corresponding

power allocation is also found. A similar approach for the effect of orthogonality factor is considered in uplink in [45] without the consideration of the optimum power allocation.

The chapter is organized as follows. Section 4.2 describes the system model as well as the problem formulation and the performance metric. Optimum power allocation is considered in Section 4.3. In Section 4.4, we extend our approach to the scenario where individual power constraints exist. Section 4.5 provides numerical examples that support our analysis, and Section 4.6 summarizes the results and concludes the chapter.

## 4.2 System Model and Problem Formulation

We consider a single cell CDMA system with  $K$  users. The base station has a maximum power budget,  $P_T$ . This power budget is assigned to users such that  $\sum_{i=1}^K p_i \leq P_T$ , where  $p_i \geq 0$  is the allocated power for user  $i$ . Figure 4.1 depicts the model of the CDMA downlink. An orthogonal code is assigned to each user and is used to modulate the signal transmitted to that user. However, due to multipath fading, orthogonality between the codes (users) is lost at the receiver side. The degree of nonorthogonality is described by the *orthogonality factor*,  $\alpha$  ( $0 \leq \alpha \leq 1$ ) [36]. Under the assumption of independent identical channels for all users, it is reasonable to work with the same average orthogonality factor for all users. The signal to interference ratio at the receiver of user  $i$  is expressed as

$$SIR_i = \frac{p_i g_i}{\alpha \sum_{j \neq i} p_j g_i + I} \quad (4.1)$$

where  $g_i$  denotes channel gain of user  $i$ .  $I$  denotes the sum of the thermal noise and the intercell interference. We define the utility of user  $i$  as follows:

$$U_i(\mathbf{p}) = \log\left(1 + k \frac{p_i g_i}{\alpha \sum_{j \neq i} p_j g_j + I}\right) \quad (4.2)$$

where  $\log$  denotes the natural logarithm. We note that the individual utility is a function of the power vector  $\mathbf{p} = [p_1, p_2, \dots, p_K]$ . The utility is an achievable rate for user  $i$ , specifically by treating the interference as noise [11]. It is assumed that adaptive modulation is employed to enable the rate determined for each user [44]. Following reference [21], we denote the factor, that captures the product of the SNR gap  $\Gamma$  and the processing gain  $N$ ,  $k = \Gamma \times N$ , where  $\Gamma$  is derived from the target bit error rate (BER),  $\Gamma = \frac{-\ln(5BER)}{1.5}$ . We should note that, in a practical system employing M-ary modulation, the transmission rate (utility) is a discrete quantity. For simplicity of analysis, and similar to previous work [41, 56], we will assume continuous rate values. We will examine the effect of this assumption in the numerical results.

The problem we consider is to determine the optimum allocation of the total transmit power from the base station to the users so as to maximize the overall system utility, i.e., sum of individual utilities. Formally, the optimization problem is formulated as:

$$\begin{aligned} \max_{\mathbf{p}} \quad & \sum_{i=1}^K \log\left(1 + k \frac{p_i g_i}{\alpha \sum_{j \neq i} p_j g_j + I}\right) \\ \text{s.t.} \quad & \sum_{i=1}^K p_i \leq P_T, \quad p_i \geq 0, \quad i = 1, \dots, K \end{aligned} \quad (4.3)$$

where we assume that  $g_1 > g_2 > \dots > g_K$ , such that user with the lower index has a higher channel gain. We note that (4.4) considers only the total power constraint. This

is the problem we will consider in Section 4.3. In Section 4.4, we will consider additional individual power constraints.

The actual outcome of optimization problem in (4.4) is the power vector. The optimum transmission strategy is implicitly included in the optimum power vector in that the users that belong to the subset of users that the base station transmits to, end up with non-zero power, and the rest with zero power. If the TDMA-mode turns out to be optimum, the power allocation is such that transmission power to only one user is positive. If the CDMA-mode turns out to be optimum, the power allocation is such that transmitted power values to multiple users are positive.

We first note that any power vector  $\bar{\mathbf{p}}$  with  $\sum_{i=1}^K \bar{p}_i < P_T$  can not be the optimum power vector. Let us define a power vector  $\mathbf{p}$  with  $p_i = \beta \bar{p}_i$  ( $\beta > 1$ ),  $i = 1, \dots, K$  such that  $\sum_{i=1}^K \beta p_i = P_T$ . It is easy to see that  $\mathbf{p}$  increases all individual utilities, and hence the system utility, as compared to  $\bar{\mathbf{p}}$ . Thus, (4.4) can be rewritten as:

$$\begin{aligned} \max_{\mathbf{p}} \quad & \sum_{i=1}^K \log\left(1 + k \frac{p_i}{\alpha(P_T - p_i) + \frac{I}{g_i}}\right) \\ \text{s.t.} \quad & \sum_{i=1}^K p_i = P_T, \quad p_i \geq 0, \quad i = 1, \dots, K. \end{aligned} \quad (4.4)$$

Observe that the utility of user  $i$  is a function of the power for user  $i$  only, i.e.,  $U_i(\mathbf{p}) = U_i(p_i)$ . Also note that, although the utility is concave in SIR, it need not be concave in power. Therefore, the optimization problem is in general not a convex program. Figure 4.3(b) emphasizes this point by plotting the individual utilities for users with different channel gains.

### 4.3 Optimum Transmit Strategy and Power Allocation

At the outset, (4.4) does not appear to be easy to solve. In an effort to gain understanding towards its optimum solution, we first consider the behavior of the individual utility by observing its derivative. Our observations motivate us to consider the system-wide approach, in which we investigate the system utility in terms of the best user's power. The investigation provided in Section 4.3.1 and 4.3.2 leads to the algorithms in Section 4.3.3.

#### 4.3.1 User Centric Approach

Consider the utility function of user  $i$  and its first and second derivative in terms of  $p_i$ , the power of user  $i$ :

$$U_i(p_i) = \log\left(1 + k \frac{p_i}{\alpha(P_T - p_i) + \frac{I}{g_i}}\right) \quad (4.5)$$

$$\frac{\partial U_i(p_i)}{\partial p_i} = k \frac{\alpha p_T + \frac{I}{g_i}}{(\alpha(p_T - p_i) + \frac{I}{g_i} + k p_i)(\alpha(p_T - p_i) + \frac{I}{g_i})} > 0 \quad (4.6)$$

$$\frac{\partial^2 U_i(p_i)}{\partial p_i^2} = k \left( \alpha p_T + \frac{I}{g_i} \right) \frac{(\alpha - k)(\alpha(p_T - p_i) + \frac{I}{g_i}) + \alpha(\alpha(p_T - p_i) + \frac{I}{g_i} + k p_i)}{(\alpha(p_T - p_i) + \frac{I}{g_i} + k p_i)^2 (\alpha(p_T - p_i) + \frac{I}{g_i})^2}. \quad (4.7)$$

Clearly,  $U_i(p_i)$  is an increasing function of  $p_i$ . We are interested in whether the utility  $U_i(p_i)$  is an increasing concave or convex in  $p_i \in [0, P_T]$ . Whether  $U_i(p_i)$  is concave ( $\frac{\partial^2 U_i(p_i)}{\partial p_i^2} < 0$ ) or convex ( $\frac{\partial^2 U_i(p_i)}{\partial p_i^2} > 0$ ) depends on the  $sign(A_i)$  of the numerator of  $\frac{\partial^2 U_i(p_i)}{\partial p_i^2}$ .  $A_i$  is given by

$$A_i = (\alpha - k)(\alpha(p_T - p_i) + \frac{I}{g_i}) + \alpha(\alpha(p_T - p_i) + \frac{I}{g_i} + k p_i).$$



By letting  $I_{ti} = \alpha(p_T - p_i) + \frac{I}{g_i}$ , we have  $A_i = (\alpha - k)I_{ti} + \alpha(I_{ti} + kp_i)$ . Thus,  $U_i(p_i)$  is an increasing function of  $p_i$  if  $\frac{p_i}{I_{ti}} > \frac{1}{\alpha} - \frac{2}{k}$ , an increasing concave function of  $p_i$  otherwise.

Clearly, by examining  $\frac{\partial^2 U_i(p_i)}{\partial p_i^2} |_{p_i=P_T}$ , we can identify the behavior of function  $U_i(p_i)$ .

When  $\frac{\partial^2 U_i(p_i)}{\partial p_i^2} |_{p_i=P_T} < 0$ ,  $U_i(p_i)$  is an increasing concave function in  $0 \leq p_i \leq P_T$  as

in Figure 4.2(a). When  $\frac{\partial^2 U_i(p_i)}{\partial p_i^2} |_{p_i=P_T} > 0$ ,  $U_i(p_i)$  is an increasing concave function in

$0 \leq p_i \leq p_i^{in}$ , while it is increasing convex function in  $p_i^{in} \leq p_i \leq P_T$ , where  $p_i^{in}$  denotes

the inflection point in  $U_i(p_i)$  (See Figure 4.3(b)). Figure 4.2(a) shows the individual

utilities of different channel gains. In this example, the individual utilities of all users

are concave in power. It is clear that when each individual utility is concave in power

rather than allocating the entire power  $P_T$  to one user, sharing the power  $P_T$  among

multiple users will yield a higher total utility. In this case, the optimization problem

in (4.4) is a convex program. However, this is no longer the case when the individual

utilities of some users are not concave, as depicted in Figure 4.3(b). In this case, we

need to have a closer look at the components that contribute to the system utility. The

following terminology is used extensively in the sequel.

- $U_i(p_i)$  is convex if  $\frac{\partial^2 U_i(p_i)}{\partial p_i^2} > 0$  in  $0 \leq p_i \leq P_T$
- $U_i(p_i)$  is concave/convex if  $\frac{\partial^2 U_i(p_i)}{\partial p_i^2} |_{p_i=0} < 0$  and  $\frac{\partial^2 U_i(p_i)}{\partial p_i^2} |_{p_i=P_T} > 0$
- $U_i(p_i)$  is concave if  $\frac{\partial^2 U_i(p_i)}{\partial p_i^2} |_{p_i=P_T} < 0$
- $p_i^*$  is said to be within the concave region of  $U_i(p_i)$ , if  $\frac{\partial^2 U_i(p_i)}{\partial p_i^2} |_{p_i=p_i^*} < 0$
- $p_i^*$  is said to be within the convex region of  $U_i(p_i)$ , if  $\frac{\partial^2 U_i(p_i)}{\partial p_i^2} |_{p_i=p_i^*} > 0$

Figure 4.3(b) depicts two possible power regions of user 1 (concave/convex user).

Following from above, we define

$$\lambda_{min}^1 = \begin{cases} \frac{\partial U_1(p_1)}{\partial p_1} \Big|_{p_1=p^*} & \text{when } U_1(p_1) \text{ is concave/convex, and } \frac{\partial^2 U_1(p_1)}{\partial p_1^2} \Big|_{p_1=p^*} = 0 \\ \frac{\partial U_1(p_1)}{\partial p_1} \Big|_{p_1=p_T} & \text{when } U_1(p_1) \text{ is concave} \end{cases} \quad (4.8)$$

$$\lambda_{max}^i = \frac{\partial U_i(p_i)}{\partial p_i} \Big|_{p_i=0} \quad (4.9)$$

and,

$$p_i(\lambda) = \begin{cases} \arg p_i \left( \frac{\partial U_i(p_i)}{\partial p_i} \Big|_{p_i=p_i(\lambda)} = \lambda \right) & \text{when } \lambda < \lambda_{max}^i \\ 0 & \text{when } \lambda > \lambda_{max}^i \end{cases} \quad (4.10)$$

where  $\lambda_{min}^1$  is the minimum derivative value of utility of user 1, while  $\lambda_{max}^i$  denotes the maximum derivative value of utility of user  $i$ . Figures 4.3(a) and (b) depict  $\lambda_{min}^1$  and  $\lambda_{max}^i$ .

The optimum policy is a function of the orthogonality factor as well as users' channel gains. Below we state the propositions that lead to characterizing the optimum policy. Our first observation states that when the orthogonality factor is larger than a certain threshold, TDMA-mode is always optimum, regardless of users' channel gains:

**PROPOSITION 4.1.** *If  $\alpha \geq \frac{k}{2}$ , TDMA-mode with  $p_1 = P_T$  yields the maximum system utility.*

**Proof:**

$\alpha \geq \frac{k}{2}$  implies  $U_i(p_i)$  is a convex function for  $\forall i$ , because  $\frac{\partial^2 U_i}{\partial p_i^2} > 0$  for all  $0 \leq p_i \leq P_T$ . When  $U_i(p_i)$  is convex for  $\forall i$ , the overall utility is convex. In this case, the maximizer of the overall utility function is at  $p_1 = P_T$ , and  $p_i = 0, i > 1$ .  $\square$

While, it is clear that the TDMA-mode is optimum when  $\alpha \geq \frac{k}{2}$ , and no further power allocation is necessary, when  $\alpha \leq \frac{k}{2}$ , we need to characterize the optimum policy which consists of the transmission strategy, i.e., TDMA-mode or CDMA-mode, and the corresponding power allocation. First, we observe the following.

**PROPOSITION 4.2.** *Suppose  $\mathbf{p}^* = (p_1^*, p_2^*, \dots, p_K^*)$  is the optimum power allocation where the  $n$  users are scheduled, i.e.  $p_i^* > 0$  for  $i = 1, \dots, n$  and  $p_i = 0$  for  $i = n + 1, \dots, K$ .*

*Then,  $p_1^* > p_2^* > \dots > p_n^*$ .*

**Proof:** Suppose the optimum power allocation is such that  $p_i^* < p_j^*$  ( $g_i > g_j$ ), for  $i, j \in \{1, \dots, n\}$ . Note that  $\frac{\partial U_i(p_i)}{\partial p_i} \Big|_{p_i=p} > \frac{\partial U_j(p_j)}{\partial p_j} \Big|_{p_j=p}$ . By exchanging the power between user  $i$  and  $j$ , we get  $U_i(p_j^*) + U_j(p_i^*) > U_i(p_i^*) + U_j(p_j^*)$ , i.e., we can always increase the system utility. Therefore, the optimum power allocation  $\mathbf{p}^*$  is such that the better channel user gets assigned a higher power value among the users with non-zero power.  $\square$

When the individual utilities of multiple users are concave/convex as in Figure 4.3(b), we have the following observation.

**PROPOSITION 4.3.** *At  $\mathbf{p}^*$ , the optimum power allocation, at most one user's power is within the convex region of its utility function. This is the user with the best channel gain.*

**Proof:** Suppose the optimum power allocation is such that two users' power values are within the convex region of their utility functions, i.e.,  $\mathbf{p}^* = [p_1^*, p_2^*, p_3^*, \dots, p_K^*]$  where  $p_1^*$  and  $p_2^*$  are within the convex region of  $U_1(p_1)$  and  $U_2(p_2)$ . Consider an alternative power allocation  $\mathbf{p}^{**} = [p_1^* + \Delta p, p_2^* - \Delta p, p_3^*, \dots, p_K^*]$ , i.e., the power of user 1 and 2 are increased by  $\Delta p$  and  $-\Delta p$ , respectively, while the rest of users' power values remain the same. By the assumption of the convexity of the utility functions,  $U_1(p_1)$  and  $U_2(p_2)$  at  $p_1^*$  and  $p_2^*$ , it follows that  $U_1(p_1^* + \Delta p) + U_2(p_2^* - \Delta p) > U_1(p_1^*) + U_2(p_2^*)$ . Thus, when the power  $p_2^*$  is within the convex region of  $U_2(p_2)$ , we can always increase the total utility. Therefore, this cannot be the optimum policy, and indeed at the optimum point, only the best user's power  $p_1$  can be within the convex region of  $U_1(p_1)$ .  $\square$

From the preceding observations, we conclude that the optimum power allocation  $\mathbf{p}^* = [p_1^*, p_2^*, \dots, p_K^*]$  has to be one of two cases in terms of the best user, i.e.,  $p_1^*$  can be either within the concave region or within the convex region of  $U_1(p_1)$ <sup>1</sup>, while the rest of the power values cannot be in the convex region of their respective utility. This observation motivates our approach to focus on the the system utility in terms of the best user.

### 4.3.2 System-Wide Approach

Let us rewrite the system utility in terms of the power allocated to the best user, i.e.,  $p_1$ :

---

<sup>1</sup>This possibility includes  $p_1^* = P_T$

$$J(p_1) = U_1(p_1) + Z(p_1) \quad (4.11)$$

$$Z(p_1) = \max[\sum_{j=2}^K U_j(p_j)]_{\sum_{j=2}^K p_j = P_T - p_1}. \quad (4.12)$$

We note that  $J(p_1)$  expends all available power,  $P_T$ ,  $p_1$  for user 1 and  $P_T - p_1$  for the rest of the users. Our aim is to find the maximizer of  $J(p_1)$  over  $0 \leq p_1 \leq P_T$ . Proposition 4.3 guarantees that  $\{U_j(p_j) (j \geq 2)\}$  are all in their concave region at the optimum power allocation. Hence,  $Z(p_1)$  can be maximized with the power constraint  $\sum_{j=2}^K p_j(\lambda) = P_T - p_1$  where  $\lambda$  is the optimum Lagrange multiplier. We note that no power should be assigned to the user  $i$  when  $\lambda_{max}^i < \lambda$ . Depending on user 1's channel condition,  $U_1(p_1)$  can be either concave or concave/convex. When  $U_1(p_1)$  is concave, the resulting optimization problem is convex and the optimum power allocation is such that  $\sum_{j=1}^K p_j(\lambda) = P_T$ . If  $U_1(p_1)$  is concave/convex as in Figure 4.3(b), we have the following observation.

**OBSERVATION 4.4.** *If  $U_1(p_1)$  is concave/convex, the optimum power allocation is one of three local optimum solutions: (i)  $p_1$  is within the concave region with  $0 \leq p_1 < p_1(\lambda_{min}^1)$ , (ii)  $p_1$  is within the convex region with  $p_1(\lambda_{min}^1) < p_1 < P_T$ , or (iii)  $p_1 = P_T$ .*

The transmission strategy for the first two cases is CDMA, while the third case ( $p_1 = P_T$ ) is TDMA. Given the fact that when  $U_1(p_1)$  is concave/convex, the resulting optimization problem is non-convex, the three possible cases described above need to be considered in detail to maximize  $J(p_1)$ .

Consider  $\sum_{i=1}^K p_i(\lambda)$ , i.e., the sum of the powers transmitted to all users, given  $\lambda$ . Observing whether  $\sum_{i=1}^K p_i(\lambda) < P_T$ , or  $\sum_{i=1}^K p_i(\lambda) > P_T$  provides us with the information whether  $J(p_1)$  is increasing or decreasing at  $p_1 = p_1(\lambda)$ :

**PROPOSITION 4.5.** *If  $\sum_{i=1}^K p_i(\lambda) < P_T$  for a given  $\lambda$ ,  $J(p_1)$  is an increasing function at  $p_1 = p_1(\lambda)$ .*

**Proof:** We can find  $\lambda^*$  such that  $p_1(\lambda) + \sum_{j=2}^K p_j(\lambda^*) = P_T$  where  $\lambda^* < \lambda$ , because  $U_j(p_j)$  ( $j \geq 2$ ) is increasing concave at the optimum power values as depicted by proposition 4.3. This implies we can increase the system utility by increasing  $p_1$  and decreasing  $p_j$  ( $j > 2$ ), while maintaining  $\sum_{j=1}^K p_j(\lambda) = P_T$ .  $\square$

**PROPOSITION 4.6.** *If  $\sum_{i=1}^K p_i(\lambda) > P_T$  for a given  $\lambda$ ,  $J(p_1)$  is a decreasing function at  $p_1 = p_1(\lambda)$ .*

**Proof:** This is the opposite situation to the previous case. We can find  $\lambda^*$  such that  $p_1(\lambda) + \sum_{j=2}^K p_j(\lambda^*) = P_T$  where  $\lambda^* > \lambda$ . This implies we can increase the system utility by decreasing  $p_1$  and increasing the  $p_j$  ( $j > 2$ ), while maintaining  $\sum_{j=1}^K p_j(\lambda) = P_T$ .  $\square$

It follows from the previous two propositions, by comparing  $\sum_{i=1}^K p_i(\lambda)$  with  $P_T$ , we can always determine whether  $J(p_1)$  is increasing or decreasing at  $p_1 = p_1(\lambda)$ . In particular, if  $\sum_{i=1}^K p_i(\lambda_{min}^1) > P_T$ ,  $J(p_1)$  is a decreasing function at  $p_1 = p_1(\lambda_{min}^1)$  and the optimum power allocation is one of three possibilities as described by Observation 4.4. If, on the other hand,  $\sum_{i=1}^K p_i(\lambda_{min}^1) < P_T$ , this implies that  $\sum_{i=1}^K p_i(\lambda) < P_T$  for all  $\lambda > \lambda_{min}^1$  where  $p_1(\lambda)$  is within the concave region<sup>2</sup>. In this case,  $J(p_1)$  is an

---

<sup>2</sup>Recall that  $p_i(\lambda_{min}^1) > p_i(\lambda)$  when  $U_i(p_i)$  is increasing concave.

increasing function when  $p_1$  is within the concave region, i.e.,  $0 \leq p_1 \leq p_1(\lambda_{min}^1)$ . This means that, no  $p_1$  value within the concave region can be optimum.

We know that the optimum power allocation dictates that  $p_1$  be either  $p_1(\lambda_{min}^1) < p_1 < P_T$ , or  $p_1 = P_T$ , and that we would have to find the local optimum solution of the sum utility function,  $\sum_{i=1}^K U_i(p_i)$ , within the convex region of  $U_1(p_1)$ . Given that the overall utility function is not necessarily unimodal, this task in general requires exhaustive search and the computational complexity associated with this task may be prohibitive for locating the optimum  $\lambda$  require a search with fine resolution. In Section 4.5, numerical example, which shows the comparison of computational complexity between the optimum solution and the near exact solution, is provided Thus, if we find a computationally inexpensive way to identify whether  $p_1^* = P_T$  is the optimum strategy, i.e., the optimality of TDMA, we can reduce the complexity of identifying the optimum policy. Next, we set out to accomplish this task, and make the following observation.

**OBSERVATION 4.7.** *If  $\sum_{i=1}^K p_i(\lambda) < P_T$  for  $\forall \lambda$  where  $p_1(\lambda)$  is within the convex region of  $U_1(p_1)$ , then  $p_1 = P_T$  is optimum power allocation.*

Observation 4.7 follows from the fact that, in this case,  $J(p_1)$  is an increasing function for  $0 \leq p_1 \leq P_T$ . Although the condition in observation 4.7 guarantees the optimality of TDMA, it still requires considerable computational complexity to verify. Notice that, as described above, when  $\sum_{i=1}^K p_i(\lambda_{min}^1) < P_T$ , the optimum power allocation does not fall within the concave region of  $U_1(p_1)$ . Thus, by adopting TDMA as the optimum policy whenever  $\sum_{i=1}^K p_i(\lambda_{min}^1) < P_T$ , we can significantly reduce computational complexity in finding the local optimum power allocation in the convex region of

$U_1(p_1)$ . In the next section, we will term this short-cut, the *near-exact algorithm*. The numerical results in Section 4.5 validate the accuracy of near-exact algorithm.

### 4.3.3 Algorithms for Transmit Strategy and Power Allocation

Following the preceding discussion in Section 4.3, we conclude that the optimality of TDMA is determined by checking  $\sum_{i=1}^K p_i(\lambda) < P_T$  for all  $\lambda$  where  $p_1(\lambda)$  is within the convex region of  $U_1(p_1)$ . Instead of this potentially computationally intensive search, we propose to simply check  $\sum_{i=1}^K p_i(\lambda_{min}^1) < P_T$ , and declare that  $p_1^* = P_T$  and  $p_i = 0, i \geq 2$  whenever this condition is satisfied.

This action, i.e. deciding that  $p_1 = P_T$  is optimum whenever  $\sum_{i=1}^K p_i(\lambda_{min}^1) < P_T$ , regardless of  $\max_{p_1} J(p_1)$  for  $p(\lambda_{min}^1) < p_1 \leq P_T$  results in sub-optimum performance whenever the optimum power allocation is such that  $p_1(\lambda_{min}^1) < p_1 < P_T$ . In our numerical results, we have observed that cases where the optimum power allocation is such that  $p_1(\lambda_{min}^1) < p_1 < P_T$ , are rare and that in most cases, the optimum power allocation is either  $0 < p_1 < p_1(\lambda_{min}^1)$  or  $p_1 = P_T$ .

We should note that there may be the cases when even though  $\sum_{j=1}^K p_j(\lambda_{min}^1) > P_T$ , TDMA can be optimum. However, as the orthogonality factor increases, the condition  $\sum_{i=1}^K p_i(\lambda_{min}^1) < P_T$  accounts for almost all of the cases where TDMA is optimum, as demonstrated by numerical results in Section 4.5. The following describes the steps of the proposed algorithm to maximize the system utility, which we term *the system utility maximizer*, A-SUM.



**A-SUM:**

STEP 1. If  $\alpha \geq \frac{k}{2}$ , then TDMA mode is optimum,  $p_1 = P_T$ , **STOP**.

STEP 2. Find  $\lambda_{max}^i$  for  $i = 1, \dots, K$ , and  $\lambda_{min}^1$ .

STEP 3. (convex region) If  $\sum_{j=1}^K p_j(\lambda_{min}^1) < P_T$ ,

then, declare that the TDMA mode is optimum, **STOP**.

STEP 4. (concave region) Find the power allocation in the concave region

$$J^*(p_1(\lambda)) = \max(J(p(\lambda))), \quad 0 \leq p_1(\lambda) \leq p_1(\lambda_{min}^1)$$

using A-PACR.

STEP 5. Choose  $\max(J^*(p_1(\lambda)), J(P_T))$ .

We re-emphasize that the reduction in the computational complexity of the *near*-exactness of the algorithm arises from the STEP 3, instead of solving for  $\max_{p_1} J(p_1)$ ,  $p_1(\lambda_{min}^1) < p_1 < P_T$ .

The optimum power allocation (STEP 4) entails selecting the users to which the base station transmits with positive power. If zero power is assigned to one user, that user is not *scheduled* for transmission. The algorithm to determine the power allocation in the concave region (A-PACR) is given below. It is assumed in A-PACR that  $\sum_{j=1}^K p_j(\lambda_{min}^1) > P_T$ . If this is not the case, there is no solution in the concave region, and A-PACR simply determines  $p_1 = P_T$ .

**A-PACR:**

STEP 1. Find  $\hat{k} = \arg_k \max \sum_{j=1}^k p_j(\lambda_{max}^k)$ , subject to  $\sum_{j=1}^k p_j(\lambda_{max}^k) \leq P_T$ ,

$$k = 1, \dots, K.$$

STEP 2. Find  $p_j(\lambda)$  ( $1 \leq j \leq \hat{k}$ ) such that  $\sum_{j=1}^{\hat{k}} p_j(\lambda) = P_T$

$$\text{where } \lambda_{min}^1 < \lambda < \lambda_{max}^{\hat{k}}.$$

The optimum number of users to which the base station transmits is selected in STEP 1. Then, optimum power values are allocated in STEP 2. Note that a numerical method, e.g., bisection [13] should be used to determine the value of  $\lambda$ .

#### 4.4 Downlink Transmission policies with individual power constraints

In this section, we consider the effect of having minimum and maximum limits on the powers that the base station transmits to individual users. Specifically, we extend our approach and present modifications to the algorithms presented in Section 4.3. We assume that each *scheduled* user, i.e., each user that the base station is designated to transmit with non-zero power, has a maximum and/or a minimum transmit power constraint. We emphasize this to convey the fact that we still may end up with non-scheduled users. This is in contrast to having a minimum power constraint for each user, which automatically sets the transmission policy to CDMA with all users simultaneously transmitted to by at least the minimum power. As a result, the optimization problem (4.4) now has additional constraints,

$$p_i^{min} \leq p_i \leq p_i^{max} \quad \forall i \quad \exists p_i > 0 \quad (4.13)$$

where  $p_i^{min}$  ensures all users selected for transmission to achieve minimum required rate  $U^{min}$ , while  $p_i^{max}$  signifies a practical limit, i.e., an arbitrary high data rate cannot be achieved, even if a user has a very high channel gain. The limits would be obtained from

the minimum and maximum rate,  $U^{min}$  and  $U^{max}$ , via

$$U^{min} \leq U_i(\mathbf{p}) \leq U^{max} \quad (4.14)$$

$$\text{with } \log\left(1 + k \frac{p_i^{min}}{\alpha(P_T - p_i^{min}) + \frac{I}{g_i}}\right) = U^{min} \quad (4.15)$$

$$\text{and } \log\left(1 + k \frac{p_i^{max}}{\alpha(P_T - p_i^{max}) + \frac{I}{g_i}}\right) = U^{max}$$

Observe the above assume that full power is expended at the base station. We will elaborate on this issue in the next section.

#### 4.4.1 Observations on the Constrained Problem

First, we consider the case when only maximum power constraints exist.

**OBSERVATION 4.8.** *When only maximum power constraints exist and the base station transmits to more than one user, full power,  $P_T$  should be expended for the optimum power allocation.*

**Proof:** Suppose the optimum power allocation expends  $\hat{P}_T$  ( $\hat{P}_T = \sum_{i=1}^K p_i^* < P_T$ ), while one user, say user 1, is at its maximum allowable utility value, i.e.  $U_1 = U^{max}$ . Observe that, we can concentrate on this case, without loss of generality, because if  $\sum_{i=1}^K p_i^* < P_T$  and  $U_1 < U^{max}$ , by proportionally increasing transmit power of all scheduled users such that  $U_1$  reaches  $U^{max}$ , the utility of each scheduled user is further increased. Thus,  $\sum_{i=1}^K p_i^* < P_T$  and  $U_1 < U^{max}$  cannot be the condition for optimum power allocation. Note that, from (4.15), it follows that by expending  $P_T$ ,  $U_1 = U^{max}$  would be achieved with  $p^{max} < p_1^*$ . Specifically,

$$U^{max} = \log\left(1 + k \frac{p_1^{max}}{\alpha(P_T - p_1^{max}) + \frac{I}{g_1}}\right) = \log\left(1 + k \frac{p_1^*}{\alpha(\hat{P}_T - p_1^*) + \frac{I}{g_1}}\right). \quad (4.16)$$

Since,  $\hat{P}_T < P_T$ , (4.16) implies that  $p_1^{max} < p_1^*$ . This means that with leftover power,  $(P_T - \hat{P}_T) + (p_1^* - p_1^{max})$ , by proportionally increasing the transmit power of all other scheduled users such that  $\sum_{j=2}^K \beta p_j^* = P_T - p_1^{max}$ , the utilities of these scheduled users are increased, while  $U_1$  is kept at  $U^{max}$ . Thus, if  $\hat{P}_T = \sum_{i=1}^K p_i^* < P_T$  and  $U_1 = U^{max}$ , the system utility can be further increased by expending full power  $P_T$ . Therefore, full power  $P_T$  should be expended for the optimum power allocation.  $\square$

*OBSERVATION 4.9. When both the maximum and the minimum power constraints exist, the optimum policy can be such that the base station transmits less than full power.*

To see why this observation is valid, consider the following argument. For simplicity of analysis, assume each scheduled user experiences interference as if full power  $P_T$  is transmitted from the base station. Then, the utility of each scheduled user is a function of its power only and the minimum and maximum power of user  $i$ ,  $p_i^{min}$  and  $p_i^{max}$  are obtained for each scheduled user  $i$  from (4.15).

Consider the case that the optimum policy schedules the first  $n$  users to be transmitted with their maximum power corresponding to the maximum utility value  $U^{max}$ , while satisfying  $\sum_{i=1}^n p_i^{max} < P_T$ . In this case, the optimum policy may try to schedule the next user with leftover power  $P_T - \sum_{i=1}^n p_i^{max}$ . If this action violates the total power constraint,  $\sum_{i=1}^n p_i^{max} + p_{n+1}^{min} > P_T$ , the transmission policy ends up with expending

less than full power. However, we note that  $p_i^{max}$  ( $i = 1, \dots, n$ ) values were obtained with the the assumption that the base station transmits full power,  $P_T$ . Noting the fact that less than full power transmission is optimum, we can see that the actual interference scheduled user  $i$  experiences is in fact less than  $\alpha(P_T - p_i^{max}) + \frac{I}{g_i}$ . In turn, the maximum utility  $U^{max}$  can be achieved by user  $i$  with power value  $p_i^{opt} < p_i^{max}$ . Fortunately, the power vector  $\mathbf{p}^{opt} = [p_1^{opt}, \dots, p_n^{opt}]$  simply is the downlink power vector that satisfies a given SIR value, i.e.  $\gamma_i = \frac{e^{U^{max}} - 1}{k}$  ( $i = 1, \dots, n$ ), and can be easily determined[64]. For convenience, we term this Power Control for Fixed Rate (PCFR).

#### 4.4.2 Utility Maximization with Individual Constraints

Proposition 4.3 where no power constraint is assumed states that at most one user can be within the convex region of the utility function. By imposing a maximum power constraint, we may have more than one user within the convex region. In this case, the utility with higher channel gain can be increased up to the maximum utility value by increasing the power of the user with higher channel gain, and decreasing the power of the user with lower channel gain, while the sum of the power of these two users remains the same. After the utility with higher channel gain reaches the maximum utility value, the power of the user with lower channel gain can be either within the concave or the convex region. This implies that, under the maximum power constraint, there can be more than one user within the convex region. However, *at most one user* expends less than maximum power within the convex region at the optimum power allocation. Otherwise, the system utility can be increased as described by Proposition 4.3.

The observation below follows from the fact that by  $\frac{\partial U_i(p_i)}{\partial p_i} \Big|_{p_i=p_i^{min}} > \frac{\partial U_j(p_j)}{\partial p_j} \Big|_{p_j=p_j^{min}}$  ( $g_i > g_j$ ), and the fact that at most one user has less than maximum power within the convex region.

OBSERVATION 4.10. *If  $p_i^{min}$  for some users are within the convex region, the optimum policy employs greedy packing of these users in the order of decreasing channel gains, i.e., allocation of maximum allowable power in the order of decreasing channel gains.*

We term such users *greedy users* and the resulting process *convex greedy packing*. If all available power is expended in this process, then the resulting power allocation is the optimum power allocation. If there is a leftover power, but is not enough to support the next user with the minimum required power, the maximum system utility is achieved with less than full power and with convex greedy packing. After greedy packing, if the leftover power is enough to support the next user with minimum required power, we need to consider the optimization problem in terms of each concave/convex user by allowing each concave/convex user to have the maximum power in the order of decreasing channel gains. To that end, we modify (4.11) and (4.12) such that

$$J(p_j)_M = \sum_{i < j} U_i(p_i^{max}) + U_j(p_j) + Z(p_j) \quad (4.17)$$

$$Z(p_j) = \max[\sum_{l > j}^K U_l(p_l)]_{\sum p_l = P_T - \sum_i p_i^{max} - p_j, \quad p_l \geq p_l^{min}} \quad (4.18)$$

where the notation  $J(p_j)_M$  denotes the fact that we have  $M$  users with minimum power requirement. The first term in (4.17) includes users which expend their maximum power  $p_i^{max}$  within the convex region. Similar to (4.12),  $J(p_j)_M$  is optimized over  $p_j$  with

remaining power  $P_T - \sum_i p_i^{max} - \sum_{l>i}^M p_l^{min}$ . The resulting solution  $\max J(p_j)_M$  only considers the case when  $p_i = p_i^{max}$  ( $i < j$ ). Recall that at most one user expends less than maximum power within the convex region at the optimum power allocation. Hence, by solving  $\max J(p_j)_M$  for all concave/convex users, we can find the optimum solution. This means that we need to solve

$$\max_j \left( \max_{p_j} J(p_j)_M \right) \quad j = k^* + 1, \dots, \min(k^{**}, M) \quad (4.19)$$

where  $k^*$ ,  $k^{**}$  denotes the number of greedy users and concave/convex users, respectively. If all individual utilities are concave, the resulting optimization problem is convex, and the solution of (4.19) is given in Section 4.3. Note that, due to the minimum power constraint, the following modifications in our previous definition (Section 4.3) are needed:

$$\lambda_{max}^i = \left. \frac{\partial U_i(p_i)}{\partial p_i} \right|_{p_i=p_i^{min}} \quad (4.20)$$

$$\lambda_{min}^i = \left. \frac{\partial U_i(p_i)}{\partial p_i} \right|_{p_i=p^*}, \left. \frac{\partial^2 U_i(p_i)}{\partial p_i^2} \right|_{p_i=p^*} = 0 \quad \text{when } U_i(p_i) \text{ is concave/convex} \quad (4.21)$$

$$p_i(\lambda) = \begin{cases} \arg p_i \left( \left. \frac{\partial U_i(p_i)}{\partial p_i} \right|_{p_i=p_i(\lambda)} = \lambda \right) & \text{when } \lambda < \lambda_{max}^i \\ p_i^{min} & \text{when } \lambda > \lambda_{max}^i \end{cases} \quad (4.22)$$

#### 4.4.3 Algorithms with Individual Power Constraints

Following the observations in Section 4.4.1, we propose modified versions of A-SUM and A-PACR in the presence of power constraints, A-SUMPC and A-PACRPC, respectively.

**A-SUMPC:**

$k^*$ : Number of greedy users

$k^{**}$ : Number of concave/convex users ( $k^{**} \geq k^*$ ,  $k^{**}$  includes  $k^*$ )

STEP 1. Find  $\lambda_{max}^i$   $i = 1, \dots, K$  and  $\lambda_{min}^i$ .

$$\text{Find } T_1 = U_1(p_1 = \min(p_1^{max}, P_T), p_2 = 0, \dots, p_K = 0),$$

set  $M = k^* + 1$ .

STEP 2. If  $k^* > 0$ , Apply Convex Greedy Packing.

STEP 3 (M-user system) If  $\sum_{i=1}^{k^*} p_i^{max} + \sum_{j=k^*+1}^M p_j^{min} > P_T$ ,  $M = M - 1$ ,

GOTO STEP 5.

$$T_M = \max_j \left( \max_{p_j} J(p_j)_M \right), j = k^* + 1, \dots, \min(M, k^{**}), \text{ via A-PACRPC.}$$

STEP 4. If  $M < K$ ,  $M = M + 1$  and GOTO STEP 3.

STEP 5.  $\max_{1 \leq i \leq M} T_i$ .

In the algorithm above,  $T_i$  denotes the maximum system utility of the  $i$ -user system. In STEP 2, convex greedy packing is applied to greedy users. Feasibility of the M-user system is checked in STEP 3, then optimum power allocation of M-users system is obtained via A-PACRPC. STEP 5 selects the largest among  $T_i$  ( $i = 1, \dots, M$ ). When the optimum power allocation expends less than full power  $P_T$ , the actual optimum power vector is found via solving M linear equations, i.e. PCFR.

**Convex Greedy Packing:**

STEP 1.  $P_{re} = P_T$ .  $i = 1$ .

STEP 2.  $p_i^* = \min(p_i^{max}, P_{re})$ ,  $P_{re} = P_{re} - p_i^*$ . If  $p_i^* < p_i^{min}$ ,  $p_i^* = 0$ .

STEP 3. If  $P_{re} = 0$  or  $p_i^* < p_i^{min}$ , STOP.

STEP 4. If  $i < k^*$ , then  $i = i + 1$ , GOTO STEP 2.



In STEP 2, maximum allowable power is assigned to greedy users in the order of decreasing channel gains. If the algorithm stops in STEP 3, and  $P_{re} = 0$ , then the resulting solution is optimum power. If  $P_{re} \neq 0$ , the actual power vector is obtained via PCFR.

**A-PACRPC:**

STEP 1.  $i = k^* + 1$ .

STEP 2. (convex region)

$$p_i^* = \min(p_i^{max}, P_T - \sum_{j=1}^{i-1} p_j^{max} - \sum_{j=i+1}^M p_j^{min}),$$

Find  $p_j(\lambda)$  ( $i < j \leq M$ ) such that  $\sum_{j=1}^{i-1} p_j^{max} + p_i^* + \sum_{j=i+1}^M p_j(\lambda) = P_T$

and corresponding system utility  $T_{Mi}^{convex}$ .

If  $\sum_{j=1}^{i-1} p_j^{max} + \sum_{j=i}^M p_j(\lambda_{min}^i) < P_T$ ,  $T_{Mi}^{concave} = 0$  and GOTO STEP 4.

STEP 3. (concave region)

Find  $p_j(\lambda)$  ( $i \leq j \leq M$ ) such that  $\sum_{j=1}^{i-1} p_j^{max} + \sum_{j=i}^M p_j(\lambda) = P_T$

and corresponding system utility  $T_{Mi}^{concave}$ .

STEP 4.  $T_{Mi} = \max(T_{Mi}^{convex}, T_{Mi}^{concave})$

If  $i < \min(M, k^{**})$ ,  $i = i + 1$ , GOTO STEP 2.

STEP 5.  $T_M = \max_{1 \leq j \leq \min(M, k^{**})} T_{Mj}$ .

Note that the near exactness of the algorithm arises from the fact that in STEP 2, we simply take  $p_i^* = \min(p_i^{max}, P_T - \sum_{j=1}^{i-1} p_j^{max} - \sum_{j=i+1}^M p_j^{min})$ , instead of solving  $\max_{p_i} J(p_i)_M$  over all  $p_i$  within the convex region.

## 4.5 Numerical Results

We provide simulation results for a range of the orthogonality factor values. The total power at the base station is  $P_T = 10$  watts. Total noise and intercell interference is  $I = 10^{-11}$  watts. Factor  $k$  in the utility function is  $k = 1.2$ , corresponding to  $\Gamma = 0.15$  and processing gain  $N = 8$ . Thus, when  $\alpha \geq 0.6$ , the individual utilities of all users are convex in power, and the TDMA-mode is optimum, regardless of the channel gains. Channel gain from the base station to mobile  $i$  is modeled as  $g_i = \frac{r_i}{d_i^4}$  where  $d_i$  denotes the distance between mobile  $i$  and the base station, which is uniformly distributed between 100m and 1000m, and  $r_i$  is the realization of the lognormal fading coefficient with variance  $8dB$ .

We have first examined the accuracy of the near-exact algorithm determining TDMA optimality. Our experiments over 10,000 channel gain realizations have demonstrated that the near-exact algorithm correctly determines TDMA optimality 97.5%, 99.6%, 99.9% of the time for  $\alpha = 0.1, 0.2, 0.3$ , respectively. As  $\alpha$  increases, as expected, the accuracy gets better since the likelihood of the case when the optimum power allocation is such that  $p_1(\lambda_{min}^1) \leq p_1 < P_T$  gradually disappears. To give the idea about the savings in complexity of the near-exact algorithm versus the optimum solution, we were able to locate the optimum solution by evaluating 1000  $\lambda$  values within the convex region of  $U_1(p_1)$  in STEP 3 of A-SUM. On the other hand, the near-exact algorithm requires a single evaluation at  $\lambda_{min}$ .

Figure 4.4 shows the percentage of channel realizations in which the policy our proposed algorithm finds is TDMA. As the number of users in the system increases, the

possibility that multiple users may have high channel gain values increases. Accordingly, the percentage decreases. As expected, the frequency of TDMA being selected increases as the orthogonality factor increases.

Figure 4.5 shows the system utility, given  $\alpha$  and the number of users  $K$  in the system. The system utility is averaged over 10,000 channel gain realizations. The optimum policy selects the number of users and the power levels for the scheduled users. In general, not all users in the system are simultaneously scheduled. When  $\alpha = 0.1$ , i.e., a low orthogonality factor, simultaneous transmissions do not result in much interference, and the optimum policy chooses the CDMA-mode. However, if the best user has a much higher channel gain as compared to the rest, the optimum policy may still end up to allocating all power to that best user. As  $\alpha$  increases, more than one user transmissions result in higher interference, and TDMA-mode becomes the preferred mode so as to avoid the interference. For example, for  $\alpha > 0.5$ , TDMA-mode is optimum in most cases. For any value of  $\alpha > 0.6$ , for example, when  $\alpha = 0.7$ , TDMA-mode is always optimum: figure 4.5 shows that when  $\alpha = 0.7$  the maximum system utility is lower than the maximum system utility values achieved for smaller  $\alpha$  values that facilitate transmissions to multiple users. The gap between the system utility for  $\alpha$  ( $\alpha < 0.6$ ) and the system utility for  $\alpha = 0.7$  can be interpreted as the gain of optimum policy that results in hybrid CDMA/TDMA over the one that results in TDMA, as a result of the difference in the orthogonality factor values. As the number of users in the system increases, the chance of selecting users with higher channel gains, multiuser diversity, increases. Thus, the system utility increases.

Figure 4.6 shows the system utility where the resulting individual utility is discretized to the integer value. With this, we attempt to investigate the performance of the proposed algorithm in a practical setting where only discrete rates are available. We observe that discretization does not lead to a significant loss in system utility especially for large  $\alpha$  values. This is because for large  $\alpha$ , TDMA results most often, and the quantization loss in utility is due to one user only.

Figure 4.7 shows the system utility gain of CDMA-mode over TDMA-mode. When the orthogonality factor is low, multiple-user transmissions has a gain over the one user transmission. The gain increases as the number of users in the system increases. As the orthogonality factor increases, however, we observe that the gain disappears, as eventually TDMA-mode becomes optimum.

Figures 4.8 and 4.9 show the system utilities and the discretized system utilities with no power constraint (NPC), minimum power constraint only (PCMIN), maximum power constraint only (PCMAX) and minimum and maximum power constraint (PC) for  $\alpha = 0.1$  and  $k = 2.4$  ( $\Gamma = 0.15$  and  $N = 16$ ). Note the loss in total system utility we have due to the presence of the maximum power constraints, because these constraints limit the throughput values of the users with high channel gains.

## 4.6 Conclusion

In this chapter, we have considered an interference limited downlink and investigated the total utility (throughput) maximizing policy which consists of the user(s) the base station selects to transmit to, and the corresponding power allocation. Depending on the channel conditions, i.e., the orthogonality factor, and the users' channel gains,

the optimum policy chooses either TDMA-mode or CDMA-mode and the corresponding power allocation. The higher the orthogonality factor, the larger the interference caused by multiple-user transmissions, rendering TDMA-mode being optimal. In contrast, multiple-user-transmissions yield a higher overall utility when the orthogonality factor is low. We observed that depending on the channel conditions, the overall system utility may or may not be a concave function and care must be given to characterizing the solution when it is not. In particular, we took the approach of examining the system utility in terms of the best user, and observed properties that helped us identify the optimal policy.

We also considered the effect of imposing minimum and maximum individual power constraints and observed that CDMA-mode becomes the choice more often when maximum power constraints are imposed.

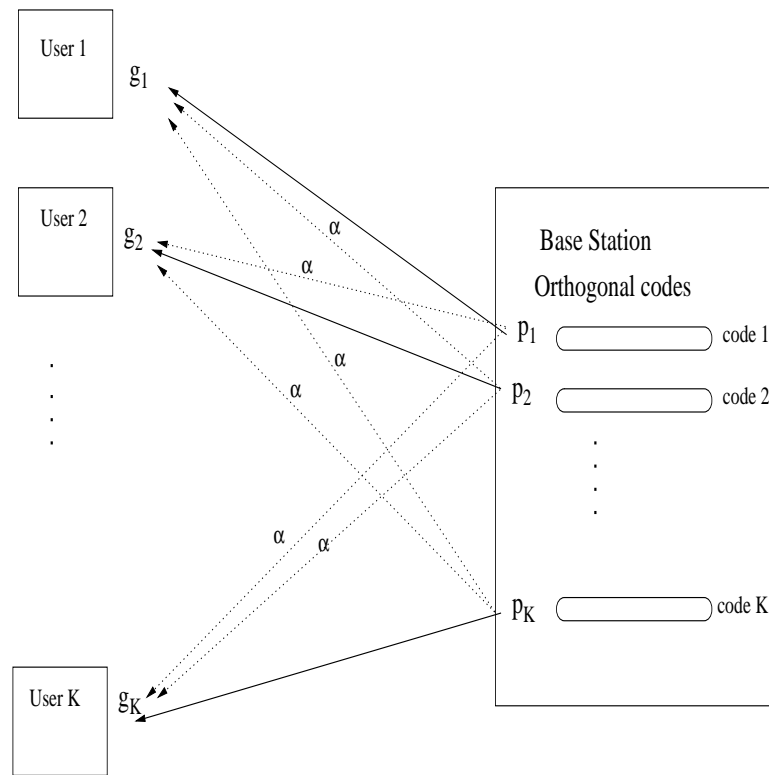


Fig. 4.1. Downlink system model.

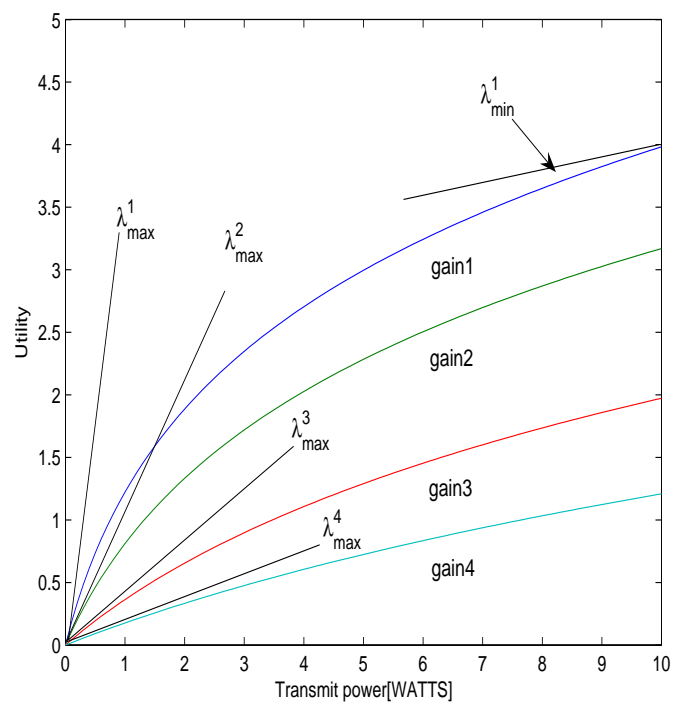


Fig. 4.2. Utility versus transmit power.  $gain_1 > gain_2 > gain_3 > gain_4$ . An example where individual utility functions for all users are concave.

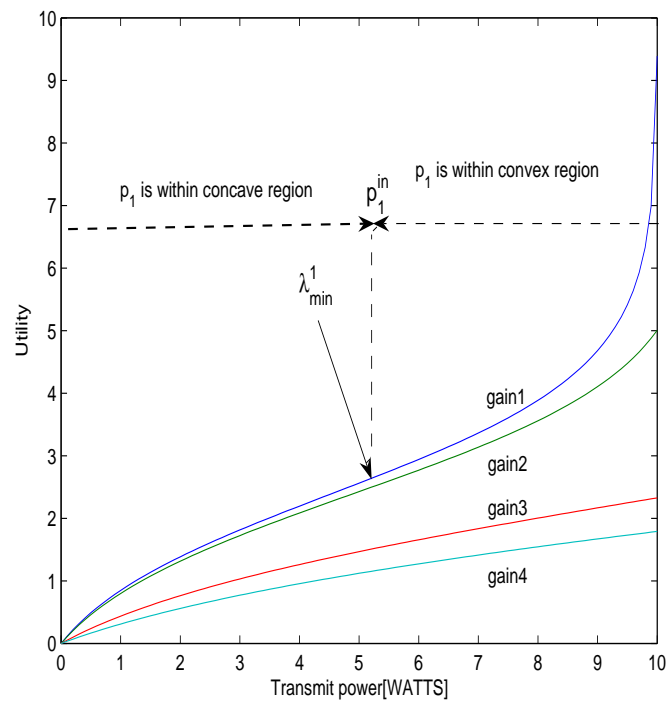


Fig. 4.3. Utility versus transmit power.  $gain_1 > gain_2 > gain_3 > gain_4$ . An example where individual utility functions for some users are not concave.



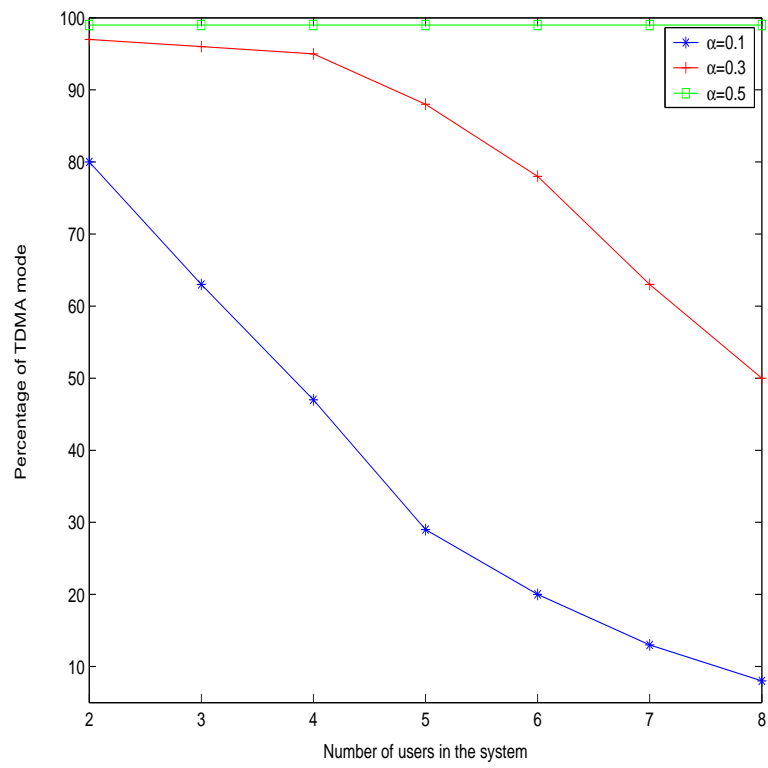


Fig. 4.4. Percentage of channel realizations in which the TDMA mode is optimum.

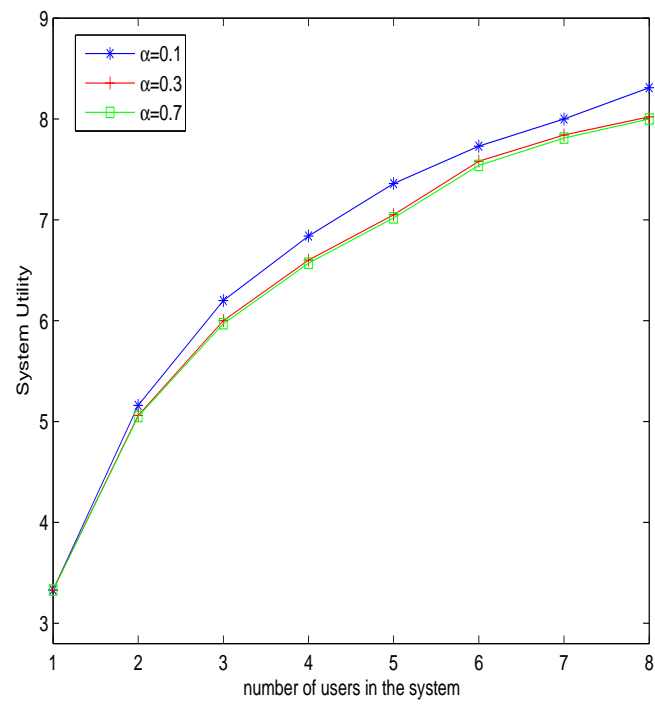


Fig. 4.5. System Utility versus number of users in the system.

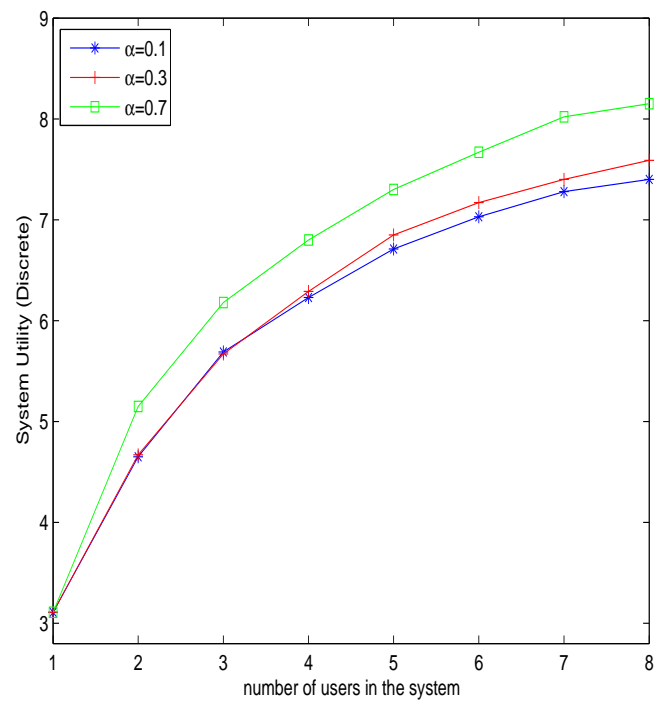


Fig. 4.6. System Utility versus number of users in the system.

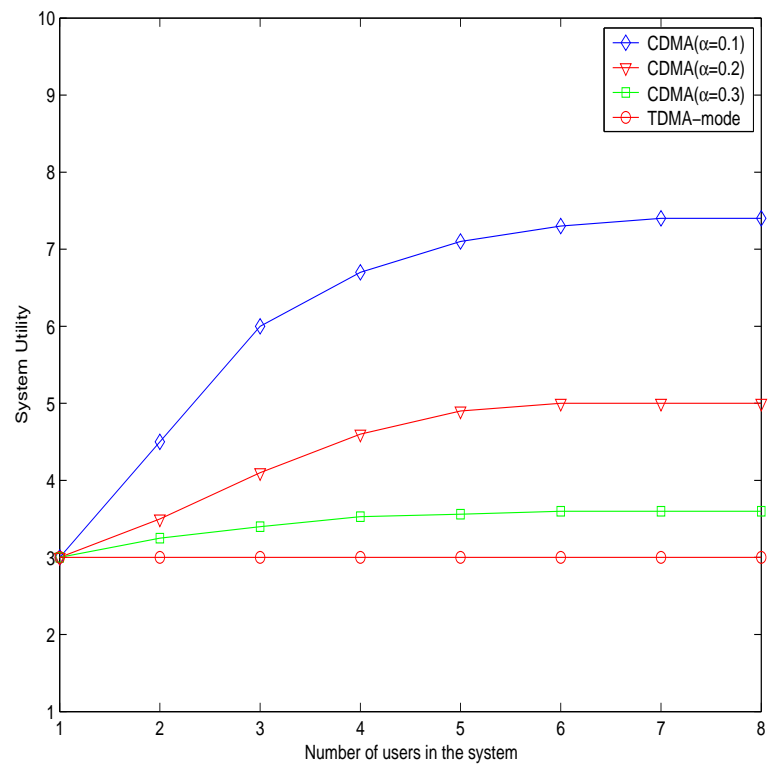


Fig. 4.7. CDMA-mode gain over TDMA-mode for different  $\alpha$  values.

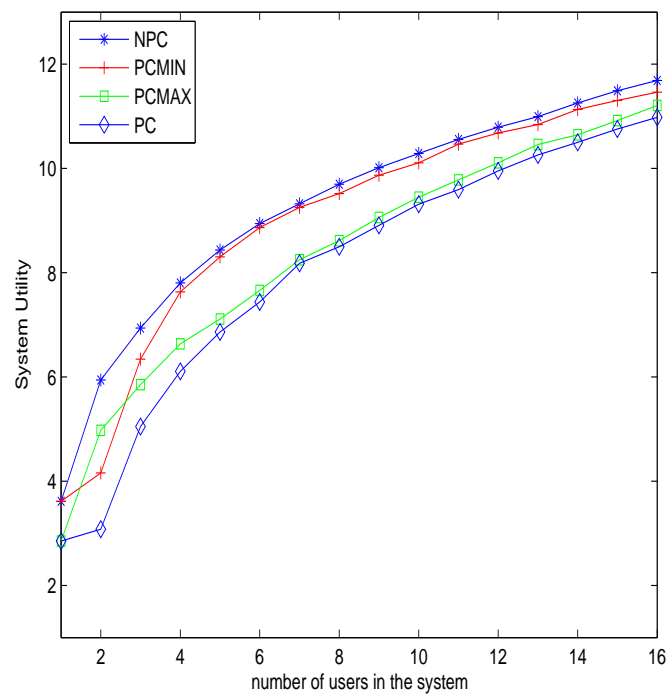


Fig. 4.8. System utilities with no power constraint (NPC), minimum power constraint (PCMIN), maximum power constraint (PCMAX) and maximum and minimum power constraints (PC).  $k = 2.4$  ( $\Gamma = 0.15$ ,  $N = 16$ ),  $\alpha = 0.1$ .

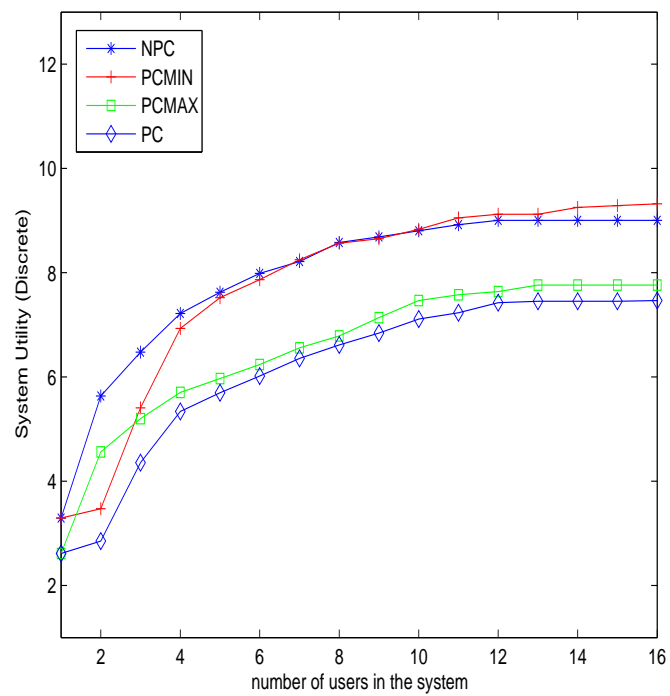


Fig. 4.9. Discrete system utilities with no power constraint (NPC), minimum power constraint (PCMIN), maximum power constraint (PCMAX) and maximum and minimum power constraints (PC).  $k = 2.4$  ( $\Gamma = 0.15, N = 16$ ),  $\alpha = 0.1$ .

## Chapter 5

# Energy Efficient Rate Scheduling for Interference Limited CDMA Systems: Short Term Throughput Fairness

### 5.1 Introduction

A considerable research effort has been directed towards energy efficient transmission techniques recently, with the objective of prolonging the battery life of mobile terminals [12, 14, 18]. The main idea is to utilize the convex relationship between power and delay: by increasing the transmission time, the transmit power required decreases, while the delay increases. In [12], power and delay tradeoff is considered for a single user system. Reference [14] considers efficient transmission scheduling by varying packet transmission time. In [18], energy minimization problem is considered with a deadline constraint for a single user system.

Typically, wireless resources are shared by simultaneous users in CDMA systems. For energy efficient transmission in CDMA systems, reference [10] investigates the energy efficient power and rate allocation with a minimum service rate requirement. In reference [10], it is shown that, by greedy packing the transmit power in the order of decreasing channel gain, the total transmit power of all users is minimized in achieving any instantaneous target system throughput, defined as the sum of the individual throughput values. In this setting, a user with a higher channel gain always has a higher instantaneous throughput. Since the channel gains of the users will be different from

each other, such a setting results in unfairness in terms of the throughput each user can achieve. To avoid such throughput unfairness, the short term average throughput requirement can be used rather than the minimum throughput requirement. This is the motivation behind our investigation of the energy efficient scheduling problem with an average throughput requirement.

In this chapter, we investigate rate scheduling and power allocation problem for a delay constrained CDMA system. Specifically, we determine a power efficient scheduling policy, while each user maintains the short term ( $n$  time slots) average throughput. We consider a multirate CDMA system facilitated by the aid of multiple codes. In each time slot, multiple codes belonging to each user become *virtual users*, and each virtual user interferes with the rest. The aim of this chapter is to schedule the virtual users into these  $n$  time slots, such that the sum of transmit power in  $n$  time slots is minimized. At the outset, this problem looks similar to the bin packing problem which is NP-complete [19]. Fortunately, the specifics of the problem enables it to admit a simple solution. We show that the total transmit power minimization problem can be solved by a shortest path algorithm. We compare the performance of the optimum scheduling with that of TDMA-type scheduling. In Section II, system model and problem formulation is described. The optimum scheduling is investigated in Section III. Numerical results is provided in Section IV. Section V concludes this chapter.



## 5.2 System Model and Problem Formulation

### 5.2.1 System Model

We consider the uplink of a single cell CDMA system where  $K$  users communicate with a base station. It is assumed that the channel gain is quasi-static, so that the channel gain of user  $i$  during the short term ( $n$  time slots) is constant and is equal to  $g_i$ . Each user may change its transmission rate by the number of codes it uses in each time slot, but maintains the average throughput during the  $n$  time slot frame. The multicode each of which corresponds to a virtual user in a time slot interfere with each other. Each code is assumed to be a randomly generated signature sequence.

The signal to interference ratio of virtual user  $i$  in the time slot  $l$  is defined as

$$\text{SIR}_{il} = N \cdot \frac{p_{il}g_i}{\sum p_{jl}g_j + I} \quad (5.1)$$

where  $I$  represents the sum of noise and the intercell interference power and  $N$  is the processing gain.  $p_{il}$  denotes the transmit power of virtual user  $i$  in time slot  $l$ . We assume that  $g_1 > g_2 > \dots > g_K$ , such that user with lower index has a higher channel gain.

In the multicode format, the rate of user  $i$  in time slot  $l$ ,  $R_{il}$ , is defined by the number of multicode,  $K_{il}$ , i.e.,  $R_{il} = K_{il} \times R_{\text{base}}$ .  $R_{\text{base}}$  is defined as  $\frac{W}{N}$  where  $W$  is the spreading bandwidth. Then, the sum of rate of user  $i$  during the  $n$  time slots is  $\sum_{l=1}^n R_{il} = \sum_{l=1}^n K_{il} R_{\text{base}}$ . We assume a common target SIR,  $\text{SIR}_{\text{target}}$ , for all virtual users.

### 5.2.2 Problem Formulation

We aim to minimize the total transmit power spent by all users in a frame subject to short term throughput constraints. More specifically, the problem is to minimize the sum of transmit power of  $K$  users in  $n$  time slots, while each user maintains the short term average throughput  $\sum_{l=1}^n \frac{K_{il}R_{base}}{n} = \bar{R}_i$ .  $\bar{R}_i$  denotes the average throughput requirement of user  $i$ . We assume that the system has a feasible solution for a given  $\{\bar{R}_i\}$ , that is, the system can accommodate all the users at their SIR target and short term throughput requirements. Formally, the optimization problem is:

$$\begin{aligned}
 \min \quad & \sum_{l=1}^n \sum_{i=1}^K \sum_{k=1}^{K_{il}} p_{il}^k & (5.2) \\
 \text{s.t.} \quad & SIR_{il} \geq SIR_{\text{target}} \quad \forall i \quad \exists p_{il} > 0 \\
 & \sum_{l=1}^n K_{il} = \frac{n\bar{R}_i}{R_{base}} \quad \forall i \\
 & p_{il} \geq 0 \quad \forall i, l
 \end{aligned}$$

where  $p_{il}^k$  is the transmit power for a virtual user  $k$  assigned to user  $i$  in time slot  $l$ . The first constraint maintains the minimum target SIR requirement of each virtual user, while the second constraint imposes the short term average throughput requirement. Because  $\sum_{l=1}^n K_{il}$  is an integer value,  $\bar{R}_i$  is assumed to be chosen such that  $\frac{n\bar{R}_i}{R_{base}}$  is an integer value. We note that user  $i$  may decrease its transmission rate to zero in any given time slot, as long as the average throughput requirement is satisfied.

Assuming  $M_l$  virtual users in the time slot  $l$ , i.e.,  $M_l = \sum_{i=1}^K K_{il}$ , the optimum received power for each virtual user is achieved when the SIR constraint in (5.2) is

satisfied with equality. The optimum equal received power for each virtual user in the time slot  $l$  is given by

$$q_l^* = \frac{\frac{I\gamma^*}{1+\gamma^*}}{1 - M_l \frac{\gamma^*}{1+\gamma^*}} \quad (5.3)$$

where  $\gamma^* = \frac{SIR_{\text{target}}}{N}$  is the SIR target normalized by the processing gain. For the resulting received power value to be feasible, we need  $q_l^* > 0$ . Hence, the maximum number of virtual users in a time slot is limited by  $\lfloor \frac{1+\gamma^*}{\gamma^*} \rfloor$ . Accordingly, a feasible solution exists when the total number of virtual users in  $n$  time slots does not exceed  $n \times \lfloor \frac{1+\gamma^*}{\gamma^*} \rfloor$ .

With optimum equal received power in (5.3), the transmit power for the virtual users in a time slot must be the same, i.e.,  $p_{il}^{k1} = p_{il}^{k2} = p_{il}$ . Accordingly, (5.2) is restated as:

$$\begin{aligned} \min \quad & \sum_{l=1}^n \sum_{i=1}^K K_{il} p_{il} & (5.4) \\ \text{s.t.} \quad & SIR_{il} \geq SIR_{\text{target}} \quad \forall i \quad \exists p_{il} > 0 \\ & \sum_{l=1}^n K_{il} = \frac{n\bar{R}_i}{R_{\text{base}}} \quad \forall i \\ & p_{il} \geq 0 \quad \forall i, l \end{aligned}$$

With the SIR equality constraint and noting that the received power is the product of the transmit power and the channel gain, i.e.,  $p_{il}g_i = q_l^*$ , the optimization problem in

(5.4) is reformulated as:

$$\begin{aligned} \min \quad & \sum_{l=1}^n q_l^* \sum_{i=1}^K \frac{K_{il}}{g_i} \\ \text{s.t.} \quad & \sum_{l=1}^n K_{il} = \frac{n\bar{R}_i}{R_{base}} \quad \forall i \end{aligned} \tag{5.5}$$

i.e., the optimization problem in (5.5) is to find  $K_{il} \forall i$  and  $\forall l$ , the number of virtual user for each user  $i$  in each time slot  $l$ , to minimize the total transmit power in  $n$  time slots, while each user  $i$  has  $T_i = \frac{n\bar{R}_i}{R_{base}}$  virtual users in  $n$  time slots. Thus,  $T = \sum_{i=1}^K T_i$  virtual users are to be scheduled in  $n$  time slots such that the total transmit power is minimized.

We note that the optimization problem considered here is different from the channel base station assignment problem [42], where multiple base station is considered, which is known as NP-complete. In our case, a single cell, i.e., one base station, is considered.

### 5.3 Optimum Scheduling

In this section, we provide the solution for optimization problem (5.5). First, we note that, the structure of the optimum scheduling policy relies on the following observation.

**OBSERVATION 5.1.** *The optimum policy schedules the virtual users in such a way that any virtual user with a lower channel gain is assigned to a time slot with a lighter load, i.e., a slot with smaller number of virtual users.*

To see why Observation 5.1 is valid, suppose the optimum policy schedules users such that one virtual user  $j$  with channel gain  $g_j$  is assigned to slot 1, and another virtual

user  $i$  with channel gain  $g_i$  ( $g_i > g_j$ ) is assigned to slot 2. It is assumed that slot 1 has more virtual users than slot 2, i.e.,  $M_1 > M_2$ . Hence,  $q_1^* > q_2^*$ . If we exchange these two virtual users  $i$  and  $j$  between two slots, slot 1 and slot 2, all the virtual users except these two need the same transmit power level, because  $q_1^*$  and  $q_2^*$  remains the same. However, the sum of these two virtual users power level is decreased, i.e.,  $\frac{q_1^*}{g_i} + \frac{q_2^*}{g_j} < \frac{q_1^*}{g_j} + \frac{q_2^*}{g_i}$ . Hence, the total transmit power is decreased.

Observation 5.1 provides a valuable information for determining the power efficient optimum scheduling policy. Define the set of virtual users in time slot  $l$  as  $s_l$ . We use  $|s_l|$  and  $M_l$  interchangeably for representing the number of virtual users in time slot  $l$ . Note that the sets of virtual users  $\{s_1, \dots, s_n\}$  should satisfy  $|s_l| \neq 0$  and  $\sum_{l=1}^n |s_l| = T$  for any valid schedule. Note also that, collection of virtual user sets resulting from *any* scheduling policy can be reordered such that  $\{s_1, \dots, s_n\}$  where  $|s_1| \leq \dots \leq |s_n|$ , termed the *reordered virtual user sets*. This reordering of virtual user sets (time slots) does not change the total power value expended as a result of this policy. That is, the performance of the scheduling policy is a function of how many virtual users are scheduled into each slot only, and not the actual location of these slots in the  $n$ -slot frame. Therefore, we only need to consider scheduling policies with the reordered virtual user sets to find the optimum scheduler.

Consider such a group of reordered virtual user sets. The following observation states how the optimum policy schedules the  $T$  virtual users to this reordered virtual user sets.

OBSERVATION 5.2. *For any given reordered virtual user sets, the optimum scheduling order of  $T$  virtual users is in the order of increasing channel gain, i.e.,*

$$\underbrace{g_K, \dots, g_K}_{T_K}, \underbrace{g_{K-1}, \dots, g_{K-1}}_{T_{K-1}}, \dots, \underbrace{g_1, \dots, g_1}_{T_1} \quad (5.6)$$

Note that the scheduling order (5.6) satisfies Observation 5.1. Hence, (5.6) is in the form of a candidate for the output of the optimum scheduler. Accordingly, the optimization problem in (5.5) is to find the best reordered virtual user set group such that the sum of total transmit power is minimized, given the optimum scheduling order in (5.6).

The optimization problem in (5.5), by an appropriate transformation, can be formulated as a graph partitioning problem with a solution that has polynomial complexity. Specifically, the optimization problem in (5.5) can be transformed into a graph partitioning problem following the approach in reference [51], as described next.

We note that (5.6) in Observation 5.2 constitutes a string [15], which is a graph where all vertices are located along a line,  $G = (V, E)$  with vertices  $V = \{v_1, v_2, \dots, v_T\}$  and edges  $E = \{(v_1, v_2), \dots, (v_{T-1}, v_T)\}$ , as in Figure 5.1. Each virtual user is represented by a vertex along the string. More specifically, each virtual user in (5.6) is sequentially mapped into the vertex of the string from the left to the right. The weight of a vertex is  $w_i = \frac{1}{g_i}$  where  $g_i$  is the channel gain of the virtual user corresponding to that vertex.

Given the string  $G = (V, E)$  as in Figure 5.1, let  $\{S_1, \dots, S_n\}$  be the partition of the set of vertices  $V$  into  $n$  subsets, and each subset  $S_l$  has a set of connected vertices. Note that in a feasible partition,  $|S_l| \neq 0$ . In this setting, the virtual user sets  $\{s_1, \dots, s_n\}$  is equivalent to  $\{S_1, \dots, S_n\}$ . Hence, we use  $s_l$  and  $S_l$  interchangeably. The cost of a virtual user set (subset)  $s_l$  is  $q_l^* \sum_{i \in s_l} \frac{1}{g_i}$  and the cost of all virtual user sets is  $\sum_{l=1}^n q_l^* \sum_{i \in s_l} \frac{1}{g_i}$ .

Therefore, the optimization problem in (5.5) is equivalent to finding a feasible  $n$ -partition such that given cost is minimized:

$$\begin{aligned} \arg \min_{\{s_1, \dots, s_n\}} \quad & \sum_{l=1}^n q_l^* \sum_{i \in s_l} \frac{1}{g_i} \\ \text{s.t.} \quad & |s_1| \leq \dots \leq |s_n| \end{aligned} \tag{5.7}$$

We note that, although the problem of optimally partitioning an arbitrary graph with an arbitrary cost function is NP-hard, partitioning a string optimally with a separable cost function can be solved in polynomial time [15]. Note that the cost function in (5.7) is separable. In this case, the problem of graph partitioning a string can be reduced to a shortest path problem with complexity  $O(nT^2)$  [53].

In the following, the solution of the partitioning problem in (5.7) by a shortest path algorithm is described. We construct a network from the string that represents the virtual users. The node that lies between the origin-destination pair are given by the set

$$\{(i, j) : 1 \leq i \leq n - 1; i \leq j \leq T - n + i\}. \tag{5.8}$$

An edge is placed from node  $(i1, j1)$  to  $(i2, j2)$  if  $i2 = i1 + 1$  and  $j2 > j1$ . Otherwise, there is no edge between  $(i1, j1)$  and  $(i2, j2)$ . There is a one-to-one relationship between the cost function of a feasible partition in a string, and the cost function of a path in the network constructed from the partitioning problem.

For instance, consider  $T = 5$  and  $n = 3$ . From the string with 5 vertices (virtual users), we first construct the network as Figure 5.2. At node  $(i, j)$ ,  $i$  and  $j$  denote the index of the time slot and the index of virtual user, respectively. The cost of a path between node  $(l - 1, t)$  and  $(l, t + w)$  is the cost of the virtual user set  $s_l$ , i.e.,  $q_l^* \sum_{i \in s_l} \frac{1}{g_i}$  where  $|s_l| = w$ . We note that the optimum policy should satisfy  $|s_1| \leq \dots \leq |s_n|$  and the maximum number of virtual users in a time slot,  $\lfloor \frac{1+\gamma^*}{\gamma^*} \rfloor$ . Hence, if a path violates any of these two constraints, the cost of that path is set to be infinity. Next, a shortest path from the origin to the destination with cost  $\min_{\{s_1, \dots, s_n\}} \sum_{l=1}^n q_l^* \sum_{i \in s_l} \frac{1}{g_i}$  is obtained by using a shortest path algorithm such as Dijkstra's method which has complexity  $O(nT^2)$ . The resulting optimum partition  $\{s_1, \dots, s_n\}$  provides  $K_{il} \forall i$  and  $\forall l$ .

## 5.4 Numerical Results

We consider the uplink of a CDMA system with a spreading bandwidth  $W = 1.228MHz$  and the processing gain  $N = 128$ . Intercell Interference is  $I = 10^{-13}$ . Target  $SIR$  is  $SIR_{\text{target}} = 5$ . With  $SIR_{\text{target}} = 5$ , maximum number of virtual users in each time slot is limited by 26.  $K = 5$  users are uniformly distributed within the cell with radius  $1km$ . The frame size is  $n = 5$  time slots. Channel gain of user  $i$   $g_i$ , is modeled as  $\frac{r_i}{d_i^4}$  where  $d_i$  is distance between the base station and the user  $i$ .  $r_i$  is the log-normal fading with variance  $8dB$ .



Figure 5.3 shows the power consumption of two scheduling methods, the optimum scheduling and the TDMA-type scheduling, for average throughput requirement  $\bar{R}_i = 9.6\text{kbps}, 19.2\text{kbps}, 28.8\text{kbps}, 38.4\text{kbps}, \text{and } 48.0\text{kbps}$ . With  $K = 5$  users, maximum average throughput is limited by 48.0kbps. In TDMA-type scheduling, user  $i$  transmits with rate  $n \times \bar{R}_i$  and users transmit in a round robin fashion. The result is obtained by averaging 10,000 channel realizations. As the average throughput requirement increases, i.e., the system load gets heavier, the gap between the performance of the optimum scheduler and that of the TDMA-type scheduling increases. This results clearly indicate the benefit of optimum scheduling for a loaded system. Note that if the channel gains of all users are identical<sup>1</sup>, the optimum scheduler and TDMA result in the same performance.

Figures 5.4 and 5.5 demonstrate the optimum transmission rate allocation for a specific channel realization into  $n = 5$  and  $n = 10$  time slot frame, respectively. The average throughput requirement is  $\bar{R}_i = 28.8\text{kbps}$ . It is shown that, for power efficient transmission, the virtual user with lower channel gain is assigned to a less loaded time slot.

Figure 5.6 shows the power consumption of two methods (optimum scheduling and equal loading) when  $K = 20$  and  $n = 10$ . In the equal loading, each time slot have equal number of virtual users. With  $K = 20$  users, maximum average throughput is limited by 48.0kbps. This example is provided to verify the performance of OS when the large number of users are in the system.

---

<sup>1</sup>A zero probability event given the fact that the channel gains are drawn from a continuous distribution.

## 5.5 Conclusion

We have considered power efficient scheduling for delay constrained multicode CDMA services. Short term average throughput requirement is imposed to maintain an average throughput for each user. It is assumed that multiple data rates are provided by means of multiple signatures (codes) each of which is treated as a virtual users. We allow codes assigned to each user to interfere with each other, as well as with codes assigned to other users. For power efficient transmission, these virtual users should be carefully scheduled. We have shown that the optimum scheduler can be obtained by solving a shortest path problem. Our numerical results demonstrate that the optimum scheduler can outperform the TDMA-type scheduler in loaded systems.

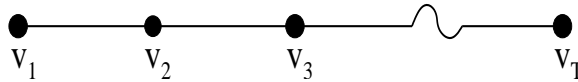


Fig. 5.1. A string constructed based on optimum virtual users scheduling ordering

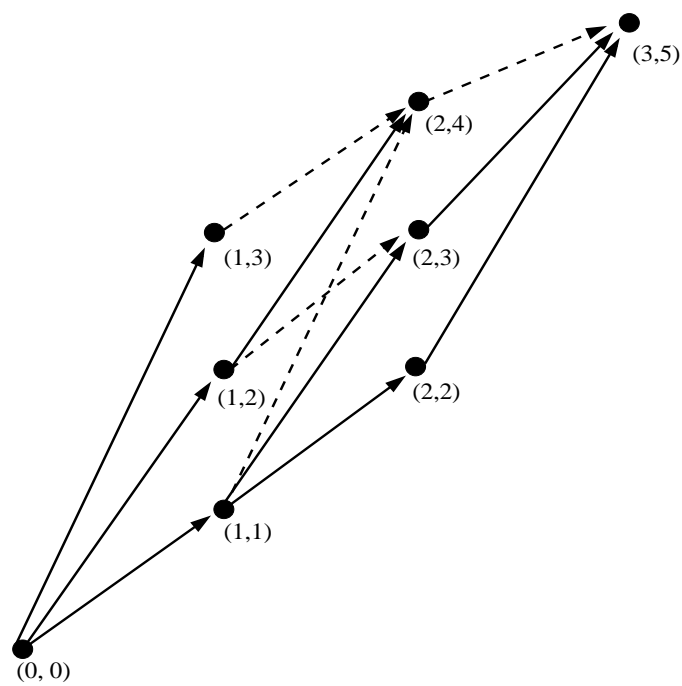


Fig. 5.2. Network constructed by 3-partitioning the string having 5 nodes ( $\cdots$  : Infeasible edge,  $-$  : Feasible edge).

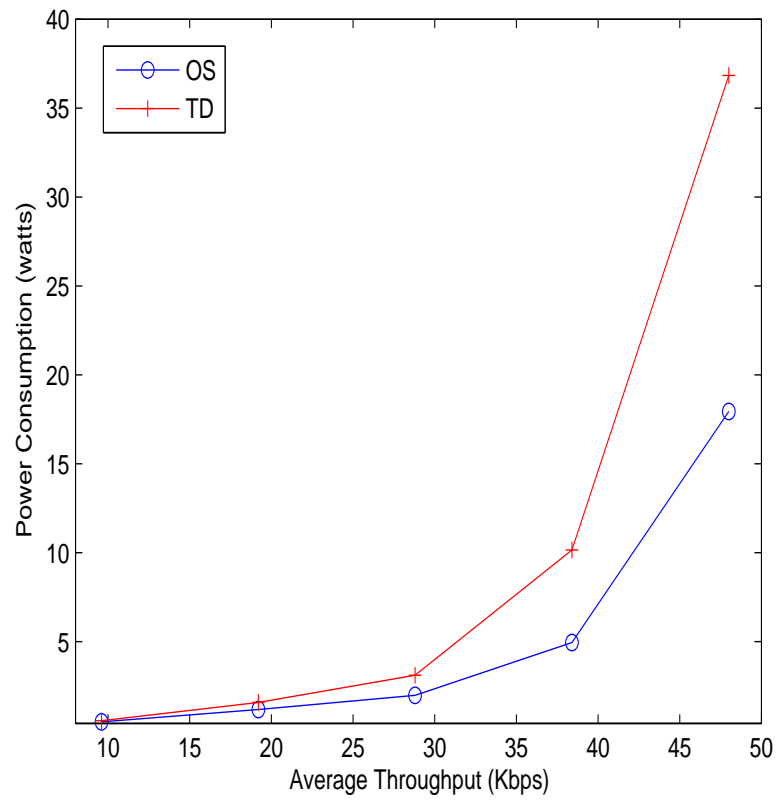


Fig. 5.3. Power Consumption of Optimum Scheduling (OS) and TDMA-type (TD)  
 $K = 5, n = 5$ .

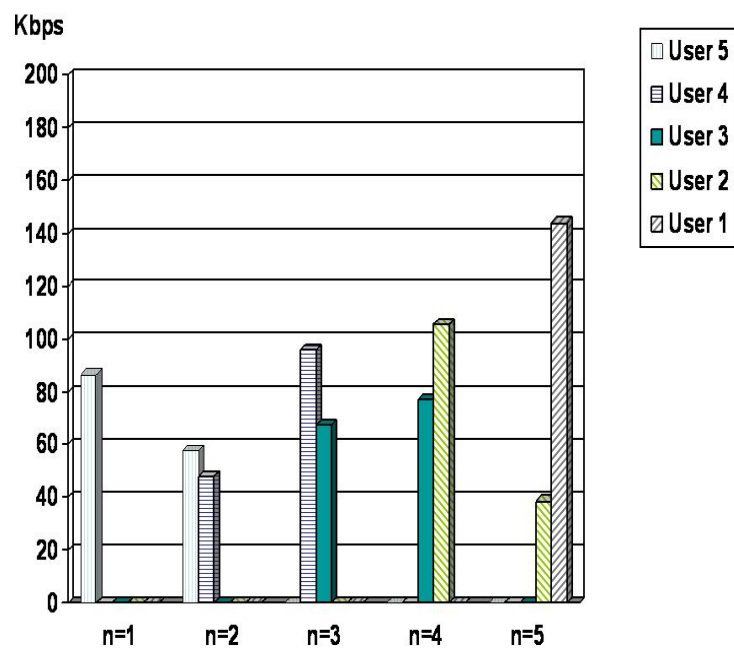


Fig. 5.4. Transmission rate allocation in time slots.  $g_1 > g_2 > g_3 > g_4 > g_5$ .

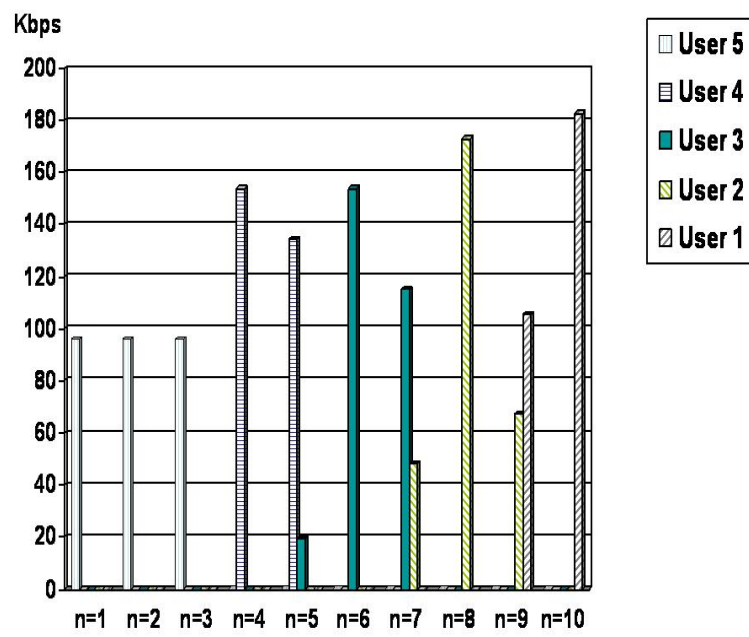


Fig. 5.5. Transmission rate allocation in time slots.  $g_1 > g_2 > g_3 > g_4 > g_5$ .

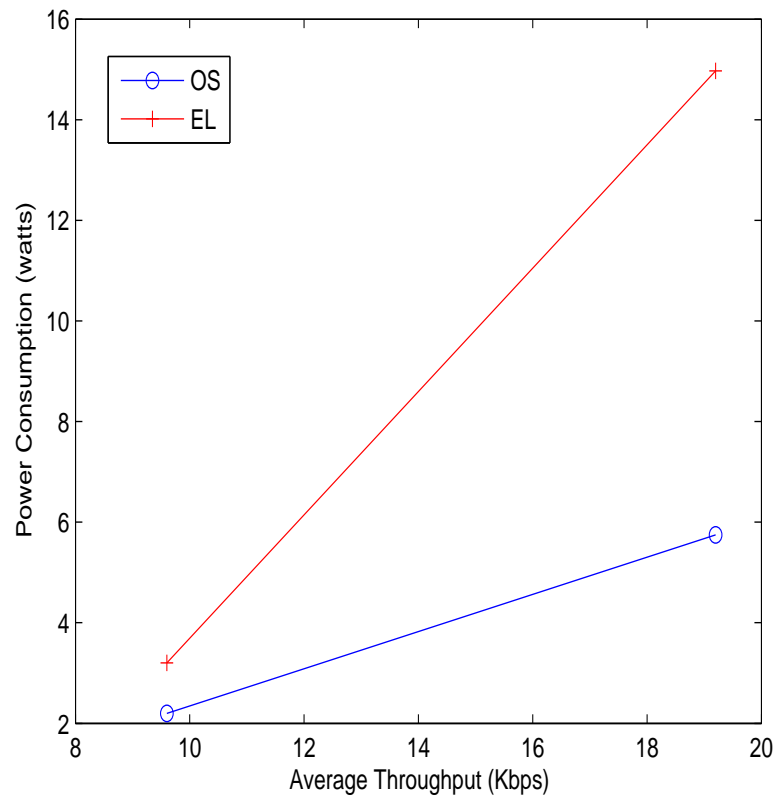


Fig. 5.6. Power Consumption of Optimum Scheduling (OS) and Equal Loading (EL),  $K = 20$ ,  $n = 10$ .

## Chapter 6

# Conclusion and Future Work

### 6.1 Thesis Summary

This thesis studies scheduling and power allocation problems in a variety of CDMA system settings by utilizing available degrees of freedom. The degrees of freedom considered in this thesis are sectored antennas, orthogonal codes, and time slots.

We have first presented the joint optimization problem of adaptive cell sectorization, power control, and linear multiuser detection for real time CDMA services to improve user capacity. When the antenna pattern is perfect, i.e., no intersector interference exists between sectored antennas, it is shown that the optimization problem can be solved by a dynamic program. In practice, the antenna pattern is imperfect which induces intersector interference. We thus remove the assumption of the perfect antenna pattern next and formulate the joint optimization problem of cell sectorization, transmit power control, and multiuser detection for both uplink and downlink. We propose an optimum algorithm as well as near optimum algorithms with reduced complexity. It is observed that intelligently combining power control, multiuser detection and cell sectorization leads to improved uplink and downlink user capacity.

We then investigate the downlink throughput maximization for interference limited multiuser system for delay tolerant CDMA services. For the CDMA downlink, the



orthogonal codes are used to communicate to each other. However, due to the multipath fading, orthogonality between codes is not preserved at the mobile side, which causes the interference between users. We model the interference level by the aid of the orthogonality factor. The aim is to find the optimum base station transmission strategy, one-user-transmission (TDMA) or more than one-user-transmissions (CDMA). We identify the optimum number of users to be scheduled and the corresponding power allocation, so as to maximize the total system utility, sum of the individual throughput, for a range of the orthogonality factor values and the users' channel gains. This thesis presents an exact and a near-exact algorithm to determine the transmission policy (TDMA or CDMA). When CDMA is optimum, the corresponding optimum power allocation is performed in the proposed algorithm.

Lastly, we consider the energy efficient temporal scheduling and power allocation problem for delay constrained CDMA services. The aim is to find the efficient optimum scheduling policy to minimize the transmit energy, while each user maintains the short term average throughput. It is observed that, for energy efficient transmission in interference limited CDMA system, the virtual user should be carefully scheduled to mitigate the interference. It is shown that the optimum scheduling can be obtained by solving a shortest path problem. We observe that by judicious scheduling, total transmit energy is decreased, especially for a loaded system.

## 6.2 Future Work

In this thesis, the scheduling and power allocation problems in CDMA systems have been investigated. Future wireless services will require higher data rates and different quality of service (QoS) levels. To satisfy these demands, recent research effort has focused on Orthogonal Frequency Division Multiple Access (OFDMA) and Multiple-Input Multiple-output (MIMO) systems [62, 47, 25, 52, 30, 29, 70, 31, 23, 38, 39]. The advantage of MIMO/OFDM systems is on the use of degrees of freedom, frequency domain, user domain, and spatial domain. These degrees of freedom can be utilized to increase the spectral efficiency. For future research, scheduling and power allocation problems in MIMO/OFDM systems can be investigated.

### 6.3 Publications

The following is a list of contributions.

#### Journal Publications

1. C. Oh, A. Yener, "Downlink Throughput Maximization for Interference Limited Multiuser Systems: TDMA versus CDMA," Submitted to IEEE Transactions on Wireless Communications 2005.
2. C. Oh, A. Yener, "Power Controlled CDMA Cell Sectorization with Multiuser Detection: A Comprehensive Analysis of Uplink and Downlink," Submitted to IEEE Transactions on Vehicular Technology 2004.

#### Conference Proceedings

1. C. Oh, A. Yener, "Downlink Throughput Maximization: TDMA versus CDMA," 39th Annual Conference on Information Sciences and Systems (CISS), March 2005.
2. C. Oh, A. Yener, "Further Results on adaptive CDMA cell sectorization with linear multiuser detection, " IEEE 37th Asilomar Conference on Signals, Systems and Computers, November 2003.
3. C. Oh, A. Yener, "Adaptive CDMA cell sectorization with linear multiuser detection," IEEE 58th Vehicular Technology Conference, October 2003.

## References

- [1] F. Adachi, M. Sawahashi, and H. Suda. Wideband DS-CDMA for next-generation mobile communication systems. *IEEE Communications Magazine*, 36(9):56–69, September 1998.
- [2] R. Agrawal, V. Subramanian, and R. A. Berry. Joint scheduling and resource allocation in CDMA systems. *Submitted, 2004*. Available at [www.ece.northwestern.edu/~rberry/opt.pdf](http://www.ece.northwestern.edu/~rberry/opt.pdf).
- [3] H. Alavi and R.W. Nettleton. Downstream power control for a spread spectrum cellular mobile radio system. In *IEEE Globecom*, 1982.
- [4] G. Alexander. *Nonnegative matrices and applicable topics in linear algebra*. Ellis Horwood, 1987.
- [5] M. Andrew, K. Kumaran, K. Ramanan, A.L. Stolyar, R.Vijayakumar, and P. Whiting. Providing quality of service over a shared wireless link. *IEEE Communications Magazine*, 39(2):150–154, 2001.
- [6] A. Bedekar, S. Borst, K. Ramanan, P. Whiting, and E. Yeh. Downlink scheduling in CDMA data networks. In *IEEE Globecom*, 1999.
- [7] P. Bender, P. Black, M. Grob, R. Padovani, N. Sindhushayana, and A. Viterbi. CDMA/HDR: a bandwidth-efficient high-speed wireless data service for nomadic users. *IEEE Communications Magazine*, pages 70–77, 2000.

- [8] F. Berggren and R. Jantti. Multiuser scheduling over rayleigh fading channels. In *IEEE Global Telecommunications Conference*, 2003.
- [9] F. Berggren and R. Jantti. Asymptotically fair transmission scheduling over fading channels. *IEEE Transactions on Wireless Communications*, 3:326–336, January 2004.
- [10] F. Berggren and S.L. Kim. Energy-efficient control of rate and power in DS-CDMA systems. *IEEE Transactions on Wireless Communications*, 3:725–733, May 2004.
- [11] F. Berggren, S.L. Kim, R. Juntti, and J. Zander. Joint power control and intra-cell scheduling of DS-CDMA non-real time data. *IEEE Journal on Selected Areas in Communications*, pages 1860–1870, 2001.
- [12] R. Berry and R. Gallager. Communication over fading channels with delay constraints. *IEEE Transactions on Information Theory*, 48(5):1135–1149, May 2002.
- [13] D.P. Bertsekas. *Nonlinear programming*. Athena Scientific, 1995.
- [14] E.U. Bıyıkoglu, B. Prabhakar, and A. El Gamal. Energy-efficient packet transmission over a wireless link. *IEEE/ACM Transactions on Networking*, 10:487–499, August 2002.
- [15] R. Diestel. *Graph Theory*. Springer, 1997.
- [16] N. Feng, S.C. Mau, and N.B. Mandayam. Pricing and power control for joint network-centric and user-centric radio resource management. *IEEE Transactions on Communications*, 52(9):1547–1557, September 2004.

- [17] G.J. Foschini and Z. Miljanic. A simple distributed autonomous power control algorithm and its convergence. *IEEE Transactions on Vehicular Technology*, 42:641–646, November 1993.
- [18] A. Fu, E. Modiano, and J. Tsitsiklis. Optimal energy allocation for delay constrained data transmission over a time varying channel. In *IEEE Infocom*, 2003.
- [19] M.R. Garey and D.S. Johnson. *A Guide to the Theory of NP-Completeness*. W. H. Freeman and Company, 1991.
- [20] R. Giuliano, F. Mazzenga, and F. Vatalaro. Adaptive cell sectorization for umts third generation CDMA systems. In *IEEE Vehicular Technology Conference, VTC'01 Spring*, May 2001.
- [21] A. J. Goldsmith and S. G. Chua. Variable-rate variable-power MQAM for fading channels. *IEEE Transactions on Communications*, 45:1218–1230, October 1997.
- [22] S.V. Hanly and D.N.C. Tse. Power control and capacity of spread spectrum wireless networks. *Automatica*, 35(12), December 1999.
- [23] R. Heath, M. Airy, and A. Laroia. Multiuser diversity for MIMO wireless systems with linear receivers. In *IEEE Asilomar Conference on Signals, Systems and Computers*, 2001.
- [24] H. Holma. *W-CDMA for UMTS: Radio Access for Third Generation Mobile Communications*. Wiley and Sons, 2002.

- [25] J. Jang and K. B. Lee. Transmit power adaptation for multiuser OFDM systems. *IEEE Journal on Selected Areas in Communications*, pages 171 – 178, February 2003.
- [26] H. Ji and C.Y. Huang. Non-cooperative uplink power control in cellular radio systems. *Wireless Networks*, 4:233–240, April 1998.
- [27] M.K. Karakayali, R. Yates, and L.V. Razoumov. Throughput maximization on the downlink of a CDMA system. In *IEEE WCNC*, 2003. Journal version: <http://www.winlab.rutgers.edu/~ryates/papers/webpreprint.html>.
- [28] M.K. Karakayali, R. Yates, and L. Razoumov. Joint power and rate control in multiaccess systems with multirate services. In *Conference on Information Sciences and Systems, CISS'03*, March 2003.
- [29] I. Kim, H. L. Lee, B. Kim, and Y.H. Lee. On the use of linear programming for dynamic subchannel and bit allocation in multiuser OFDM. In *IEEE Global Telecommunications Conference*, 2001.
- [30] D. Kivanc and H. Liu. Subcarrier allocation and power control for OFDMA. In *IEEE Thirty-Fourth Asilomar Conference on Signals, Systems and Computers*, 2000.
- [31] E. Lawrey. Multiuser OFDM. In *In proc. International Symposium on Signal Processing and Its Applications*, 1999.
- [32] J.C. Liberti and T.S. Rappaport. *Smart antennas for wireless communications : IS-95 and third generation CDMA applications*. Prentice Hall, 1999.

- [33] R. Lupas and S. Verdu. Linear multiuser detectors for synchronous code-division multiple access channels. *IEEE Transactions on Information Theory*, 35:123–136, January 1989.
- [34] U. Madhow and M.L. Honig. MMSE interference suppression for direct-sequence spread spectrum CDMA. *IEEE Transactions on Communications*, 42:3178–3188, December 1994.
- [35] R.J. McEliece. *Finite Fields for Computer Scientists and Engineers*. Boston:Kluwer, 1987.
- [36] N.B. Mehta, L.J. Greestein, T.M. Willis, and Z. Kostic. Analysis results for the orthogonality factor in WCDMA downlinks. *IEEE Transactions on Wireless Communications*, pages 1138–1149, November 2002.
- [37] R. W. Nettleton and H. Alavi. Power control for a spread spectrum cellular mobile radio system. In *IEEE Vehicular Technology Conference*, 1983.
- [38] K.W. Ng, R.S. Cheng, and R.D. Murch. Iterative bit and power allocation for V-BLAST based OFDM MIMO system in frequency selective fading channel. In *IEEE WCNC*, 2002.
- [39] K.W. Ng, R.S. Cheng, and R.D. Murch. A simplified bit allocation for V-BLAST based OFDM MIMO systems in frequency selective fading channel. In *IEEE ICC*, 2002.



- [40] C. Oh and A. Yener. Adaptive CDMA cell sectorization with linear multiuser detection. In *IEEE Vehicular Technology Conference, VTC'03 Fall*, September 2003.
- [41] S.J. Oh and K.M. Wasserman. Optimality of greedy power control and variable spreading gain in multi-class CDMA mobile networks. In *ACM/IEEE Mobicom*, 1999.
- [42] S. Papavassiliou and L. Tassiulas. Joint optimal channel base station and power assignment for wireless access. *IEEE/ACM Transactions on Networking*, 4:857 – 872, December 1996.
- [43] B. Prabhakar, E.U. Biyikoglu, and A. El Gamal. Energy-efficient transmission over a wireless link via lazy packet scheduling. In *IEEE Infocom*, 2001.
- [44] X. Qiu and K. Chawla. On the performance of adaptive modulation in cellular systems. *IEEE Transactions on Communications*, pages 884–895, 1999.
- [45] K. Ramanan and L. Qian. Uplink scheduling in CDMA packet-data systems. In *IEEE Infocom*, 2003.
- [46] F. Rashid-Farrokhi, K.J.R. Liu, and L. Tassiulas. Downlink power control and base station assignment. *IEEE Communications Letters*, 1(04):102–104, July 1997.
- [47] W. Rhee and J.M. Cioffi. Increase in capacity of multiuser OFDM system using dynamic subchannel allocation. In *IEEE Vehicular Technology Conference Proceedings, spring*, 2003.

- [48] A. Sabharwal, D. Avidor, and L. Potter. Sector beam synthesis for cellular systems using phased antenna arrays. *IEEE Transactions on Vehicular Technology*, pages 1784–1792, September 2000.
- [49] C.U. Saraydar, N.B. Mandayam, and D.J. Goodman. Pricing and power control in a multicell wireless data network. *IEEE Journal on Selected Areas in Communications*, 50(2):1883–1892, October 2001.
- [50] C.U. Saraydar, N.B. Mandayam, and D.J. Goodman. Efficient power control via pricing in wireless data networks. *IEEE Transactions on Communications*, 50(2):291–303, February 2002.
- [51] C.U. Saraydar and A. Yener. Adaptive cell sectorization for CDMA systems. *IEEE Journal on Selected Areas in Communications*, 19(6):1041–1051, June 2001.
- [52] Z. Shen, J.G. Andrews, and B.L. Evans. Optimal power allocation in multiuser OFDM systems. In *IEEE Global Telecommunications Conference*, 2003.
- [53] C. De Simone, M. Lucertini, S. Pallottino, and B. Simeone. Fair dissections of spiders, worms, and caterpillars. *Networks*, 20:323–344, 1990.
- [54] J.E. Smee and H.C. Huang. Mitigating interference in wireless local loop DS-SSMA systems. In *IEEE PIMRC*, 1998.
- [55] D.N.C. Tse and S.V. Hanly. Linear multiuser receivers: effective interference, effective bandwidth and user capacity. *IEEE Transactions on Information Theory*, 45:642–657, March 1999.

- [56] S. Ulukus and L.J. Greenstein. Throughput maximization in CDMA uplinks using adaptive spreading and power control. In *IEEE ISSSTA*, 2000.
- [57] S. Ulukus and R. Yates. Adaptive power control and MMSE interference suppression. *ACM Wireless Networks*, 4:489–496, November 1998.
- [58] S. Ulukus and R. Yates. Iterative construction of optimum signature sequence sets in synchronous cdma systems. *IEEE Transactions on Information Theory*, pages 1989–1998, July 2001.
- [59] S. Ulukus and A. Yener. Iterative transmitter and receiver optimization for CDMA networks. *IEEE Transactions on Wireless Communications*, pages 1879–1884, November 2004.
- [60] S. Verdú. *Multuser Detection*. Cambridge University Press, 1998.
- [61] P. Viswanath, V. Anantharan, and D.N.C. Tse. Optimal sequences, power control, and user capacity of synchronous cdma systems with linear mmse multiuser receivers. *IEEE Transactions on Information Theory*, pages 1968–1983, September 1999.
- [62] C.Y. Wong, R.S. Cheng, K.B. Lataief, and R.D. Murch. Multiuser OFDM with adaptive subcarrier, bit, and power allocation. *IEEE Journal on Selected Areas in Communications*, pages 1747 – 1758, October 1999.

- [63] M. Xiao, N.B. Shroff, and E.K.P. Chong. A utility-based power-control scheme in wireless cellular systems. *IEEE/ACM Transactions on Networking*, 11:210–221, April 2003.
- [64] R. Yates. A framework for uplink power control in cellular radio systems. *IEEE Journal on Selected Areas in Communications*, 13:1341–1348, September 1995.
- [65] R. D. Yates and C. Y. Huang. Integrated power control and base station assignment. *IEEE Transactions on Vehicular Technology*, 44(3):638–644, August 1995.
- [66] A. Yener, R. Yates, and S. Ulukus. Interference management for CDMA systems through power control, multiuser detection and beamforming. *IEEE Transactions on Communications*, 49(7):1227–1239, July 2001.
- [67] J. Zander. Performance of optimum transmitter power control in cellular radio systems. *IEEE Transactions on Vehicular Technology*, 41:57–62, February 1992.
- [68] J. Zander and M. Frodigh. Comment on performance of optimum transmitter power control in cellular radio systems. *IEEE Transactions on Vehicular Technology*, 43, August 1994.
- [69] J. Zhang et al. An efficient algorithm for adaptive cell sectoring in CDMA systems”. In *IEEE International Conference on Communications, ICC’03*, May 2003.
- [70] Y. Zhang and K.B. Letaief. Optimizing power and resource management for multiuser MIMO/OFDM systems. In *IEEE Global Telecommunications Conference*, 2003.

## Vita

- 1999** B.S. in Electrical Engineering, Yonsei University, Seoul, Korea
- 2001** M.S. in Electrical Engineering, The Pennsylvania State University,  
University Park
- 2005** Ph.D. in Electrical Engineering, The Pennsylvania State University,  
University Park